Calorimetry in Medical Applications

PET & SPECT

(Positron Emission Tomography and Single-Photon Emission Tomography)

Chin-Tu Chen, Ph.D.

Department of Radiology &

Committee on Medical Physics

Pritzker School of Medicine &

Biological Sciences Division

The University of Chicago

- Introduction
- PET/SPECT Fundamentals
- Uses in Clinics and R&D
- Advances in PET/SPECT and HEP Calorimetry
- Conclusion

Gamma (Anger) Camera – Planar Scintigrraphy
with Rotation for Angular Sampling ===➔
Single-Photon Emission Computed Tomography (SPECT)

Nuclear Medicine Imaging

Radioisotope-Labeled Chemicals

Tracer Kinetics & Distribution

Function & Physiology

(Beyond Structural and Anatomy)

Planar Scintigraphy

ECT (Emission Computed Tomography)

Single-Photon ECT (SPECT)

Positron ECT (PET)

Nuclear Medicine Imaging
Unclear Medicine Imaging

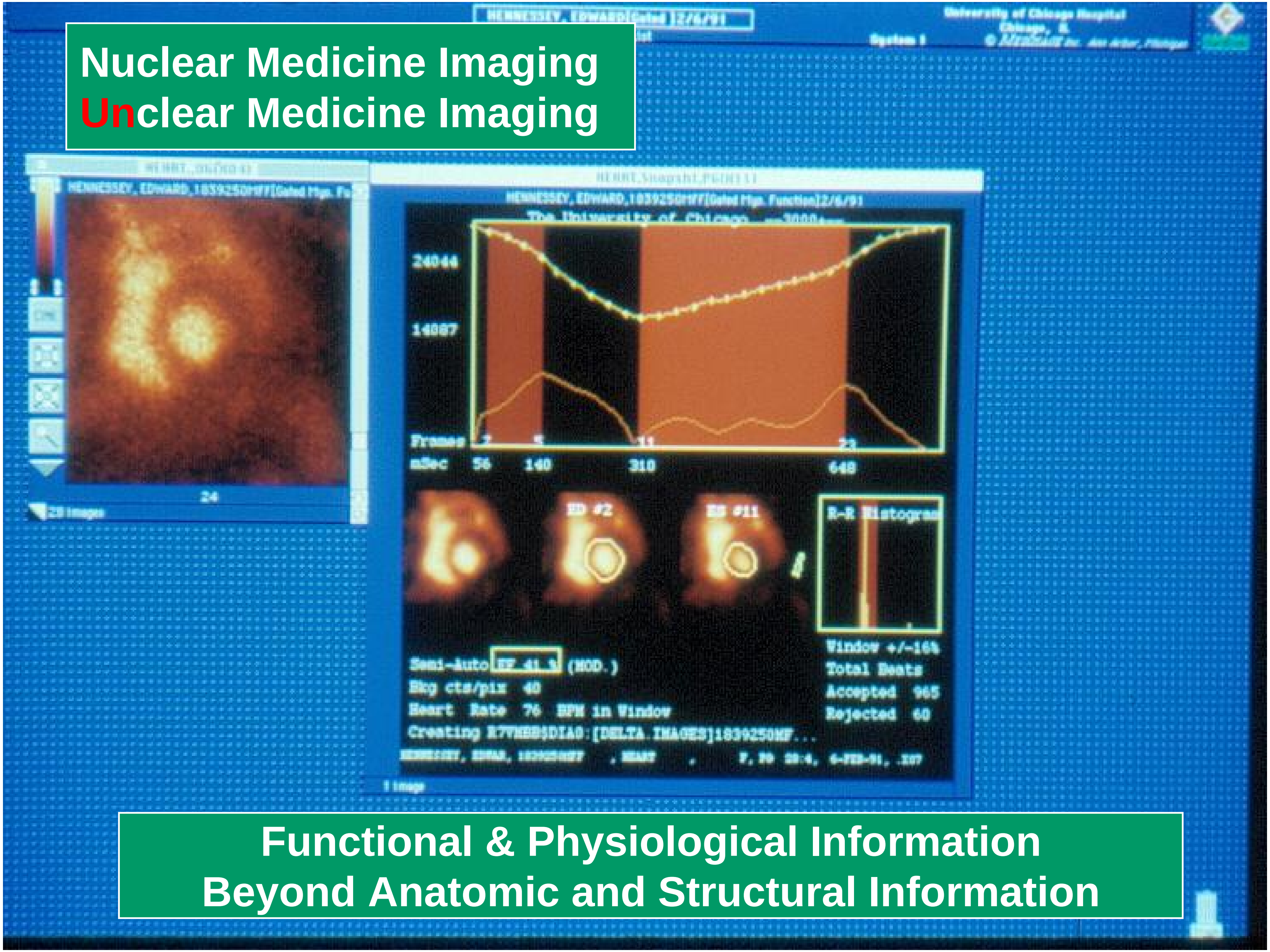

Functional & Physiological Information
Beyond Anatomic and Structural Information

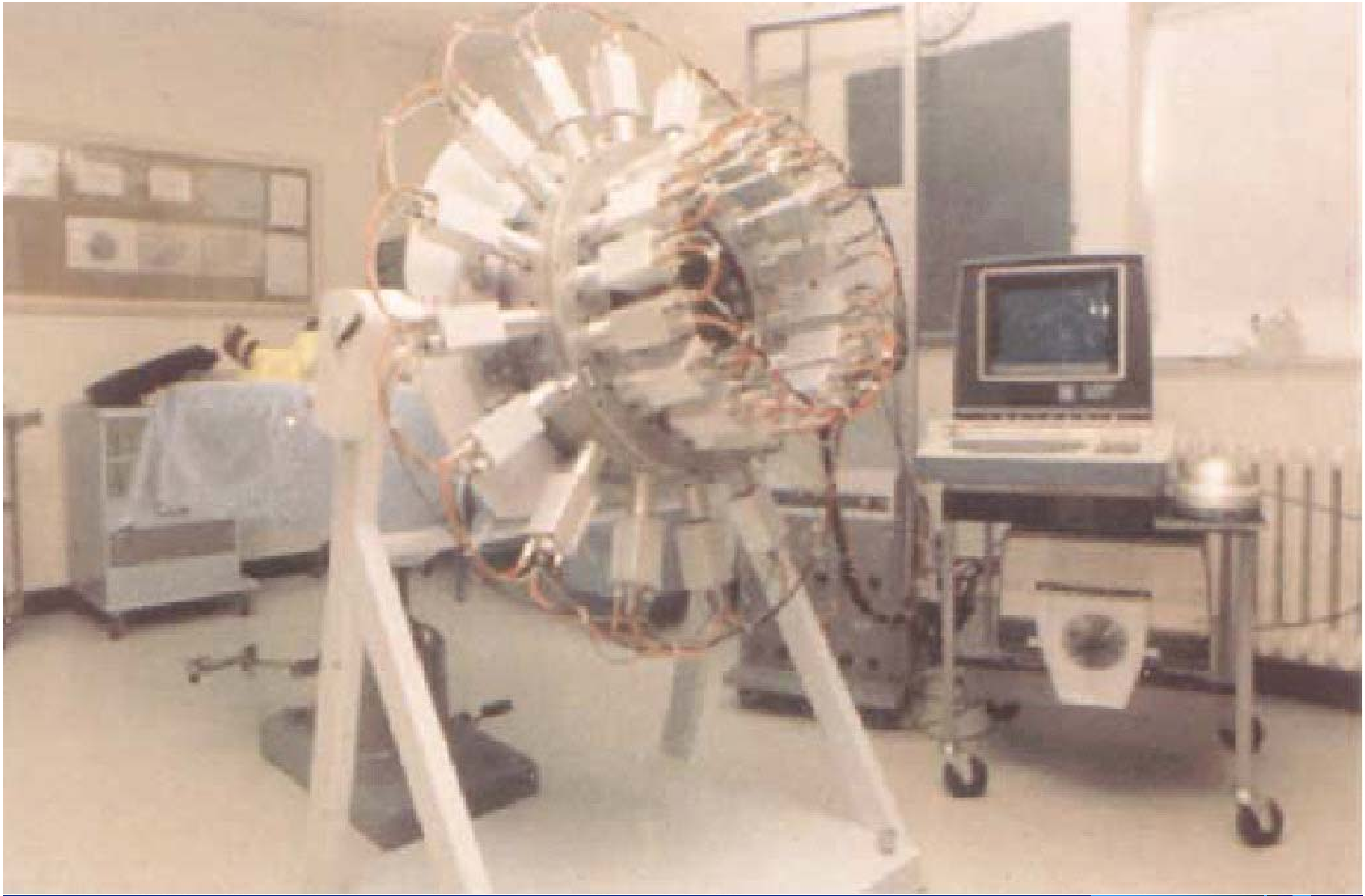

Early PET (Positron Emission Tomography)

32-Detector Circular Array (1973, Brookhaven)

Imaging of Life and Life Processes

Live Brain 1

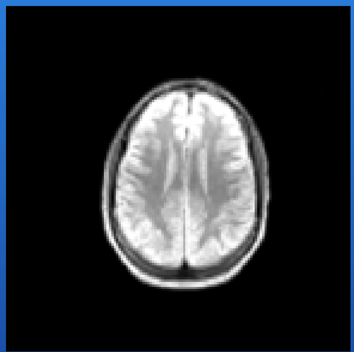

MR

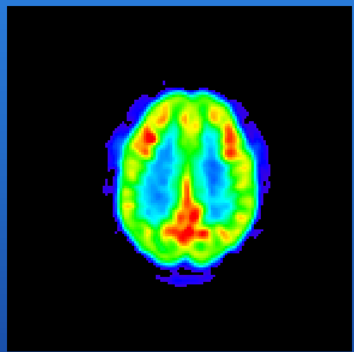

PET

Dead Brain 2

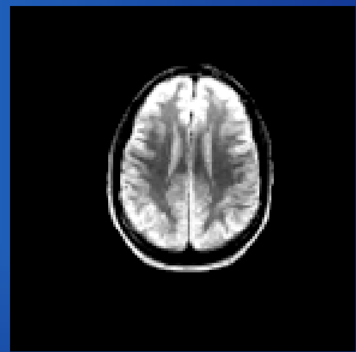

MR

PET

PET Principle

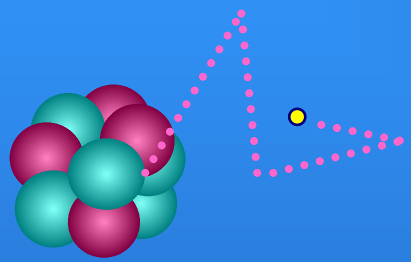

$P \longrightarrow N + e^{+} + n + \text{energy}$

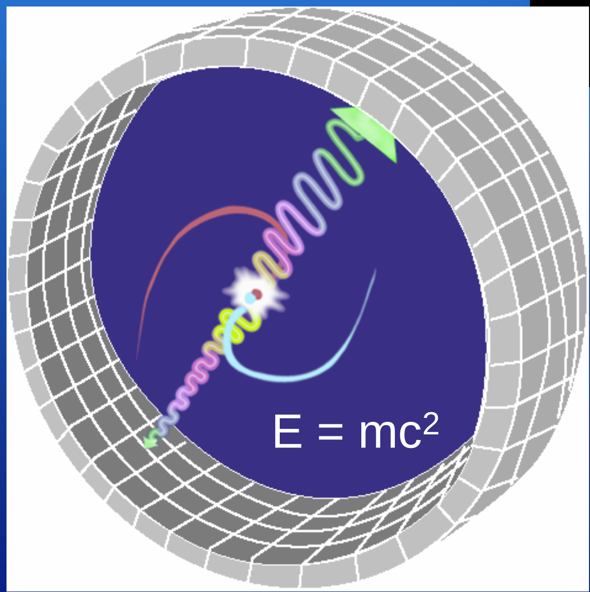

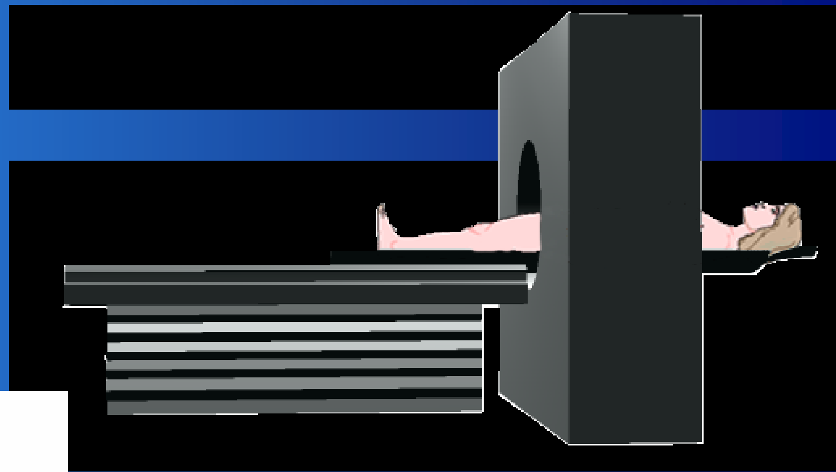

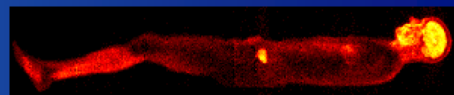

Production of Isotopes
(Mini-Cyclotron)

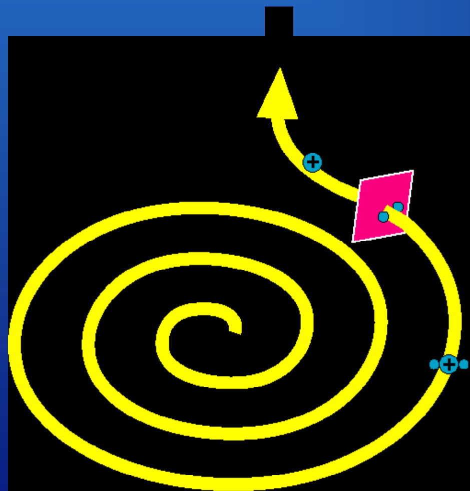

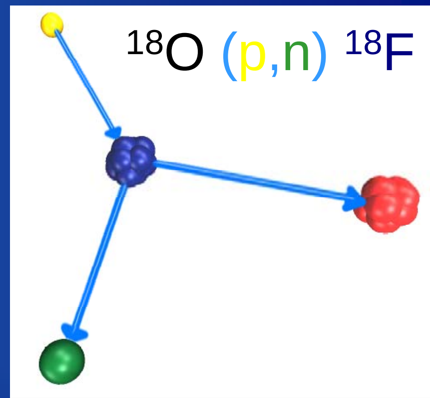

PET Isotopes

^{15}O

^{13}N

^{11}C

^{18}F

^{64}Cu

^{82}Rb

^{124}I

PET Tracers

$[^{15}O]$-O_2 $[^{15}O]$-H_2O

$[^{15}O]$-H_2O $[^{15}O]$-CO

$[^{13}N]$-NH_3 $[^{18}F]$-FDOPA

$[^{13}N]$-glutamate $[^{18}F^-]$

$[^{11}C]$-acetate $[^{18}F]$-FDG

$[^{11}C]$-palmitate

[11C]-methionine

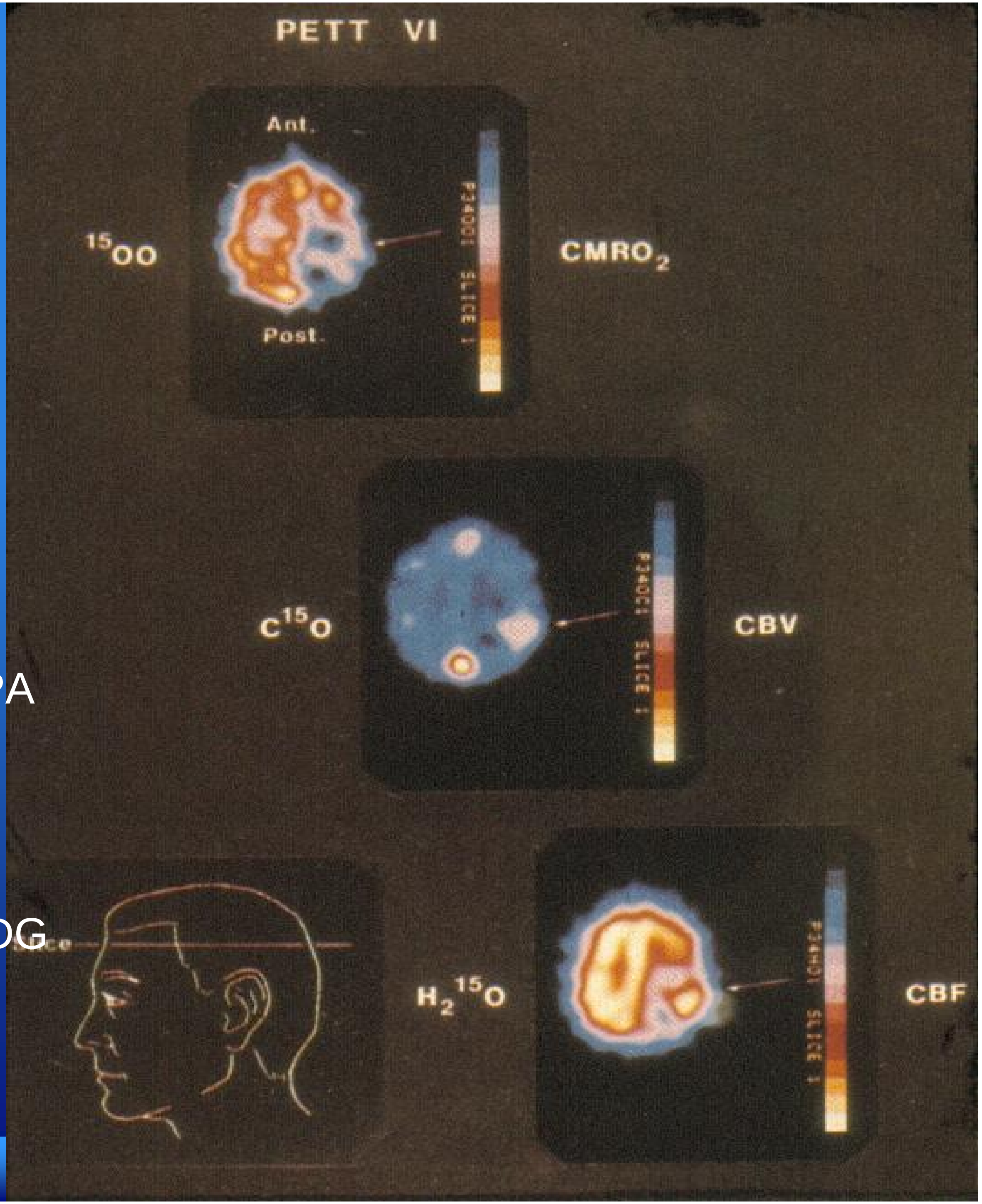

^{18}Fluoro-2-deoxy-D-glucose

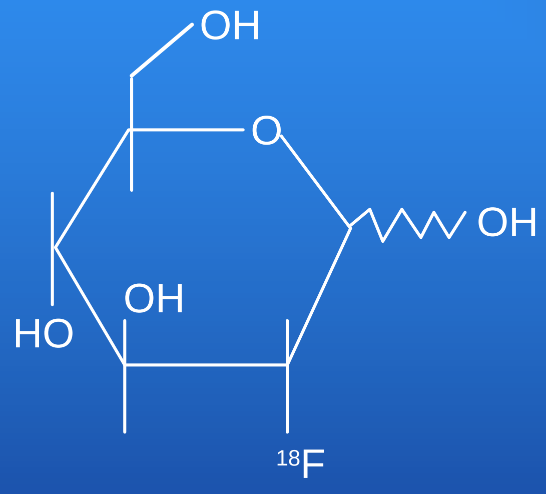

[^{18}F]–FDG

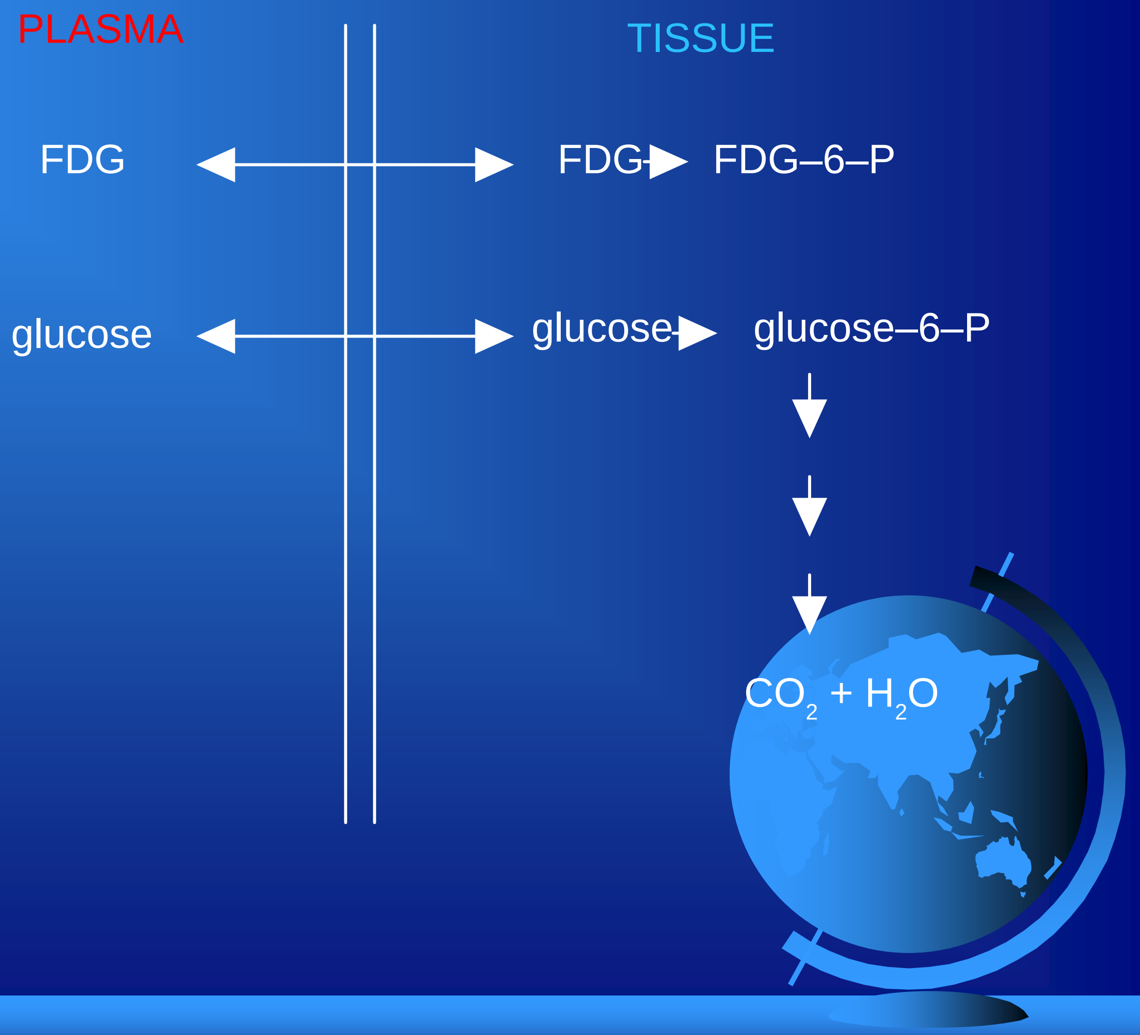

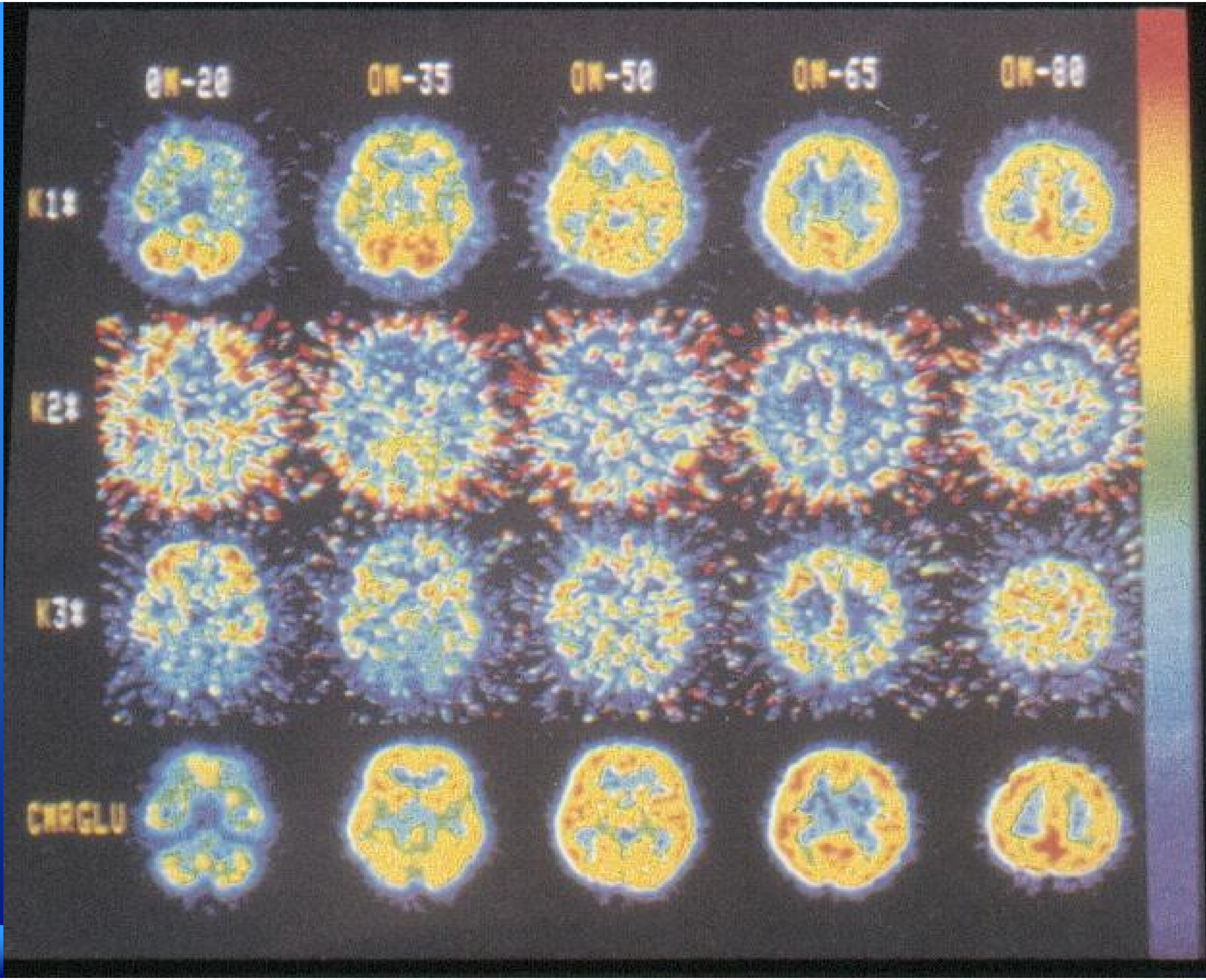

OM-20
OM-35
OM-50
OM-65
OM-80
K1*
K2*
K3*
CMRGLU

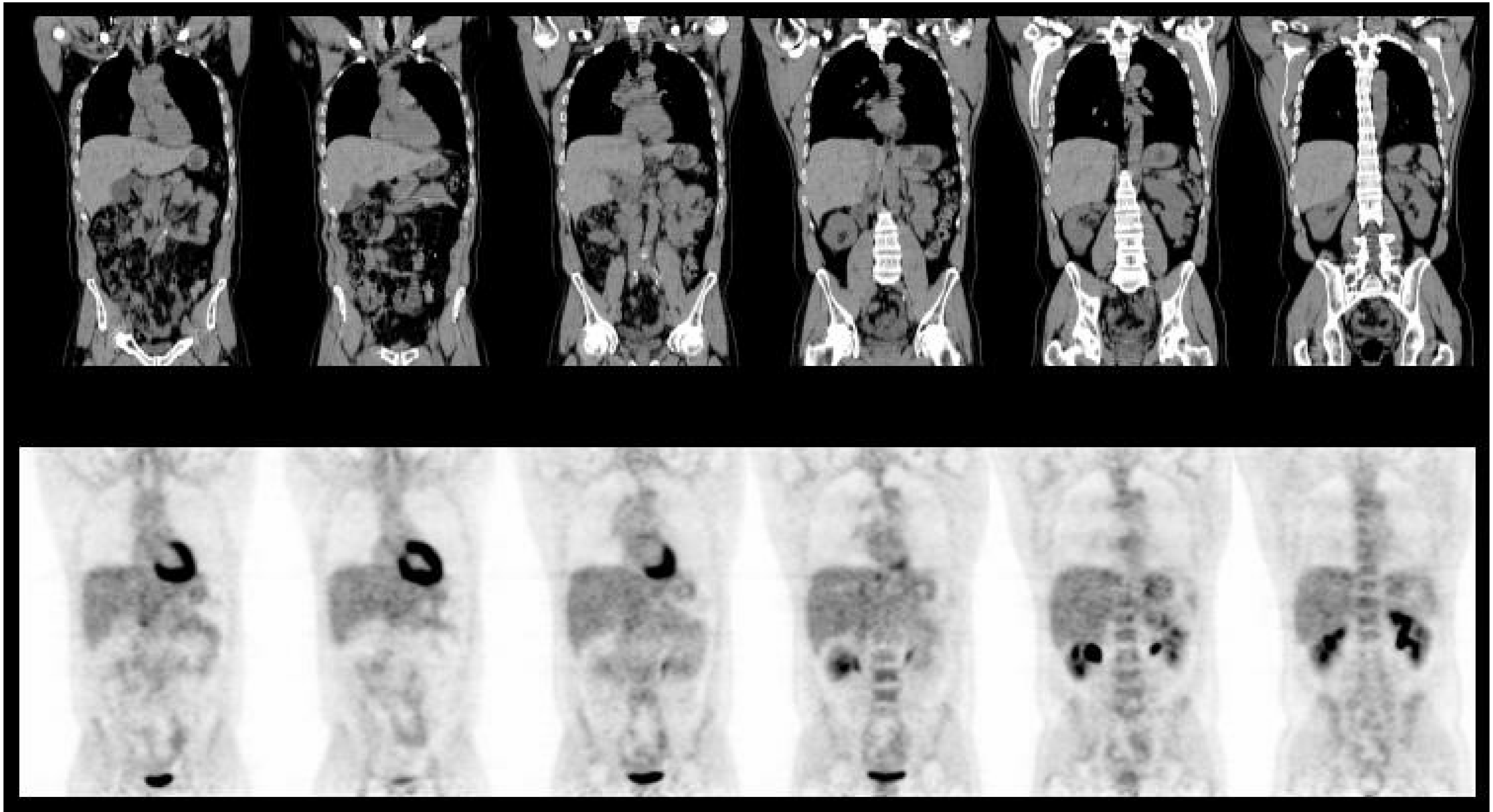

Human PET: 3-4mm; Target: 1-2mm
Animal PET: 1-2 mm; Target: <0.5mm

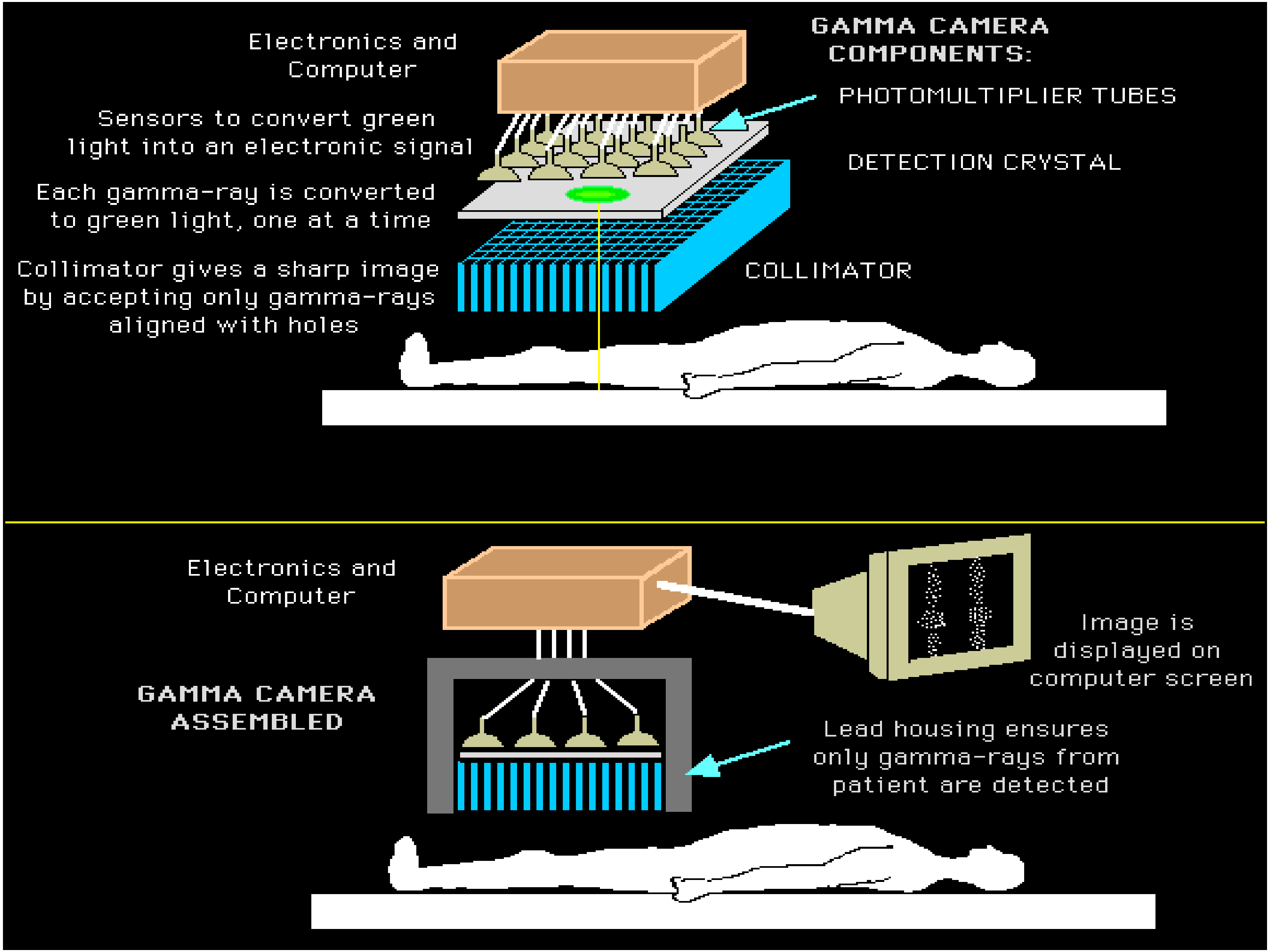
GAMMA CAMERA COMPONENTS:
Electronics and Computer
Sensors to convert green light into an electronic signal
PHOTOMULTIPLIER TUBES
DETECTION CRYSTAL
Each gamma-ray is converted to green light, one at a time
Collimator gives a sharp image by accepting only gamma-rays aligned with holes
COLLIMATOR
Electronics and Computer
GAMMA CAMERA ASSEMBLED
Image is displayed on computer screen
Lead housing ensures only gamma-rays from patient are detected

Cross section of a gamma camera

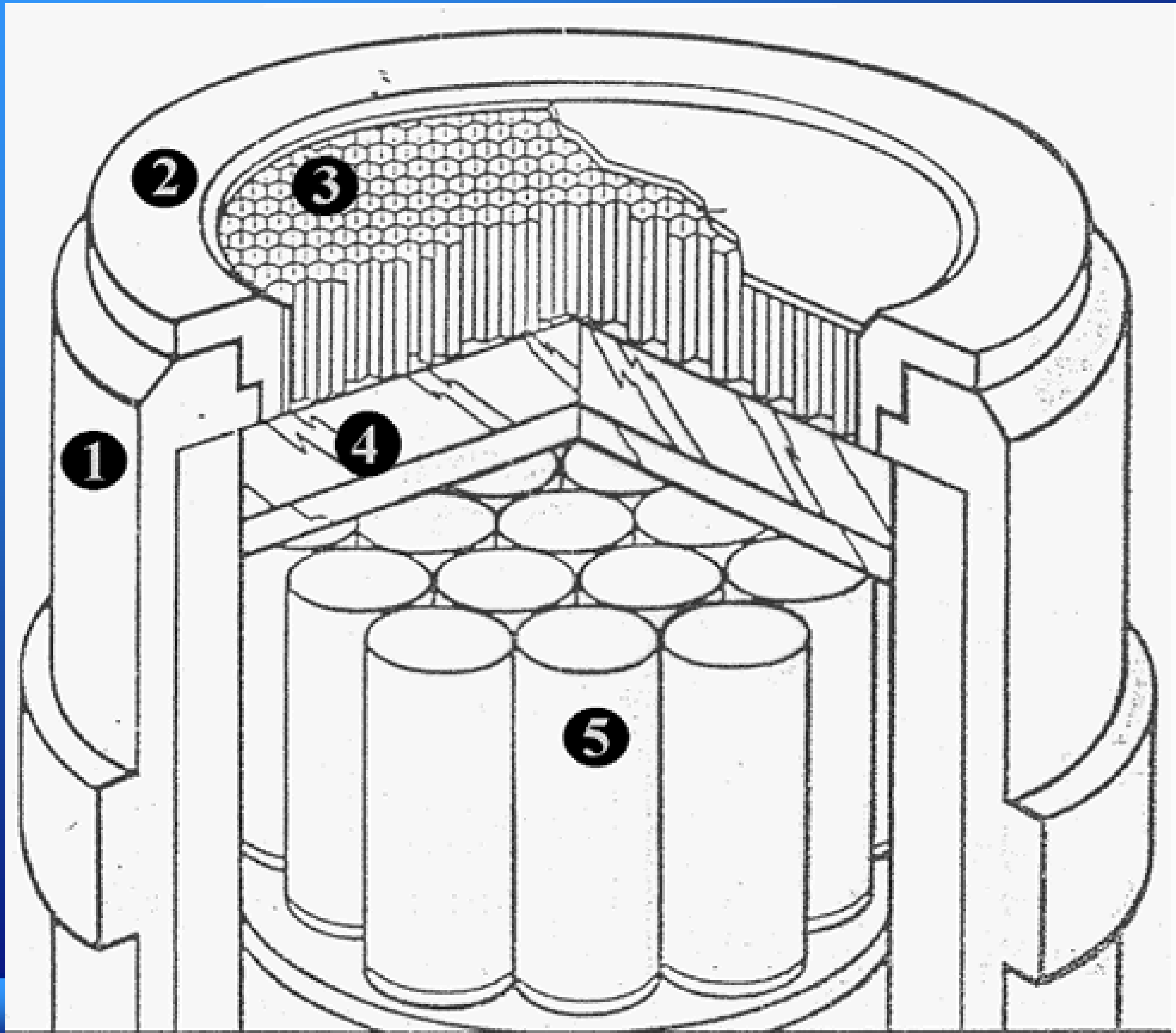

Single-Photon Radionuclides

Name	$T_{1/2}$	γ or x-ray (keV)	abundance
^{133}Xe	5.3 days	81	0.38
^{99m}Tc	6.0 hrs	140	0.89
^{111}In	2.8 days	171	0.90
		245	0.94
^{123}I	13 hrs	159	0.99
^{67}Ga	3.3 days	92	0.38
		184	0.23
		300	0.16

Single-Photon Radionuclides

Name	$T_{1/2}$	γ or x-ray (keV)	abundance
^{201}Tl	3.0 days	69	0.27
		71	0.46
		80	0.16
		83	0.04
		135	0.03
		167	0.10

0.93

Ga-67 Citrate Whole Body Study

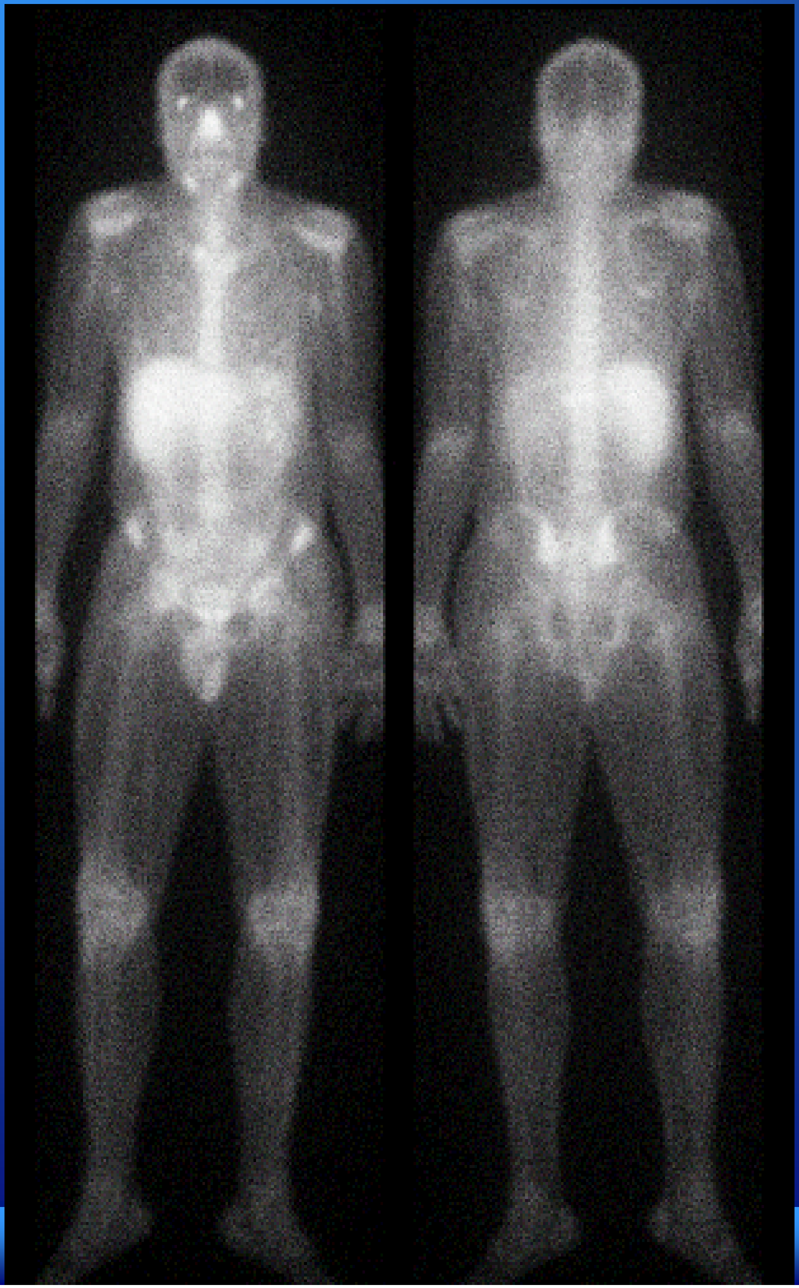

Triple-Head SPECT Scanner

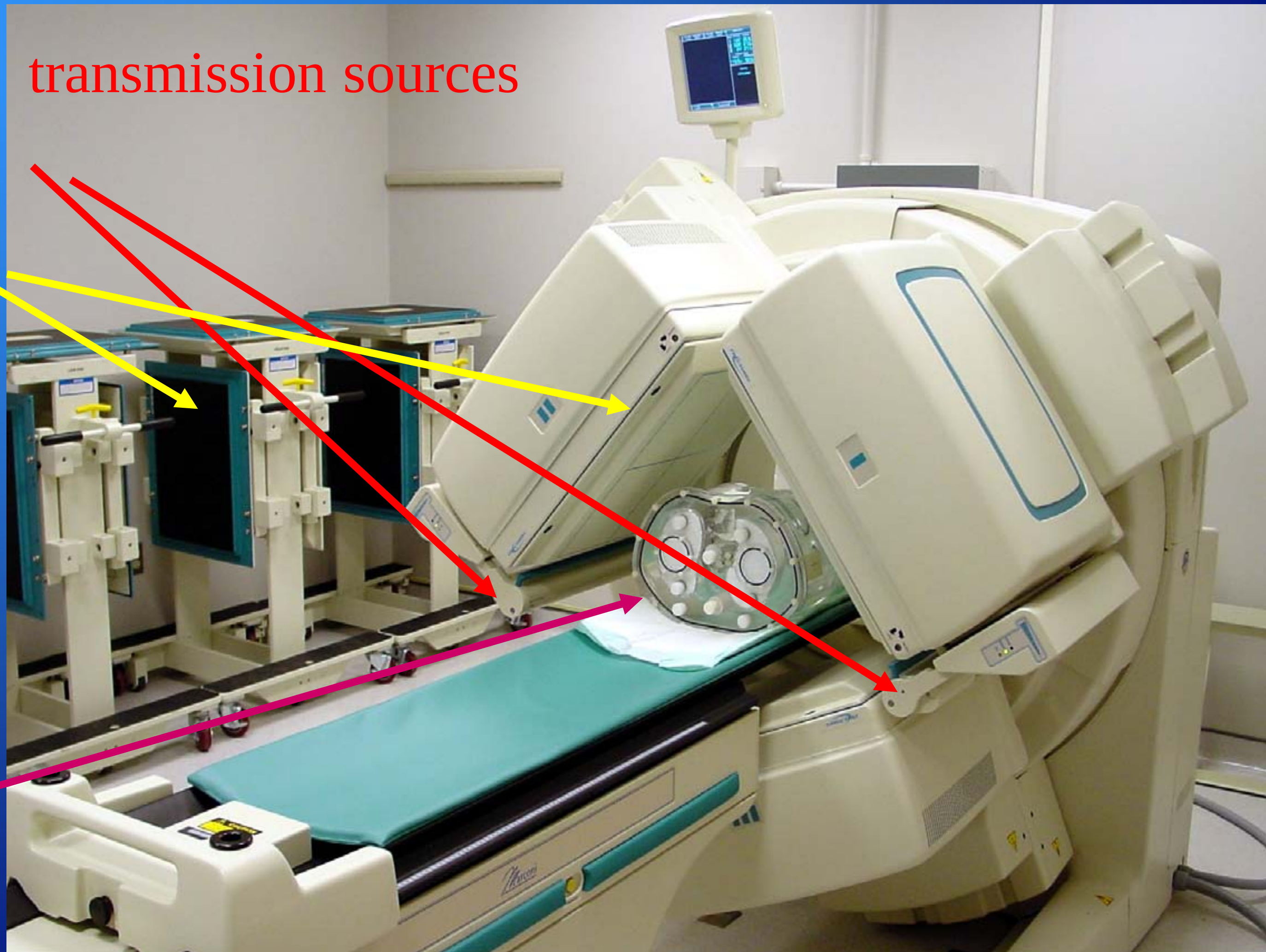

Technology Evolution

PET Scanner Family

REVEAL PET/CT
function + anatomy

ECAT EXACT HR^{+}
High performance

ECAT ACCEL
High throughput

ECAT EXACT
Clinical versatility

ECAT ART
Clinical efficiency

^{18}FDG Brain Tumor

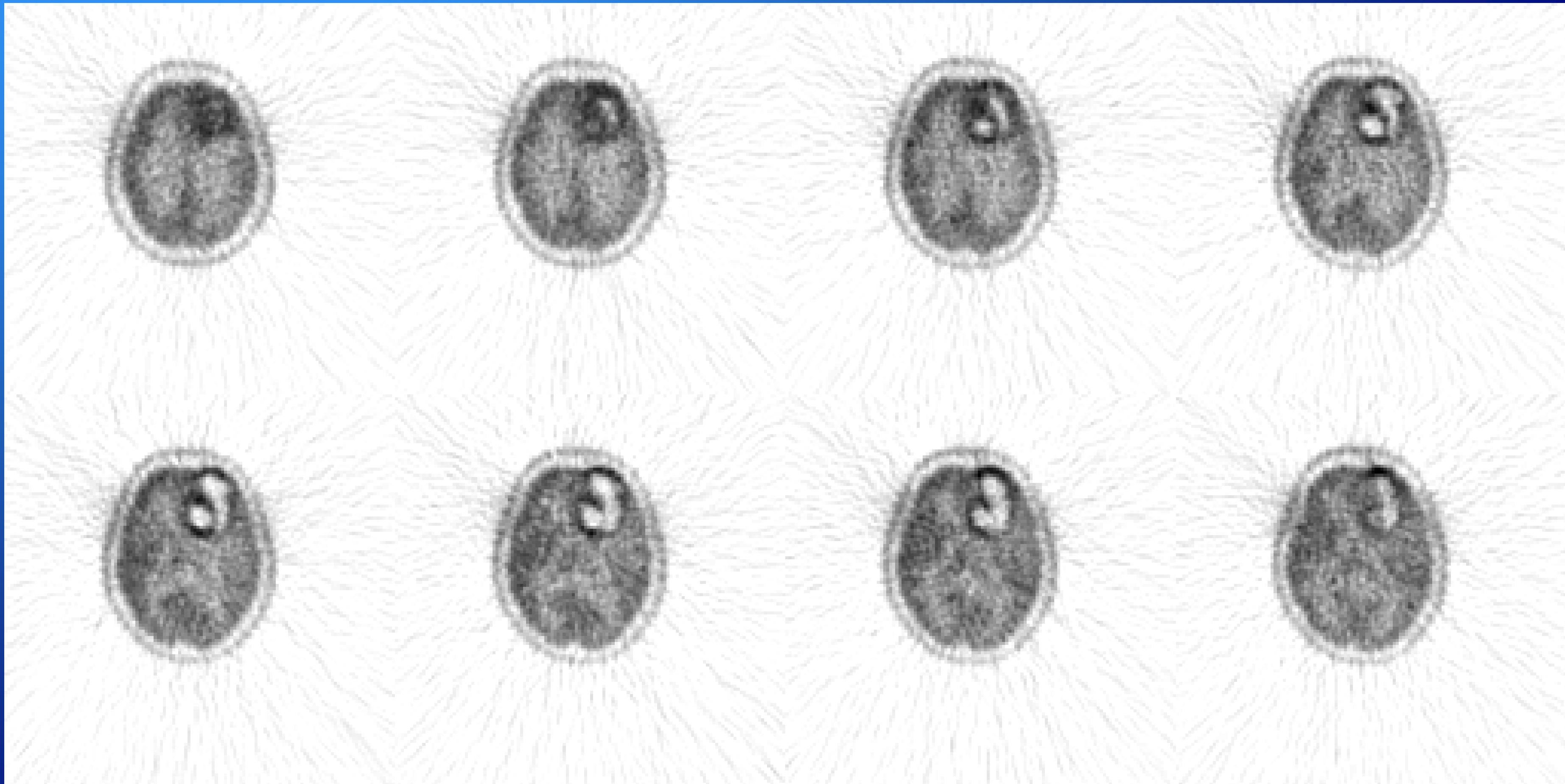

Alzheimer's Disease

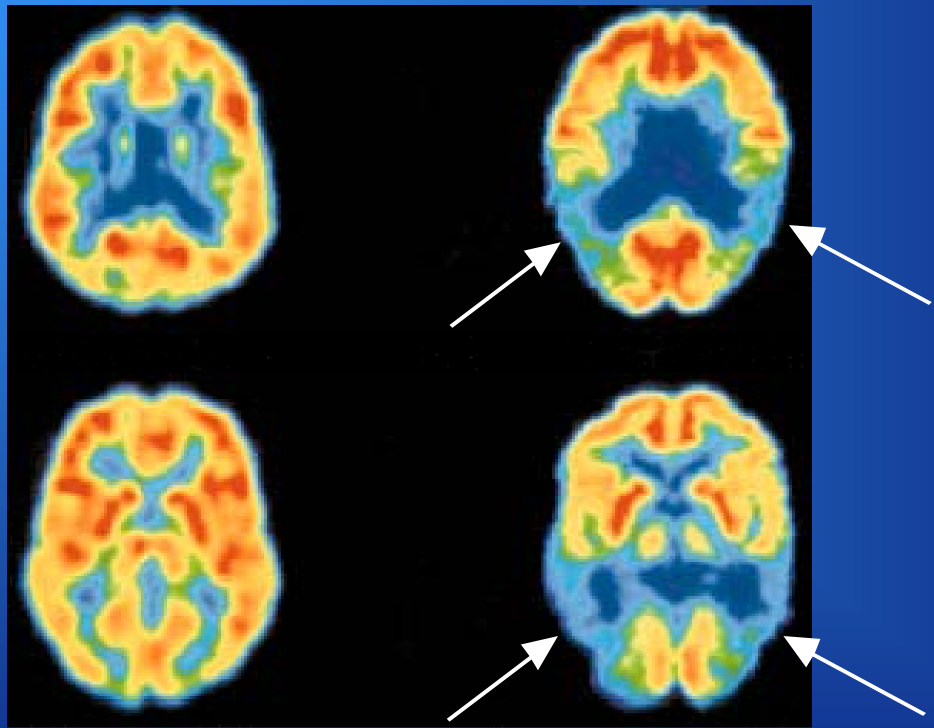

Normal

Alzheimer' s Disease

Cardiac Viability

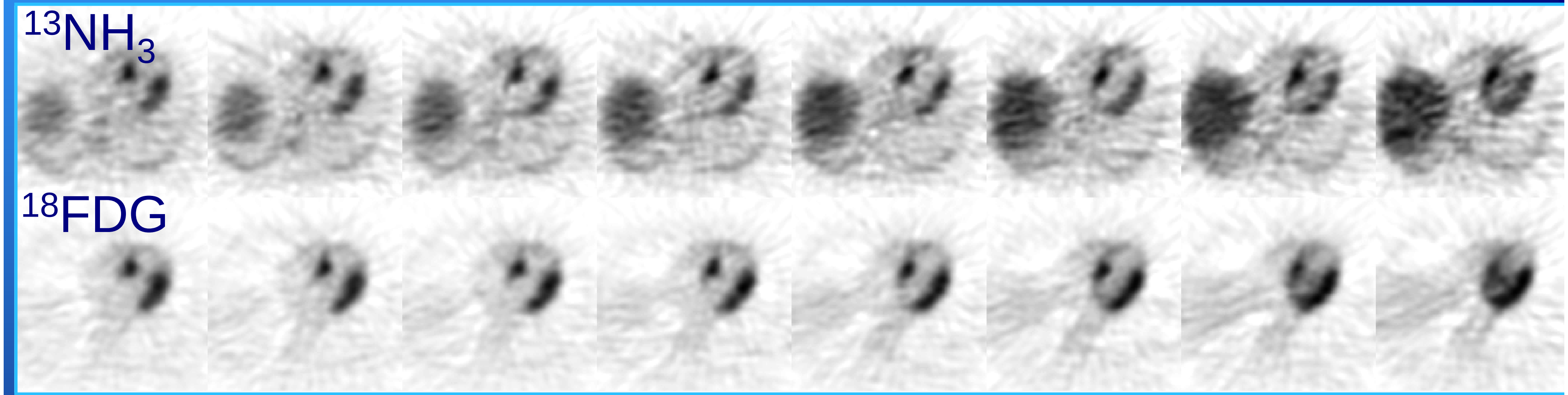

Lung Cancer

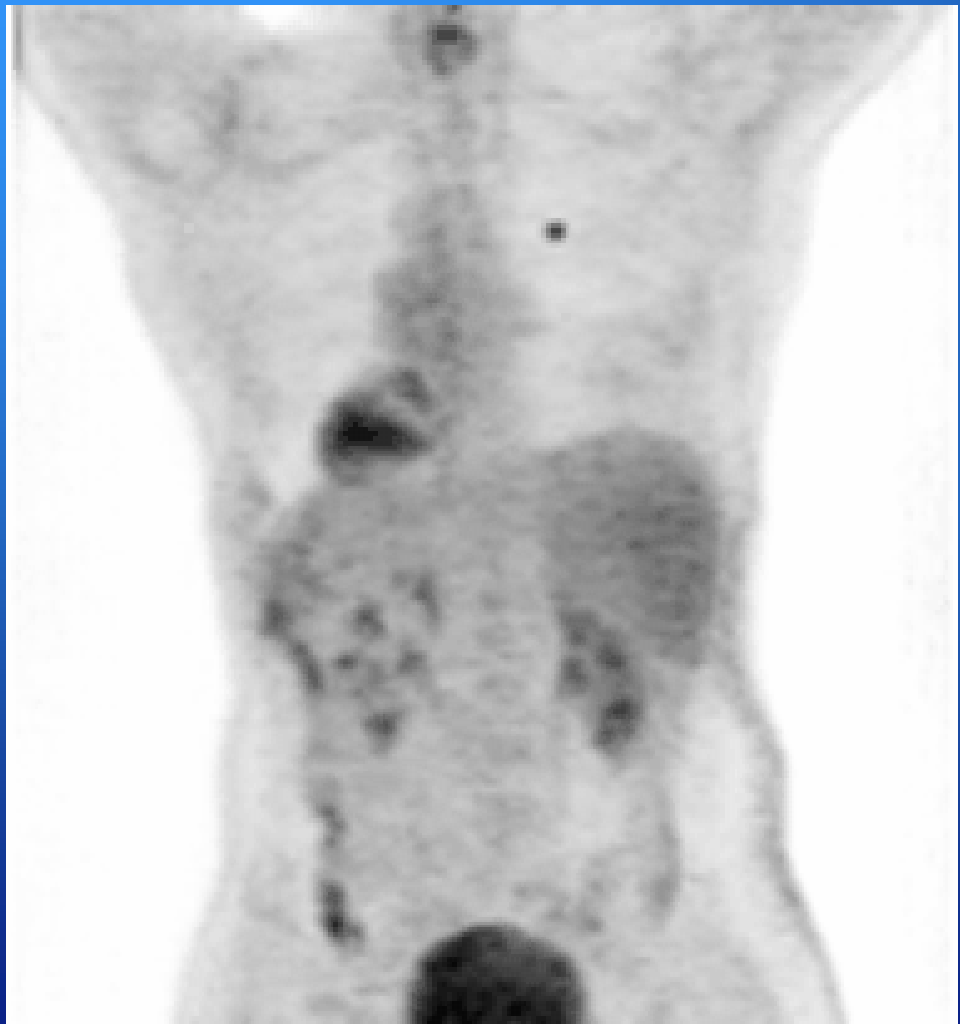

57-year-old male with lung cancer

ECAT EXACT, 15 mCi FDG,
5 min/bed emission,
2 min/bed segmented transmission, OS-EM iterative reconstruction

Data courtesy of Mallinckrodt Institute of Radiology/Barnes Hospital, St. Louis

Breast Cancer

40-year-old female with breast cancer had lumpectomy along with chemo/radiation therapy one year prior. The patient experienced pain in the right shoulder 10 months later.

Bone scan negative. CT scan initially read as negative.

Whole-body, FDG PET scan found numerous lymph node metastases in the upper chest.

Treatment plan based on conventional diagnostic techniques would have been watchful waiting. PET scan found a number of lymph node metastases, and patient was put back on chemo/radiation therapy. Re-read of CT after PET still could not accurately gauge extent of disease.

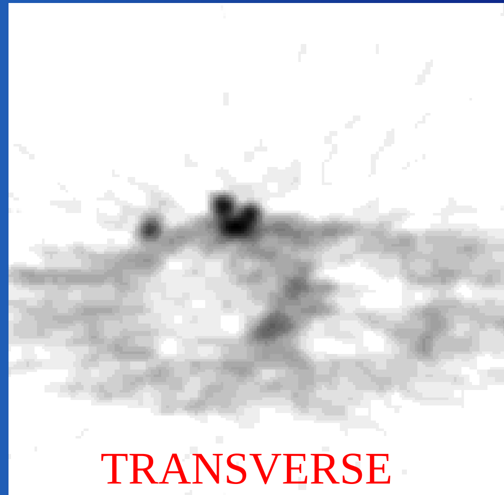

Courtesy of Amjad Ali, M.D. • Rush-Presbyterian-St. Luke's Medical Center

Colorectal Cancer

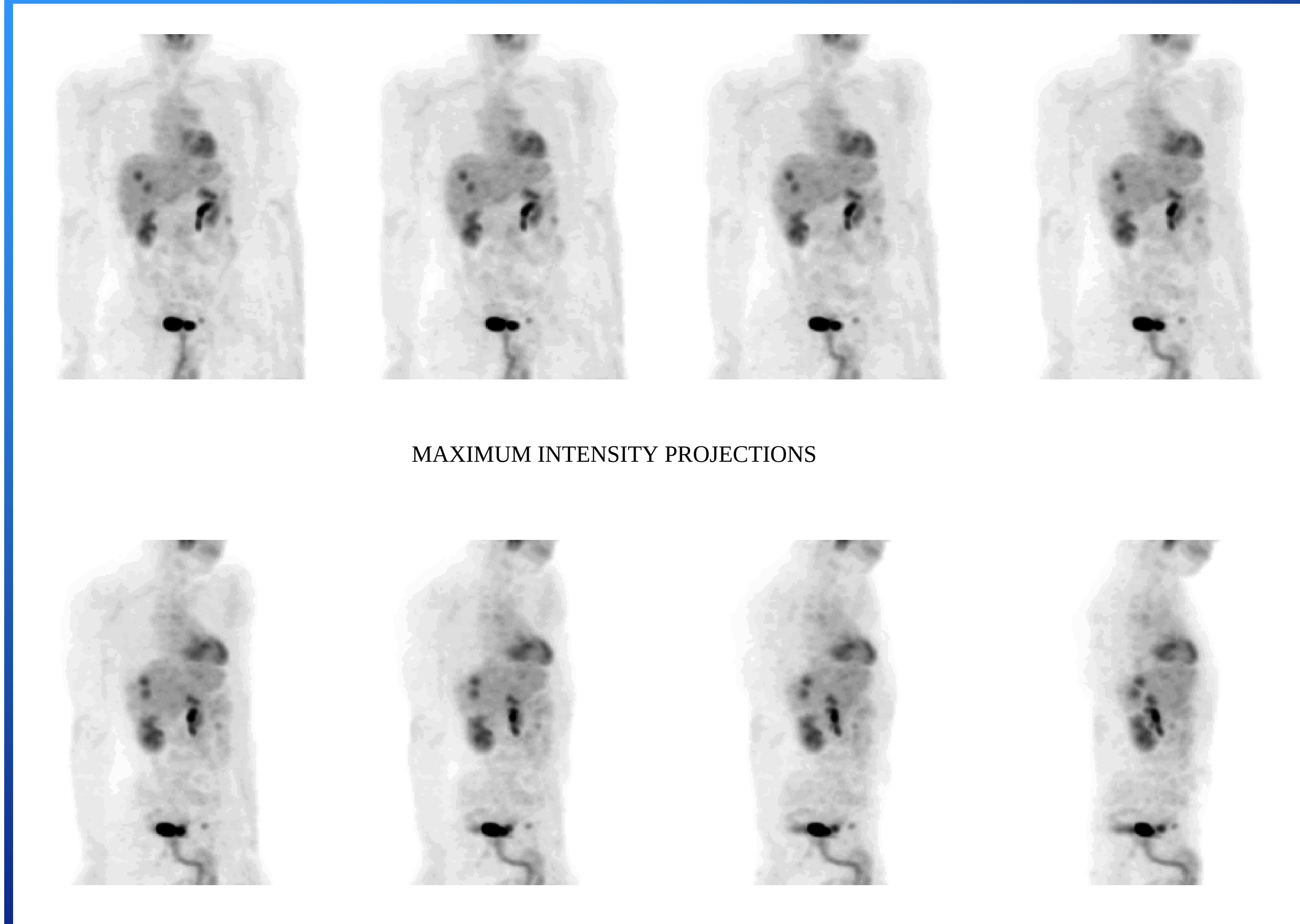

44-year-old male with colon ca. and liver metastases

ECAT EXACT, 10 mCi FDG, 8 min/bed emission, 5 min/bed segmented transmission, OS-EM iterative reconstruction

Data courtesy of Rush

Metastatic Melanoma

71-year-old male with metastatic melanoma on left shoulder discovered 12/94.

CT performed on 7/10/95 demonstrated tumor of the distal femur with negative findings in the abdomen. Bone scan on 7/13/95 showed an abnormal femur and four spine lesions.

Whole-body FDG PET scan demonstrates numerous lesions throughout the body.

Patient was scheduled for an amputation and total knee replacement based on CT and bone scan results. After PET found multiple lesions, surgery was cancelled, avoiding both the cost and the trauma of an operation that would not be effective.

Courtesy of Amjad Ali, M.D. • Rush-Presbyterian-St. Luke's Medical Center

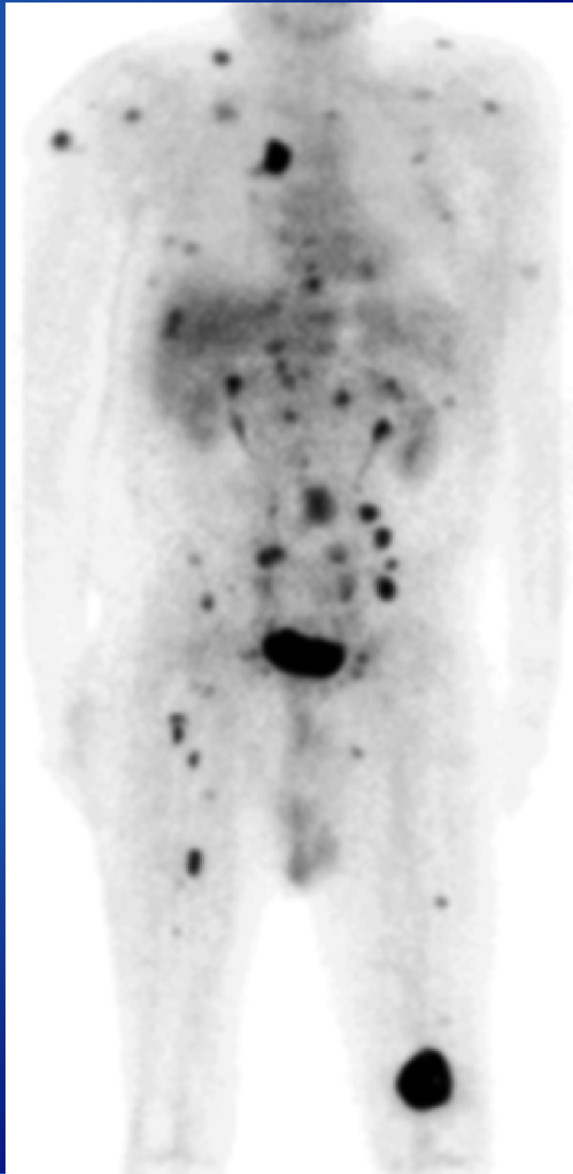

AP PROJECTION

Clinical Applications of PET
— In Cancer & Therapy Monitoring

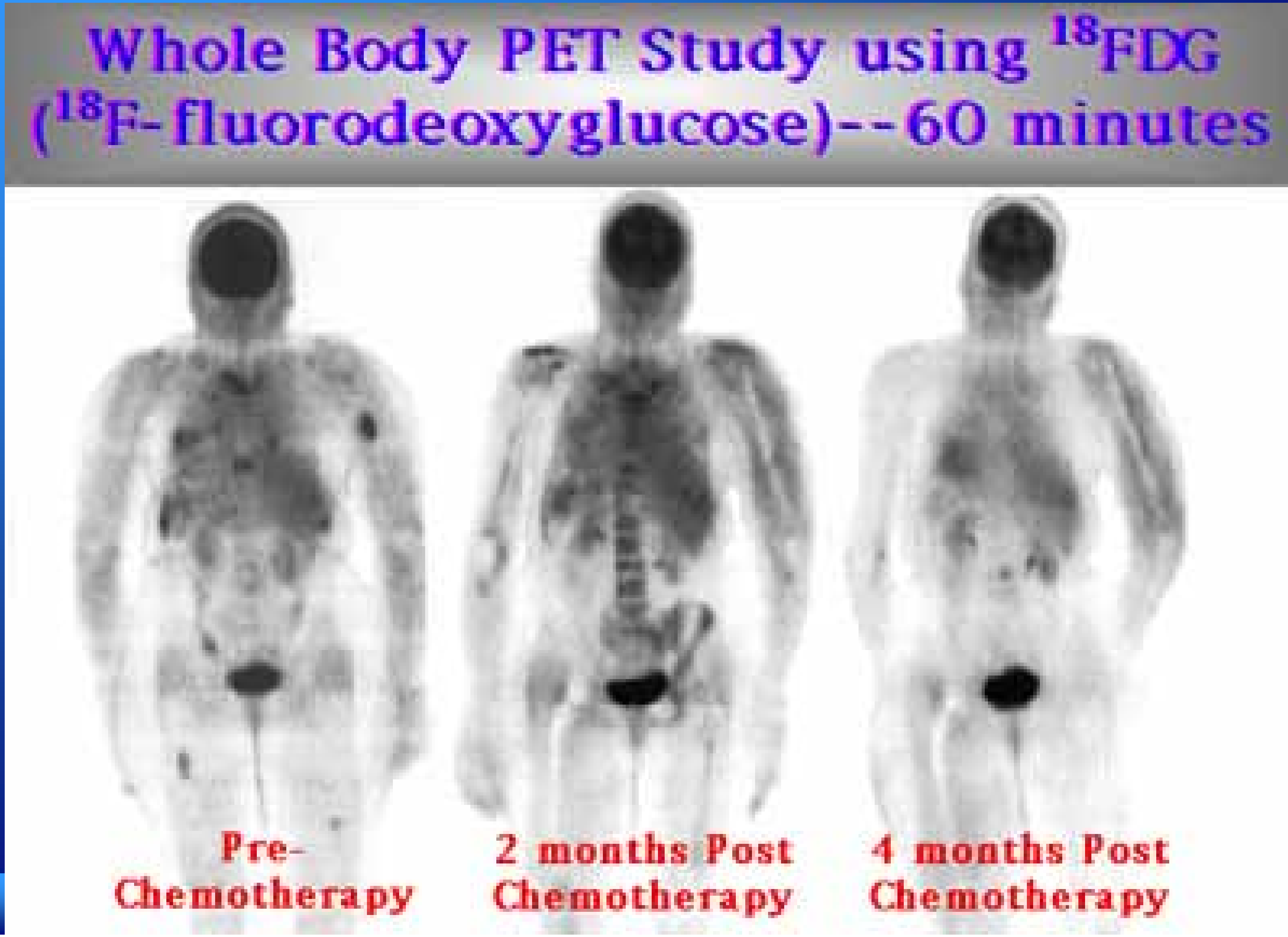

PET in Drug Development

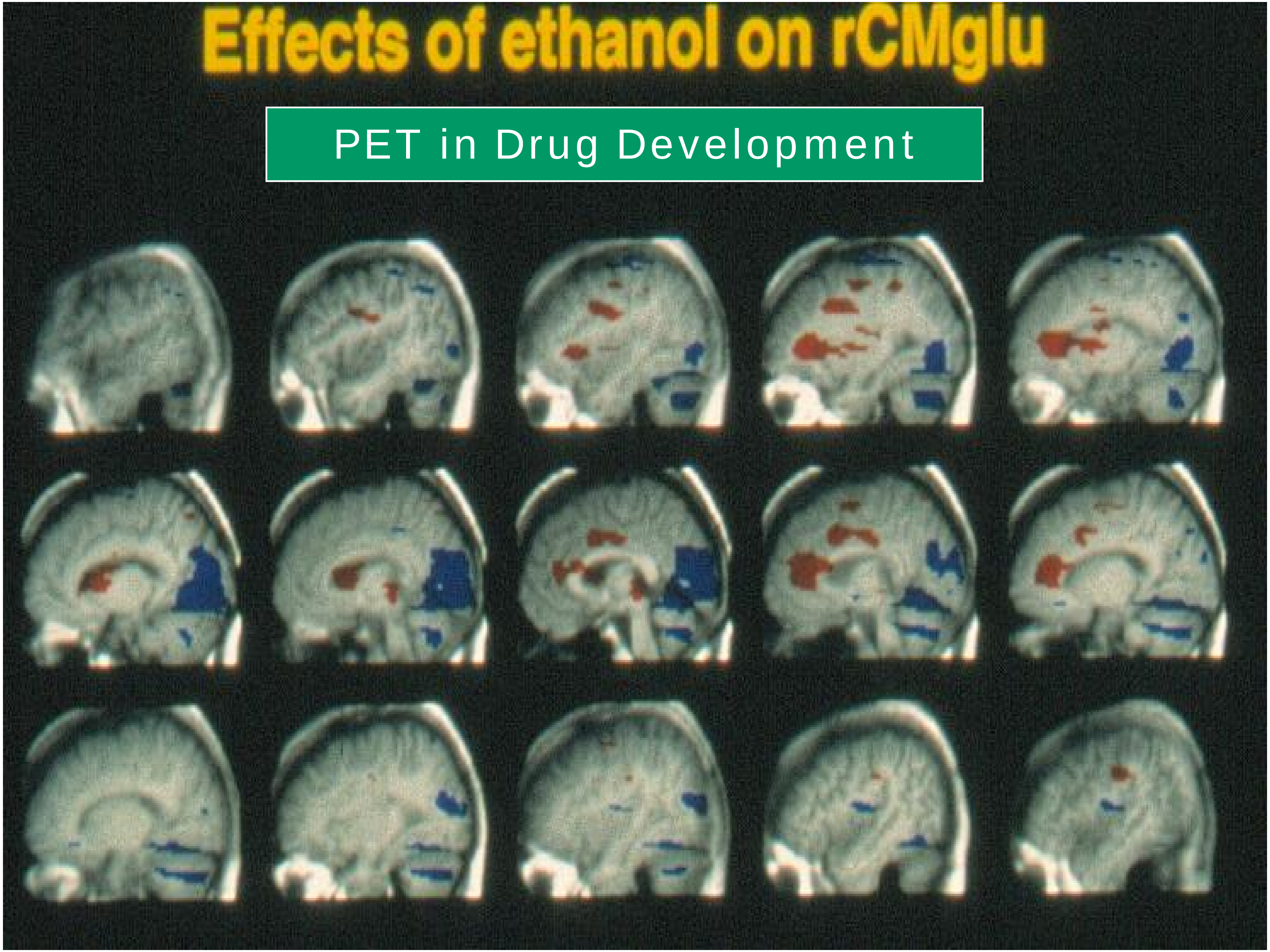

I-123 Thyriod Scan

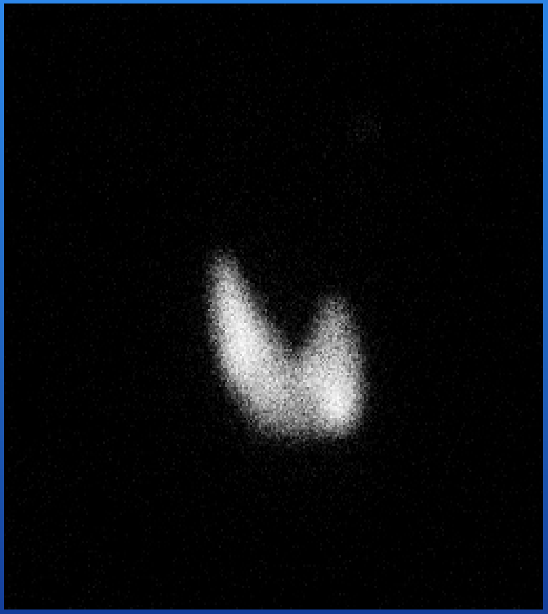

Rt-Ant-Obl

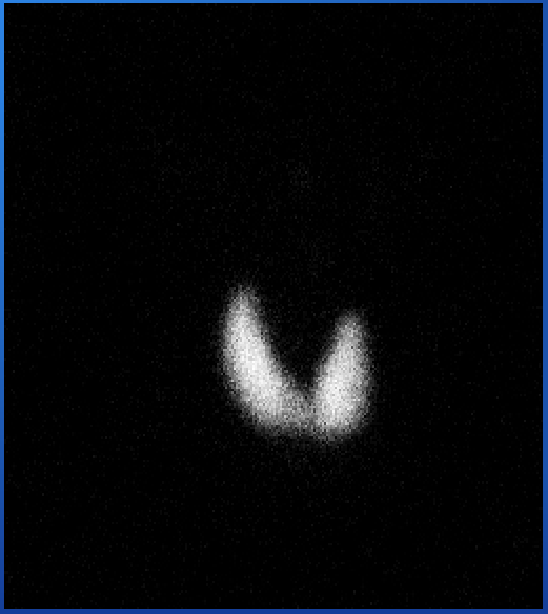

Anterior

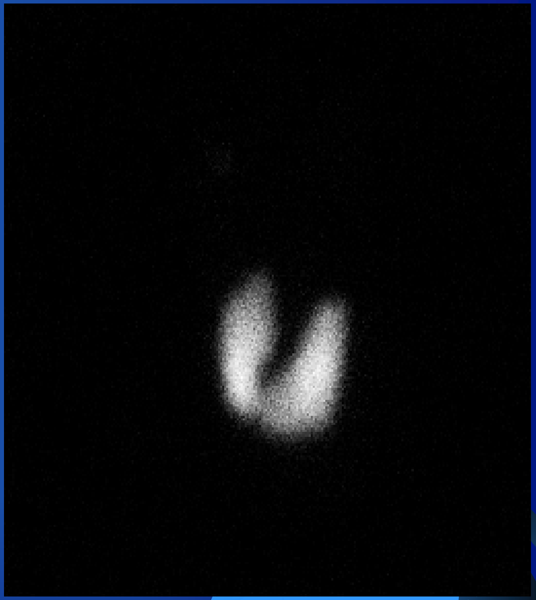

Lt-Ant-Obl

Lung ventilation/perfusion images

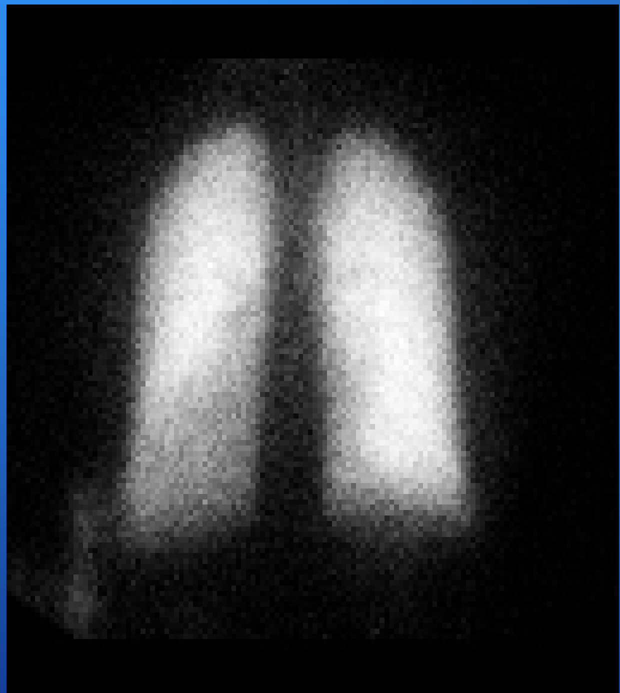

Xe-133 ventilation   Tc-99m MAA perfusion

HDP Whole Body Bone Study

Tc-99m sestamibi parathyroid scan

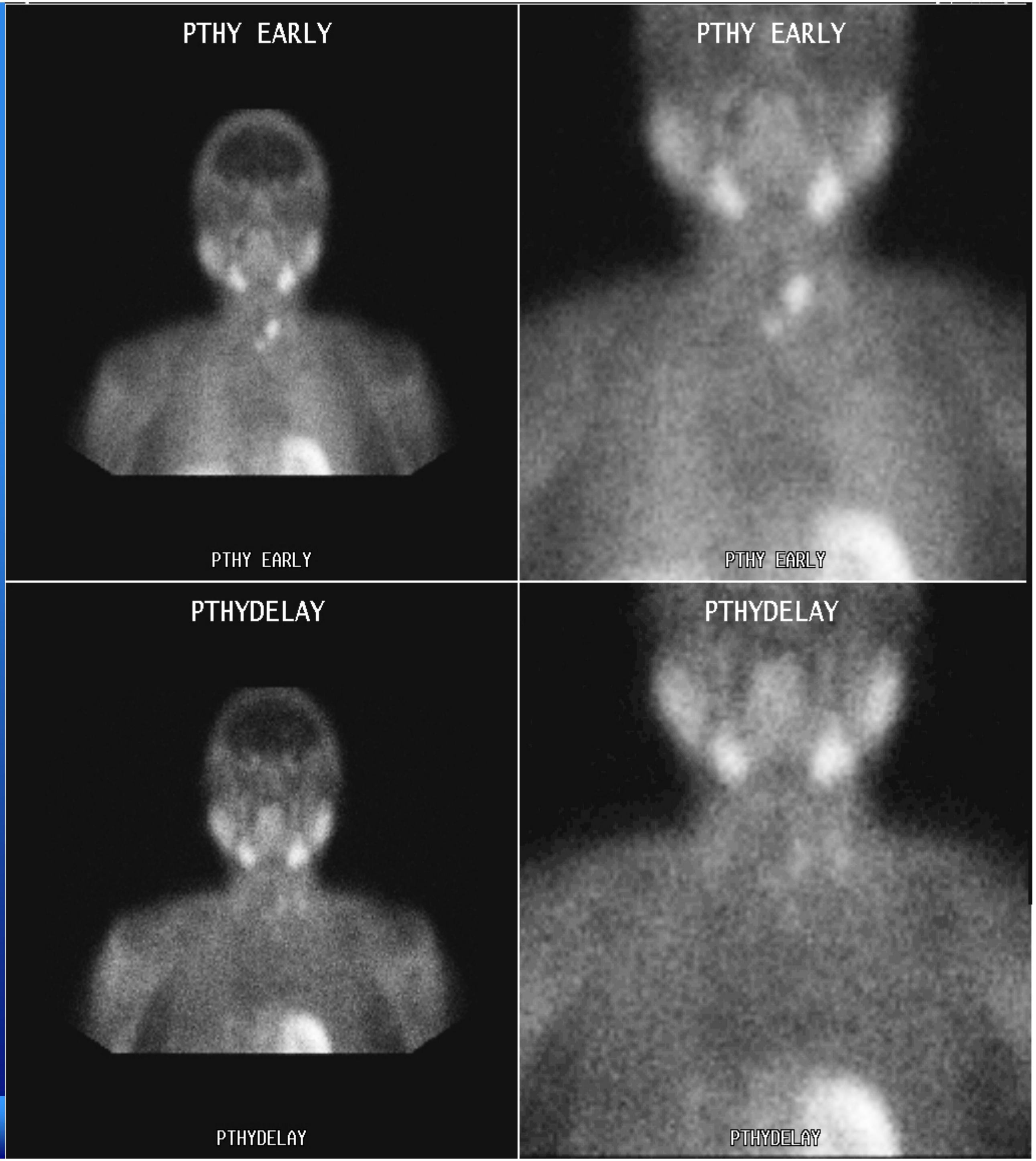

Tc-99m tetrofosmin SPECT myocardial images

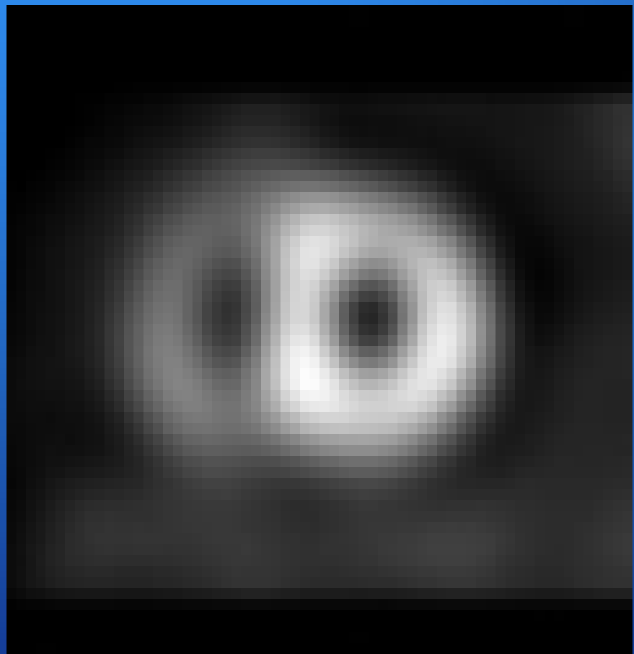

short axis

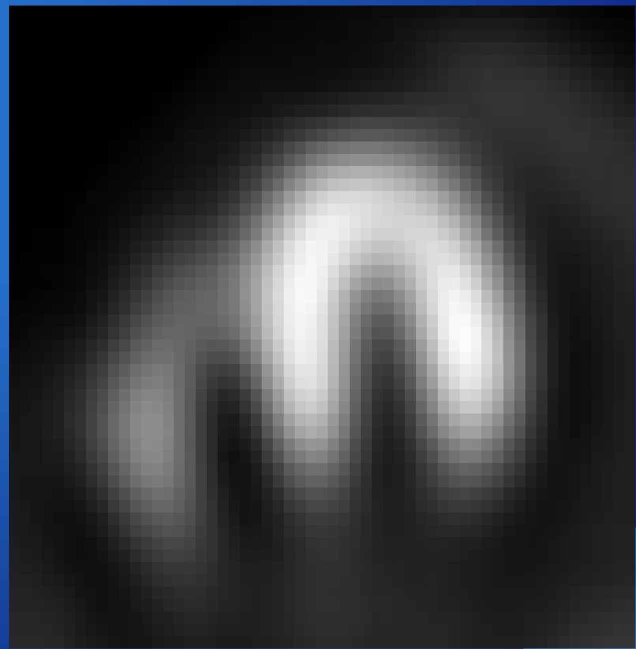

long axis

FBP

IR-AC

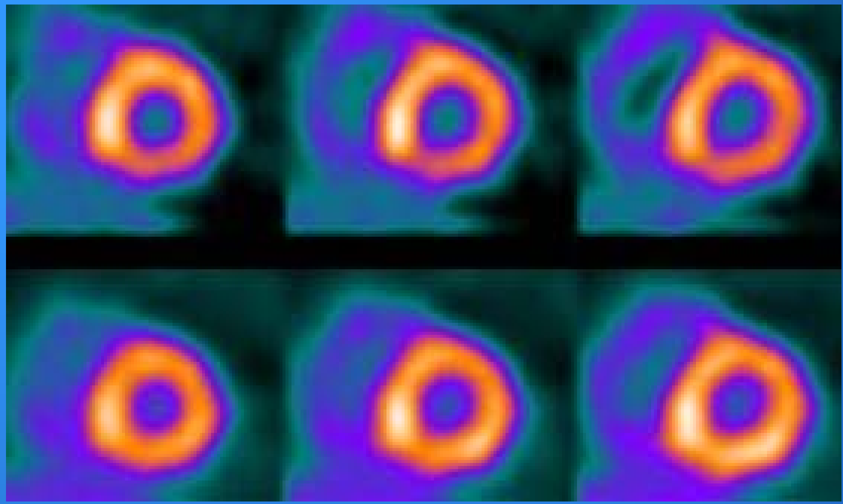

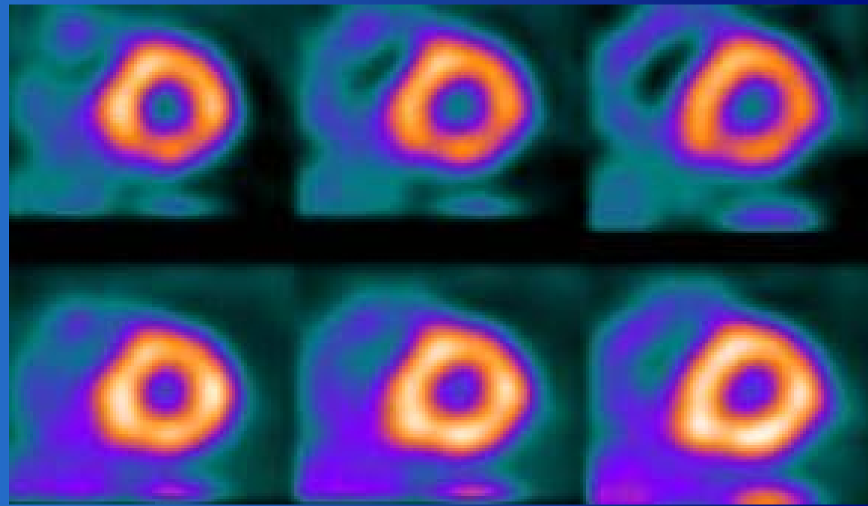

FBP

IR-AC

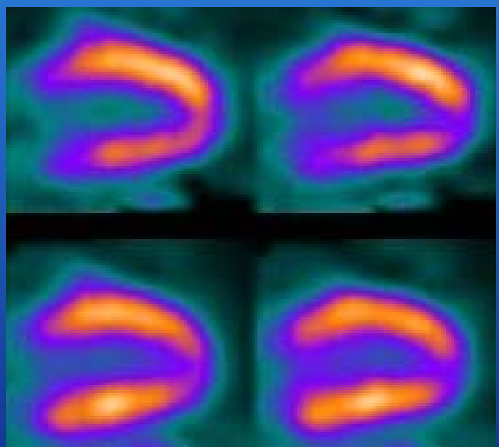

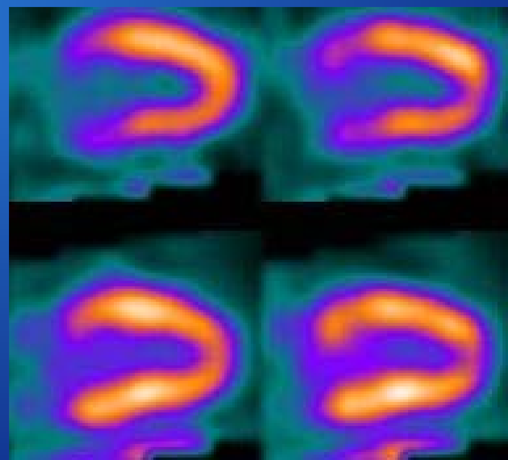

Stress

Rest

In-111 labeled Prostascint whole body scan

Tc-99m TRODAT

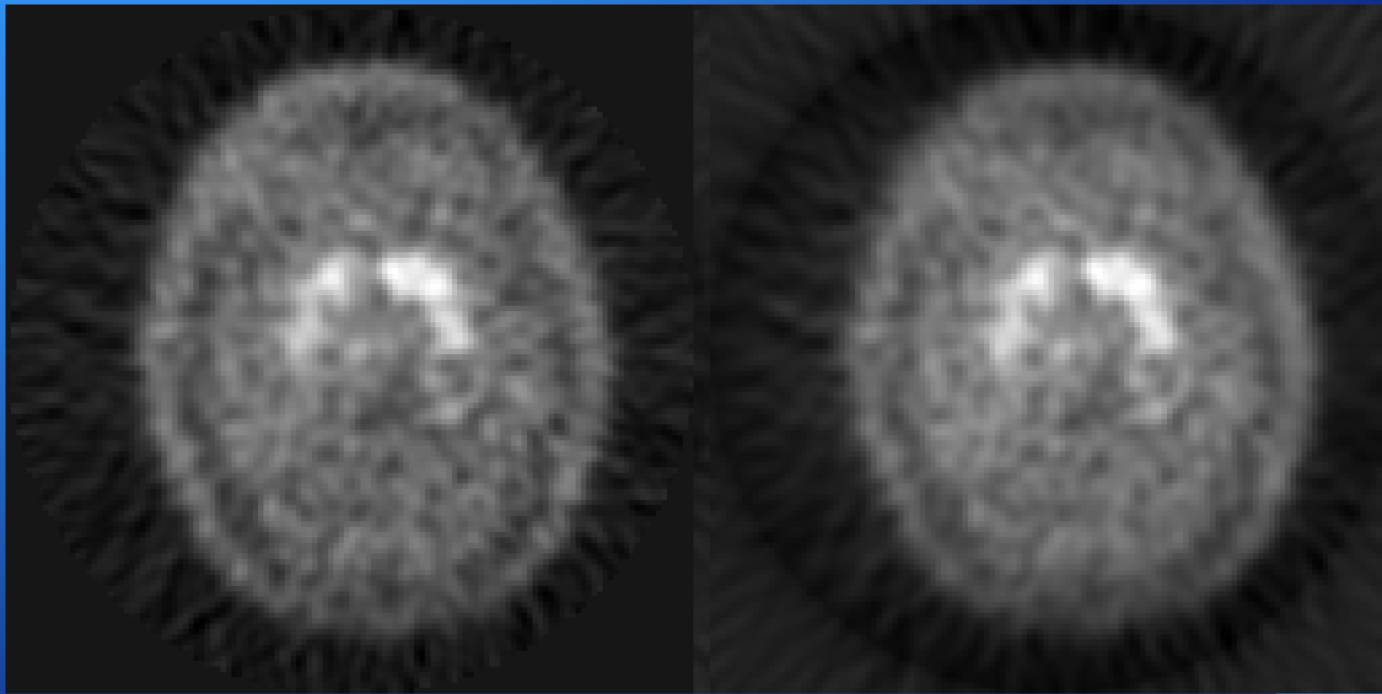

Biochemical Imaging with Small Animals

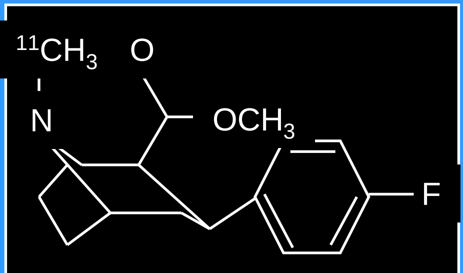

$[^{11}C]$WIN 35,428

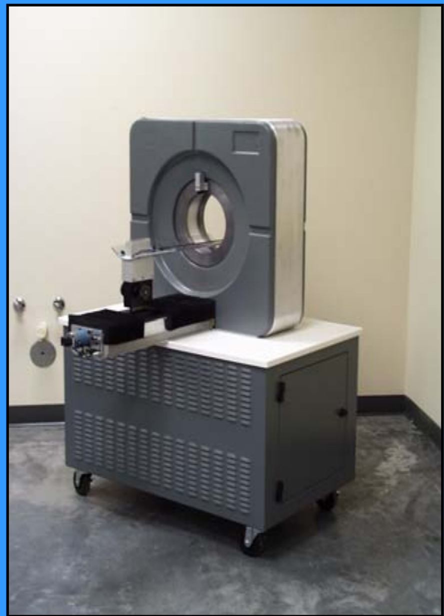

microPET

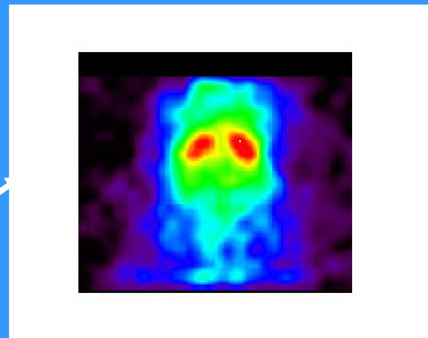

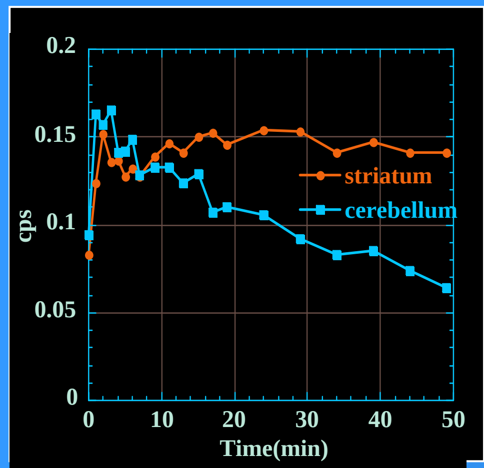

microPET Images

baby rhesus monkey brain phantom (25 cc) - 1.2 mCi ^{18}FDG 1hr. acquisition

microPET

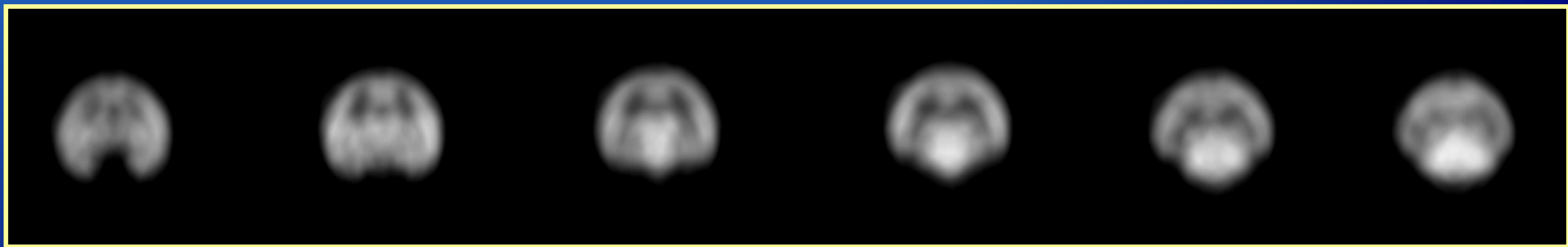

EXACT HR+

Animal Studies: ^{11}C-WIN 35,428

in collaboration with Bill Melega

	Vervet Monkey	Rat	Mouse
		x2	x2
Transverse	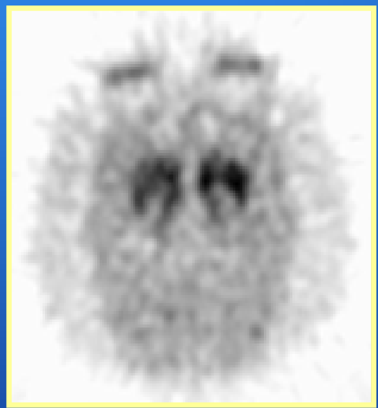	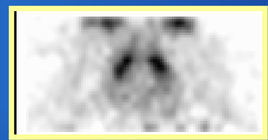	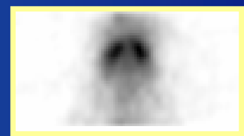
Coronal	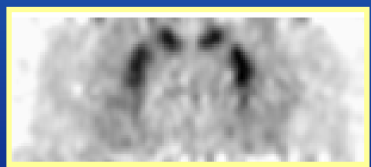	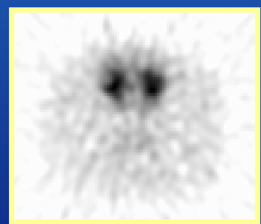	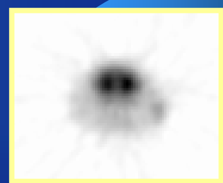

Vervet Monkey Brain - FDG

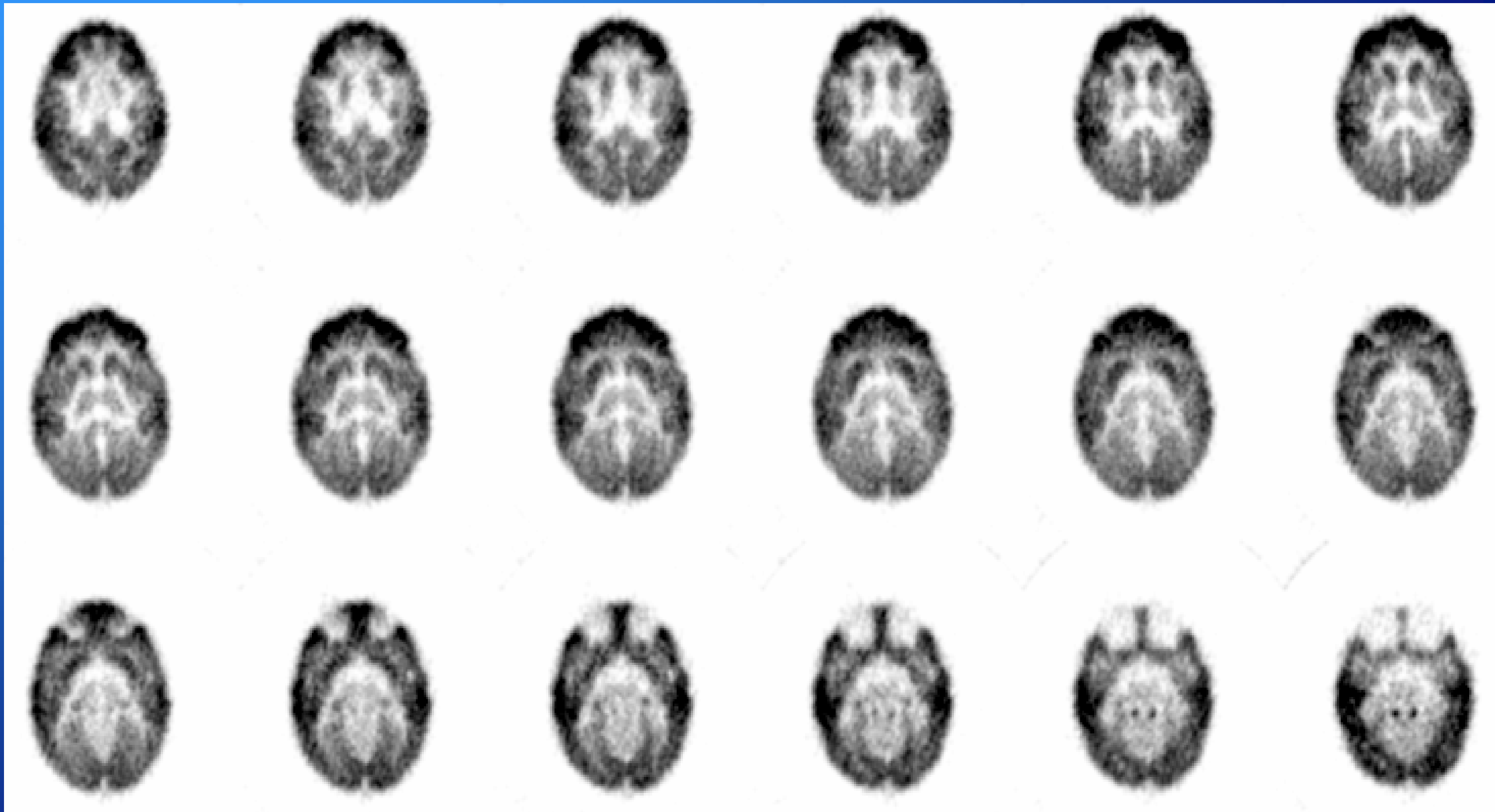

Injected dose: 1.8 mCi **Imaging time: 60 min.**

FDG Whole Body Rat Study

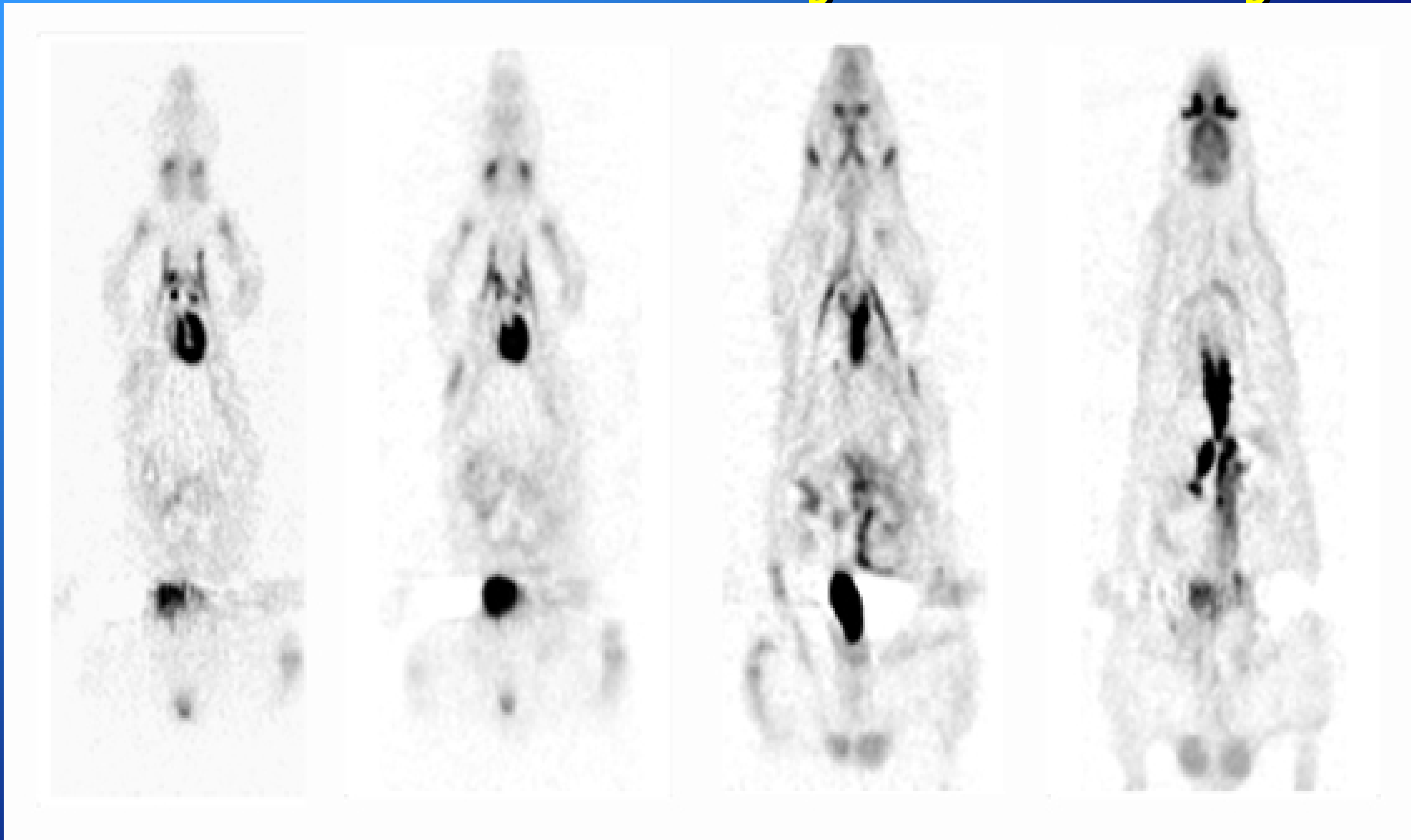

Injected dose: 2.5 mCi   Imaging time: ~2 hrs.

FDG Rat Heart

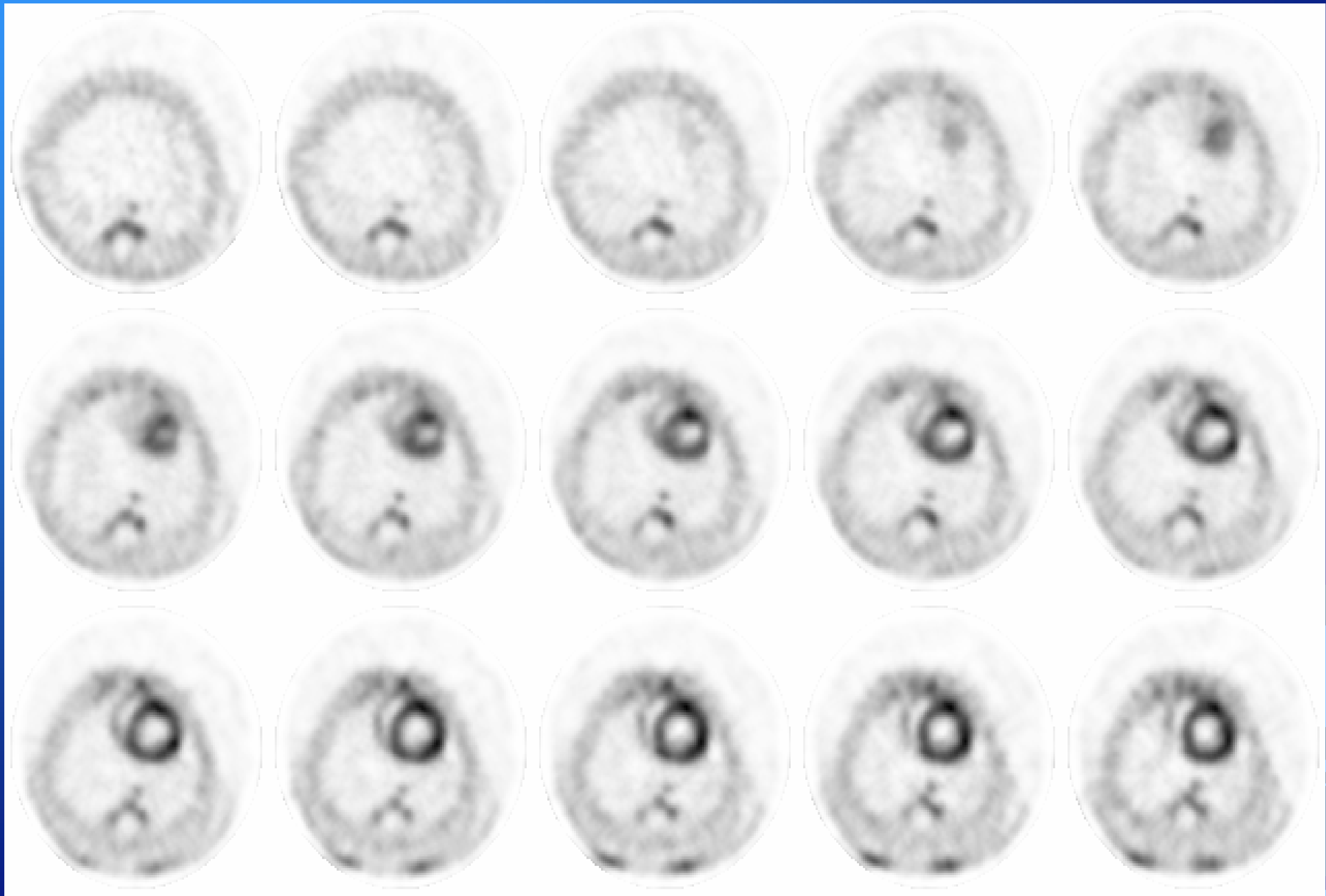

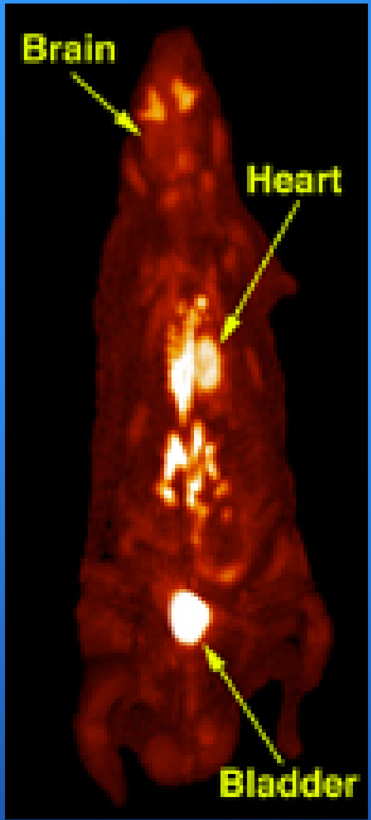

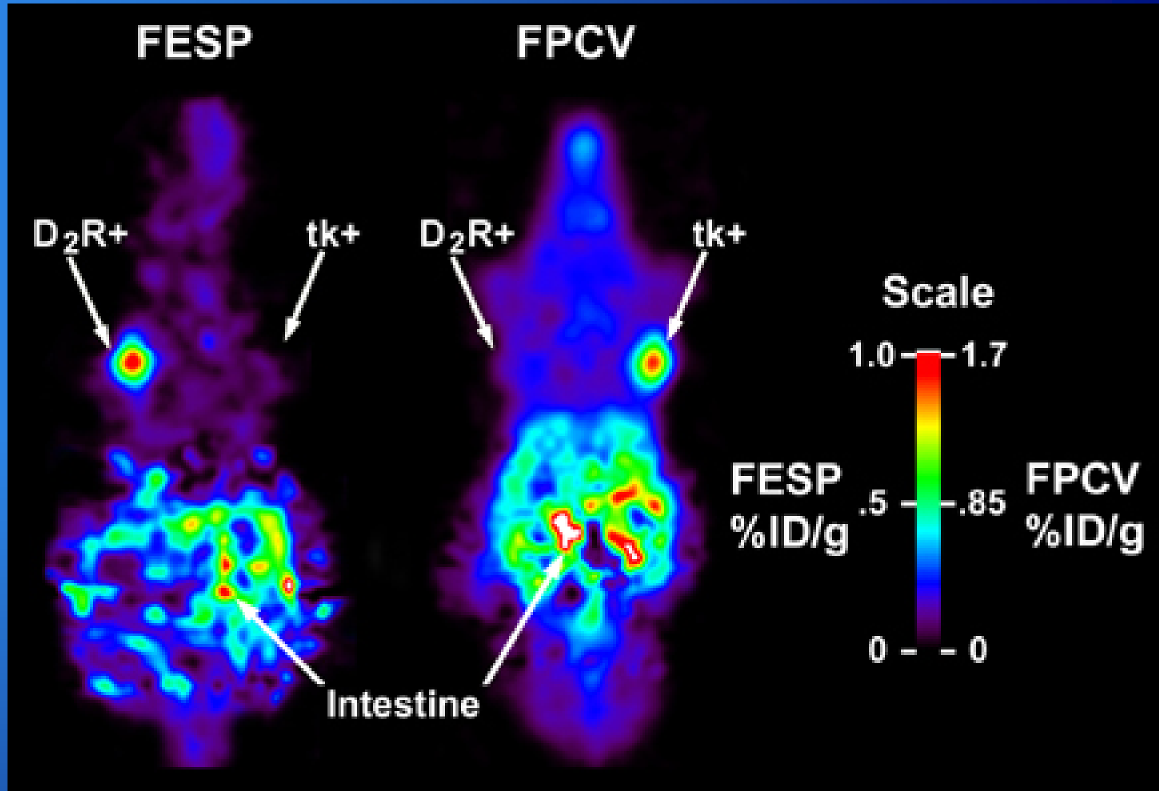

Mouse model with one tumor on each shoulder. The left tumor expresses the D2 receptor gene and uptakes FESP, while the tumor on the right, represses the tk gene and uptakes FPCV.

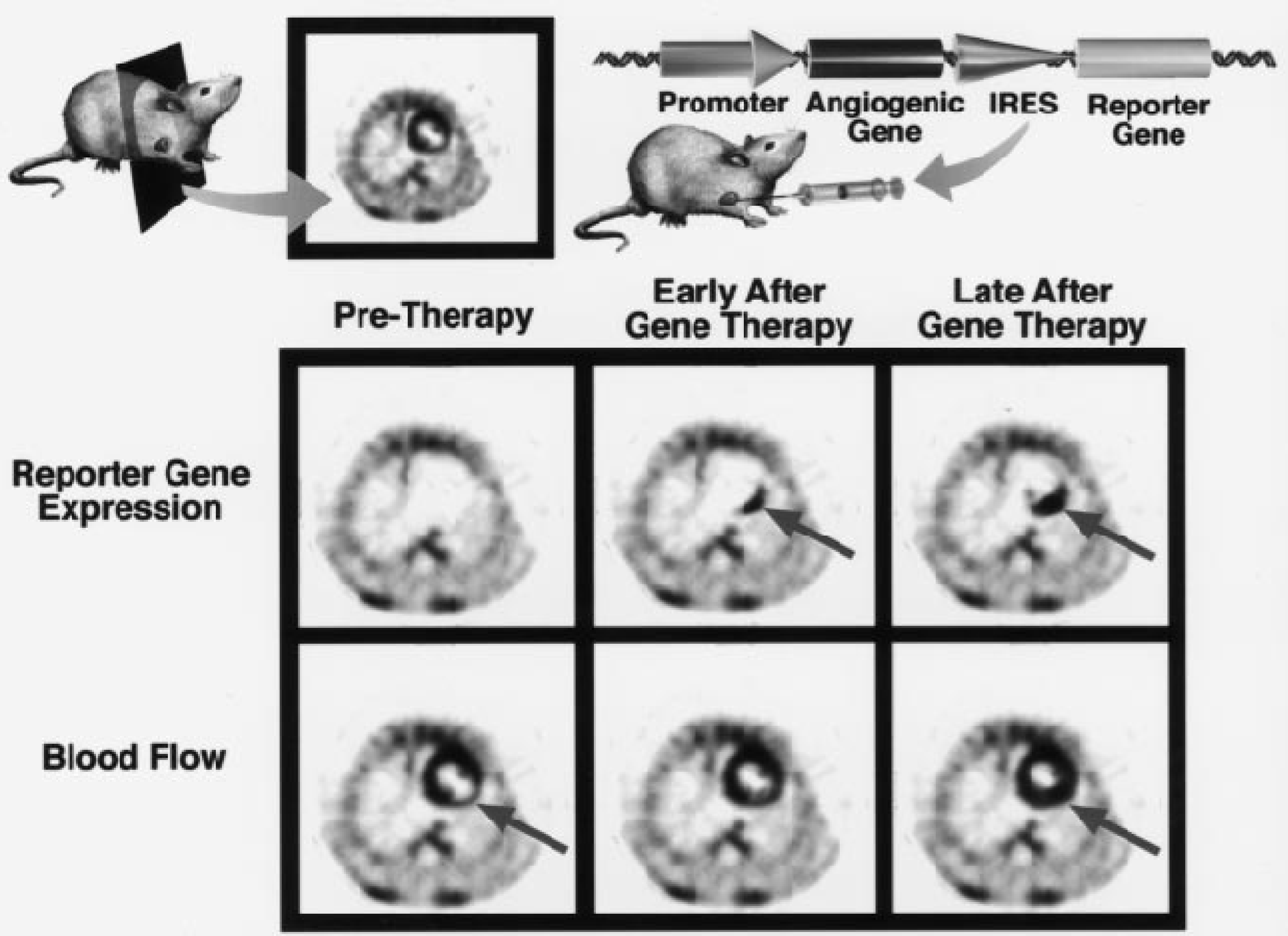

Promoter
Angiogenic Gene
IRES
Reporter Gene
Pre-Therapy
Early After Gene Therapy
Late After Gene Therapy
Reporter Gene Expression
Blood Flow

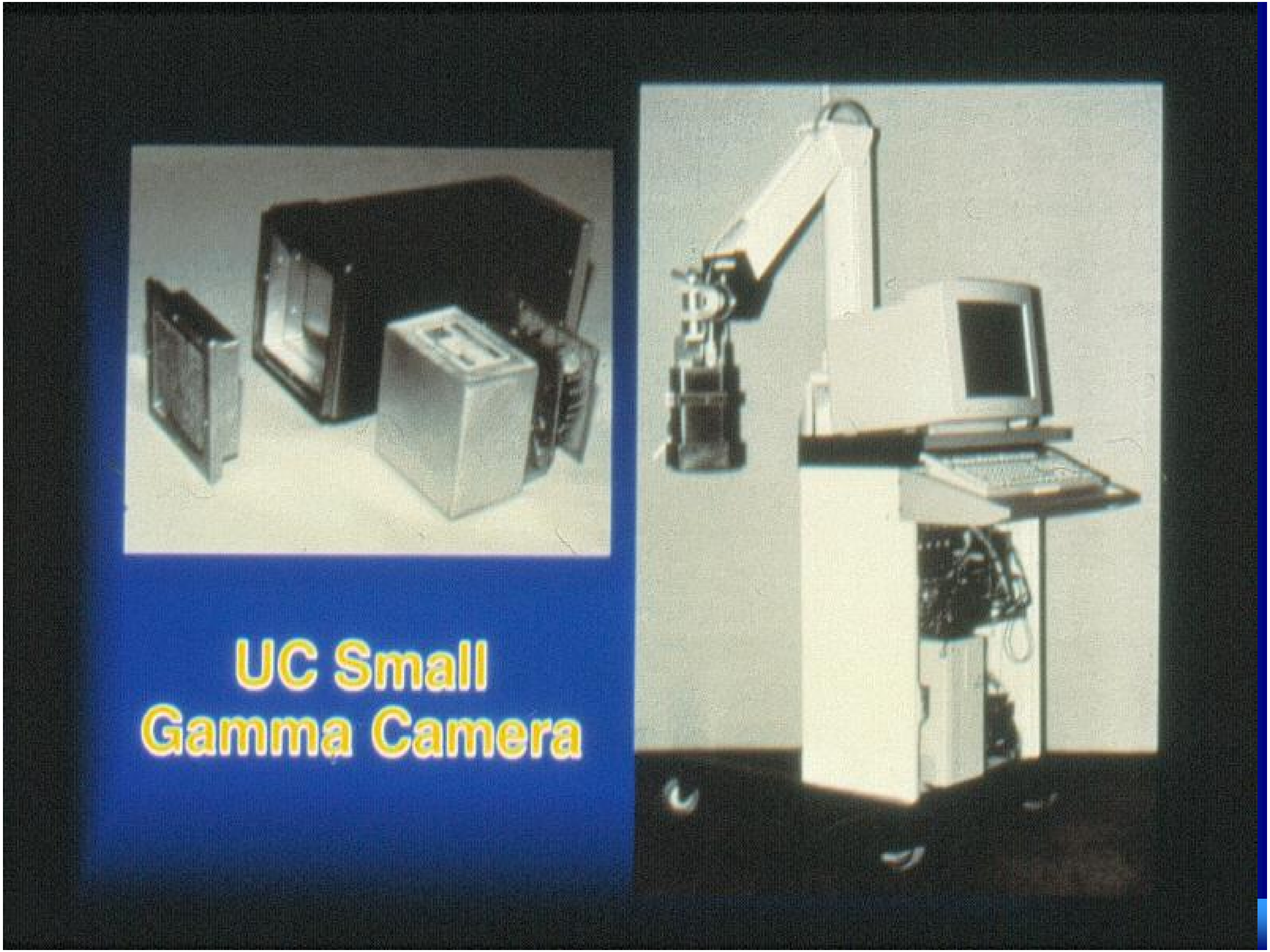
UC Small
Gamma Camera

Application-Specific Imaging Devices

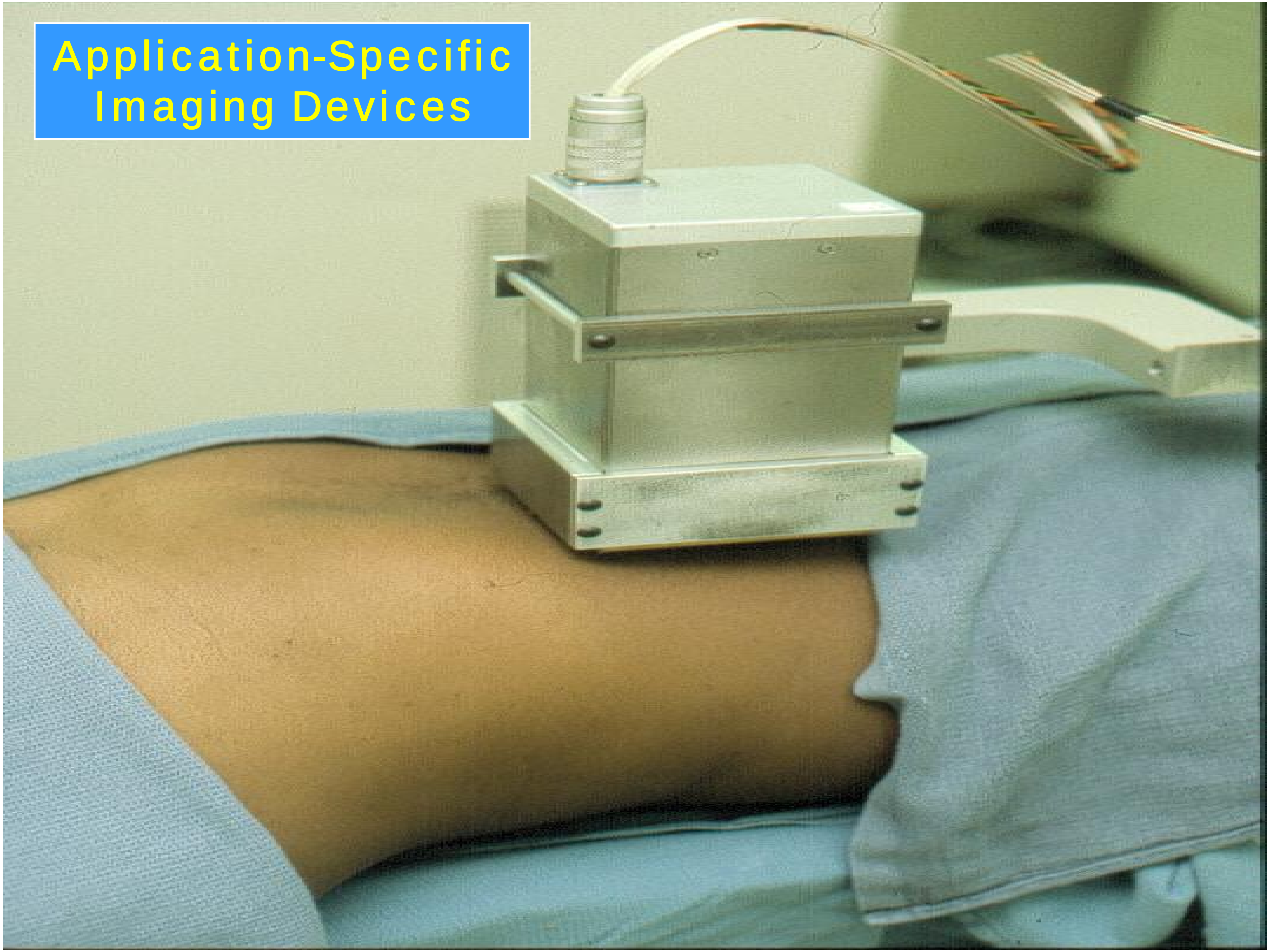

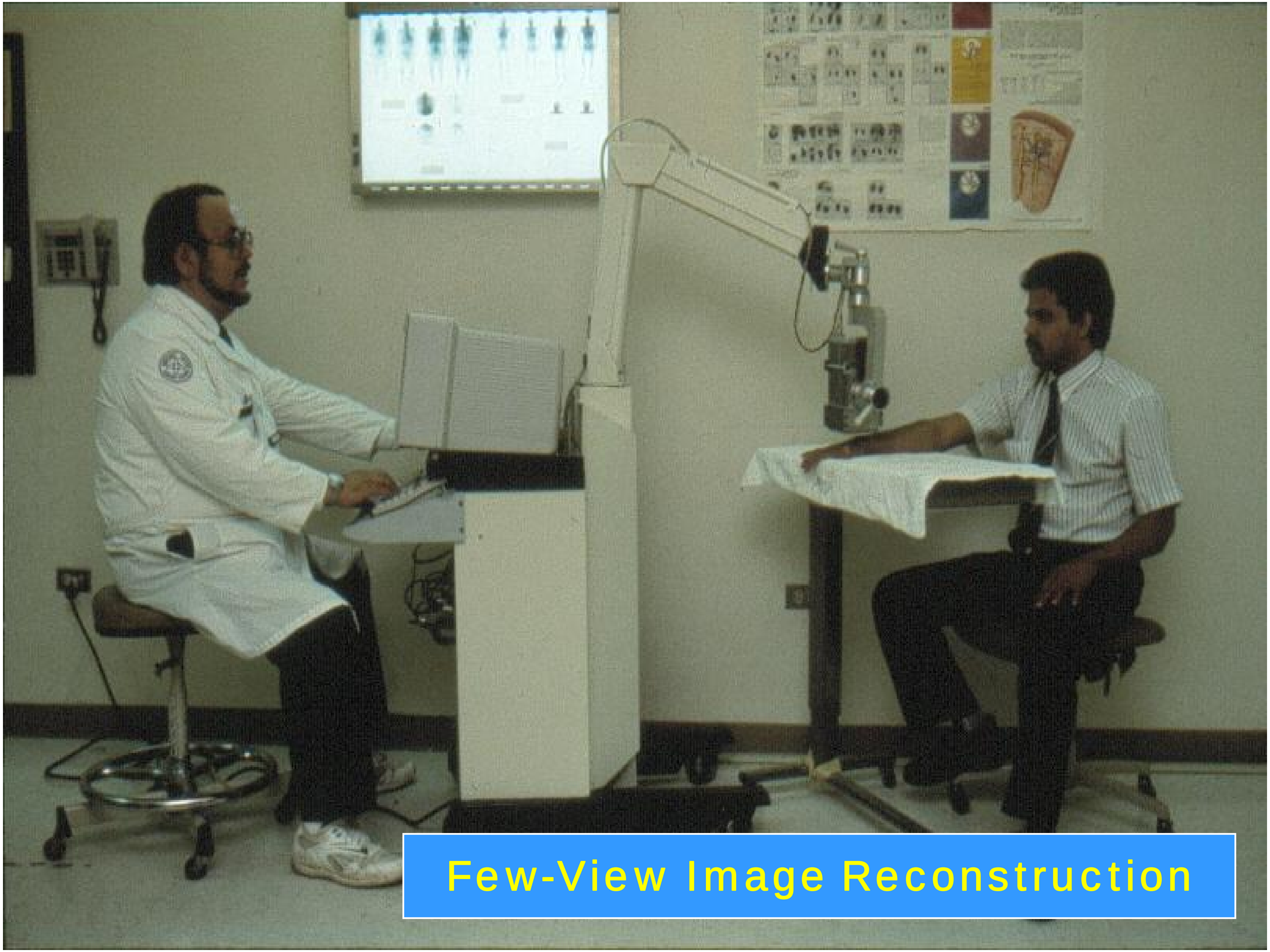

Few-View Image Reconstruction

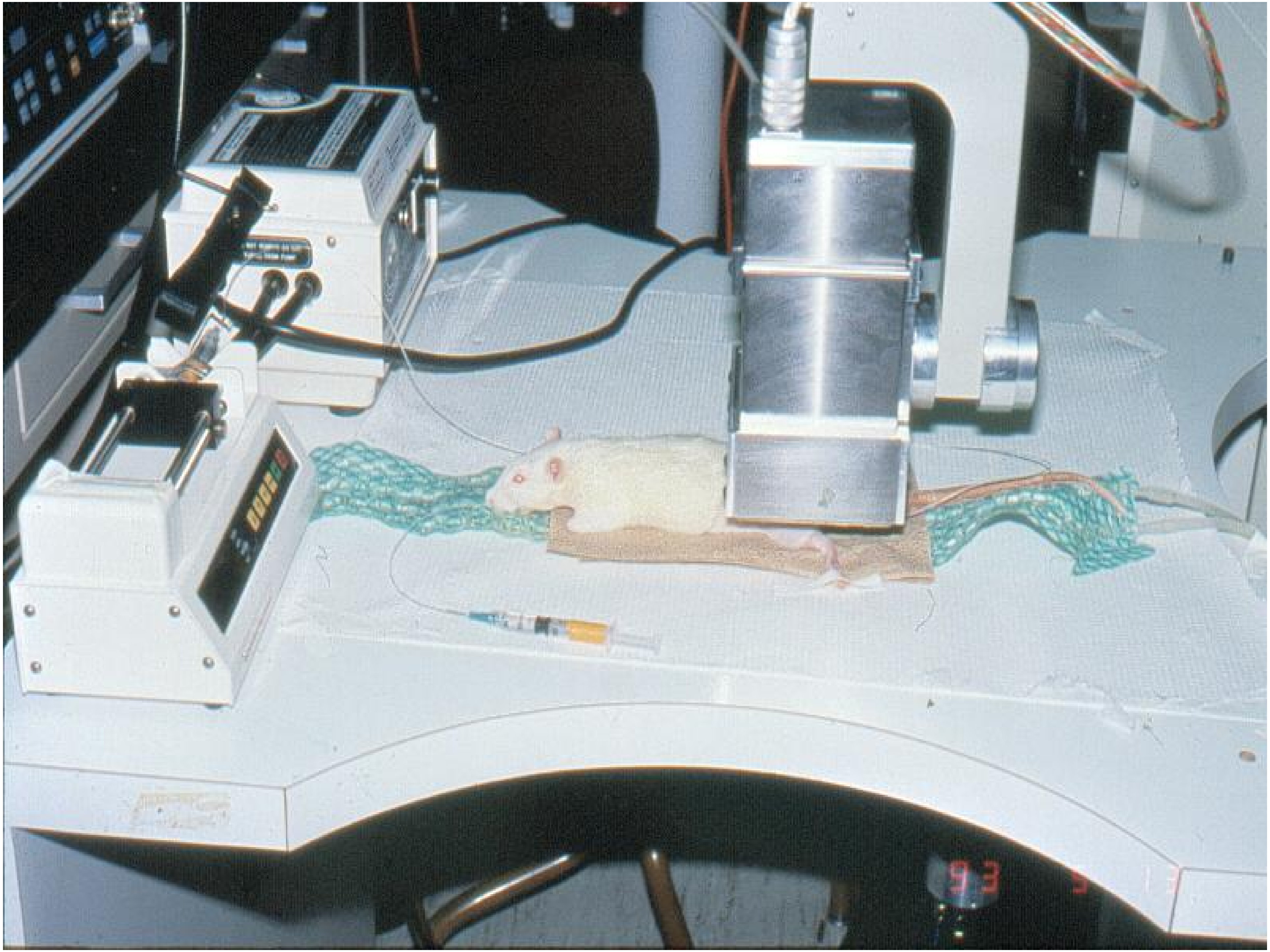

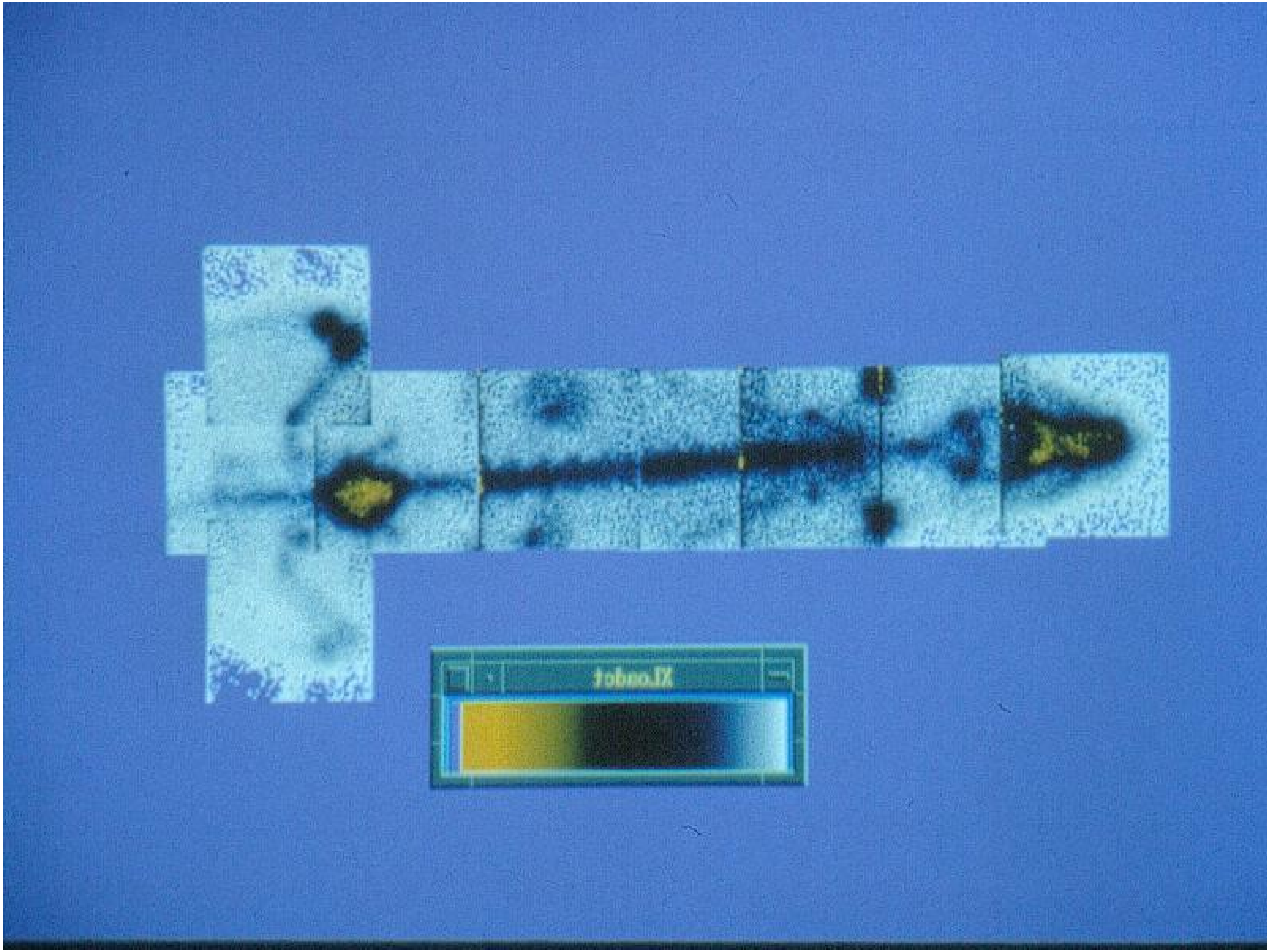

External Appearance

Upper Right Extremity

Source: 4000 volts

Diagnostic Images

0.1T - MRI

injured muscle

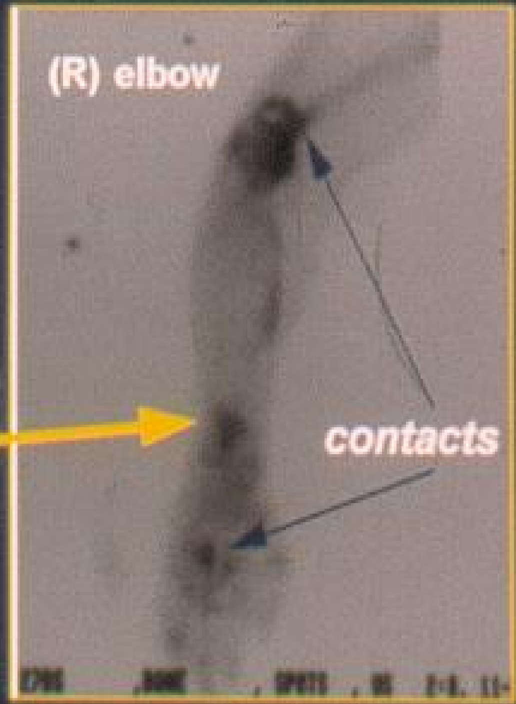

Tc-99m PYP scan

Tc99m-PYP Uptake After Pulsed Shock Exposure

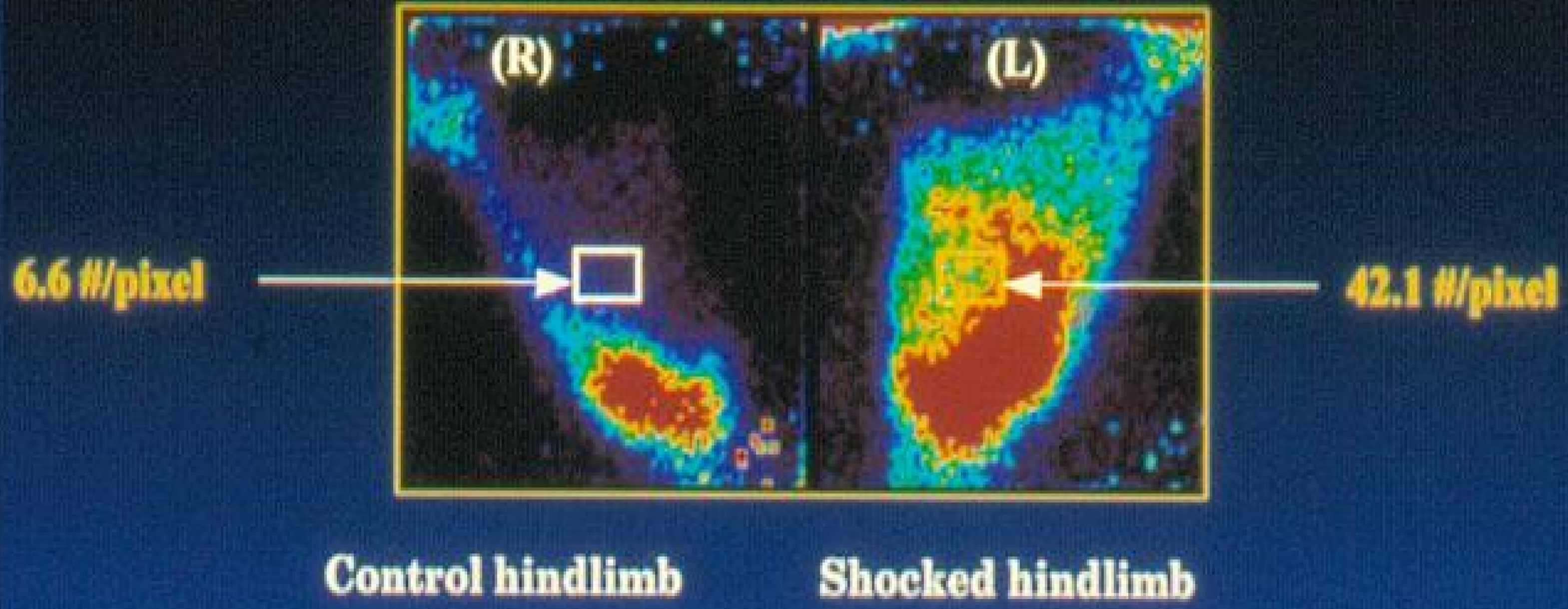

⇨ Exposure: 2-amp, 4-msec/ 10 sec, 2000-volt pulses, ankle-to-tail x12.

Unshocked/Saline vs Shocked/Saline

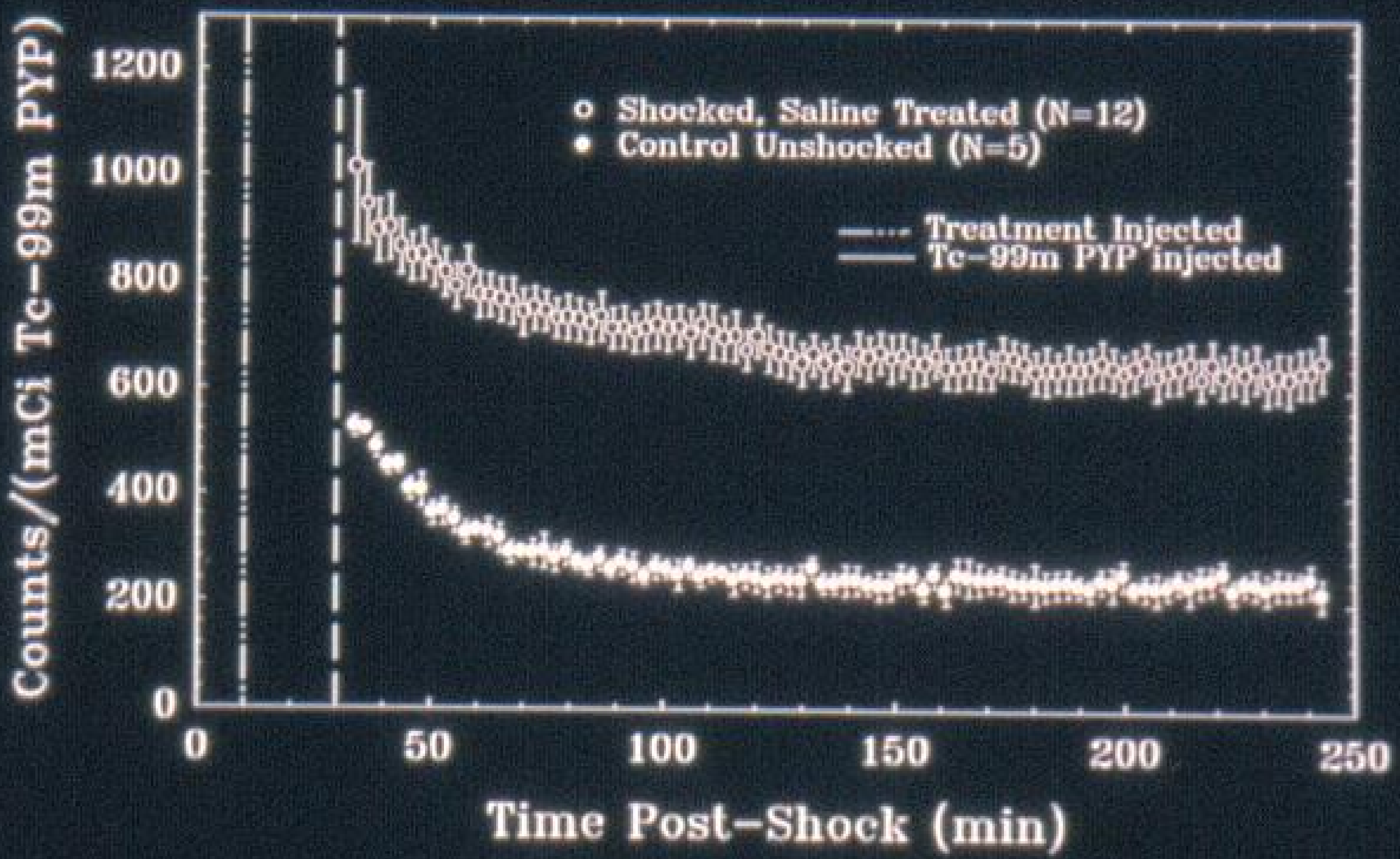

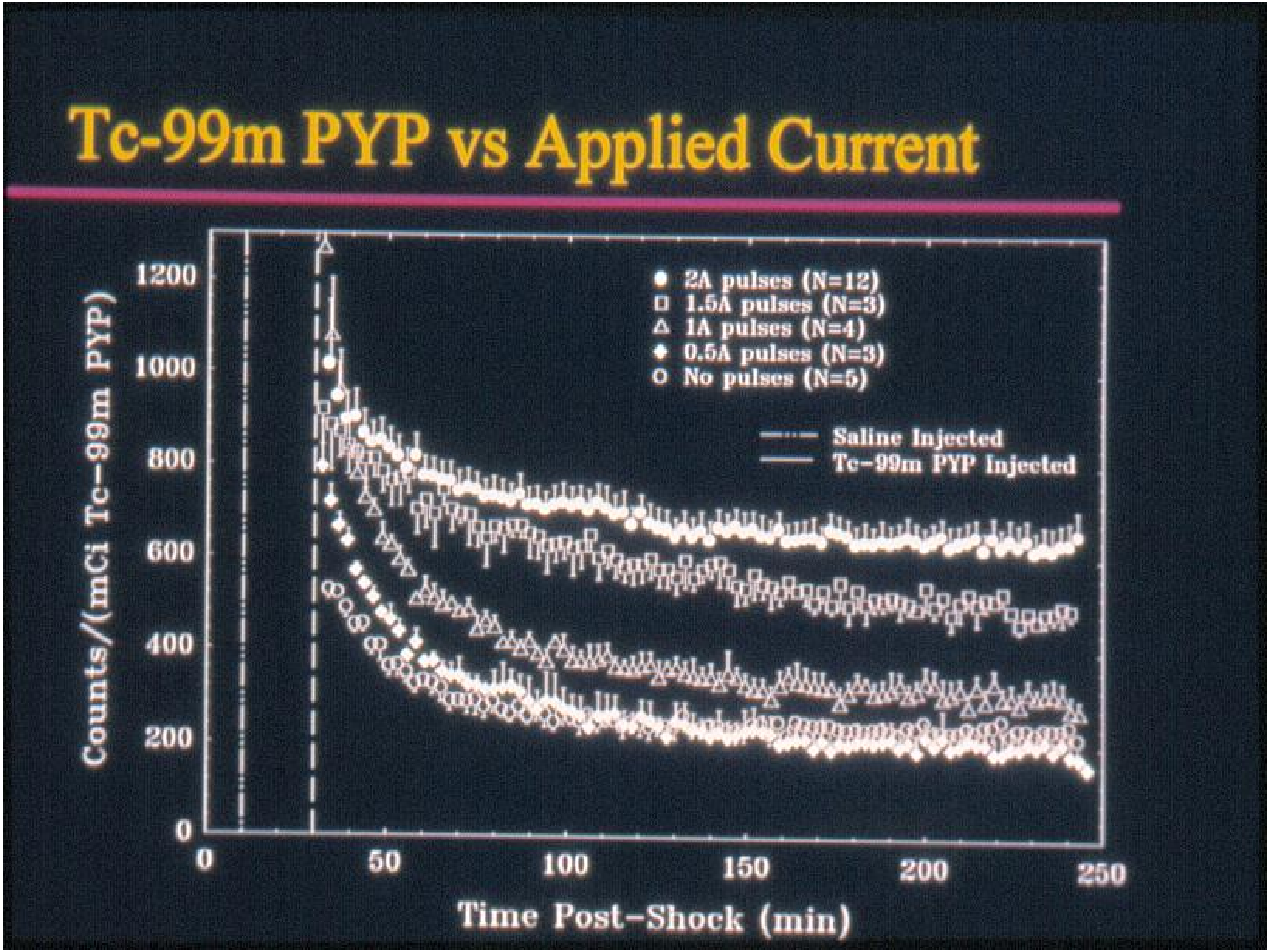

Tc-99m PYP vs Applied Current
2A pulses (N=12)
1.5A pulses (N=3)
1A pulses (N=4)
0.5A pulses (N=3)
No pulses (N=5)
Saline Injected
Tc-99m PYP Injected
Counts/(mCi Tc-99m PYP)
0
200
400
600
800
1000
1200
0
50
100
150
200
250
Time Post-Shock (min)

^{99m}Tc PYP: Poloxamer-188 Data

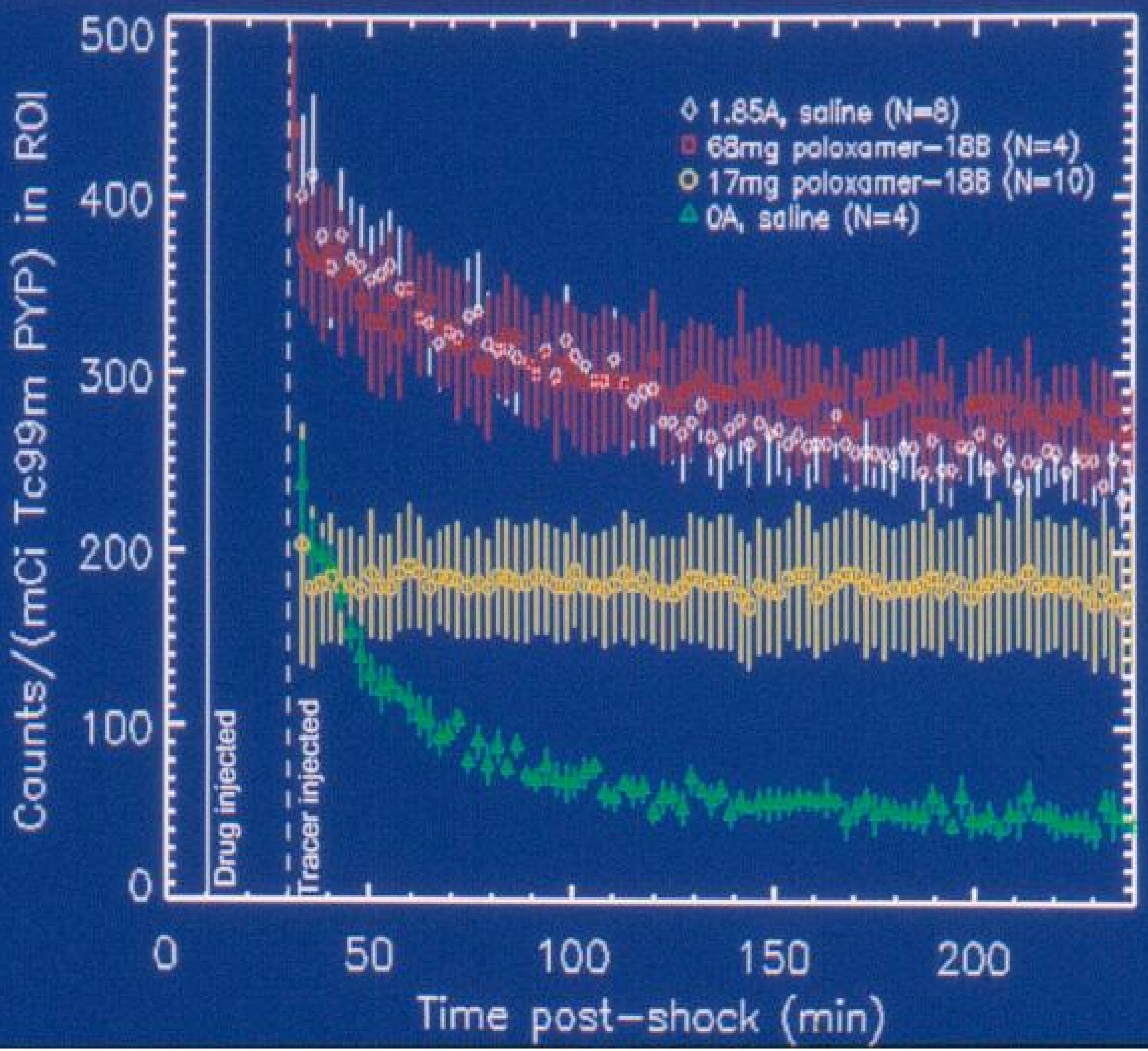

PET Scintillators

- **Sodium Iodide - NaI (1940s, Hofstadter)**
  - pros: high light output
  - cons: hygroscopic, low atomic number, low density, slow

ECAT II, 1977

- **Bismuth Germanate - BGO (1970s, Weber)**
  - pros: high density and atomic number, rugged and nonhygroscopic
  - cons: low light output, slow

ECAT 911, 1982

- **Gadolinium Oxyorthosilicate - GSO (1980s, Takagi)**
  - pros: high density, fast, nonhyygroscopic
  - cons: low atomic number, low light output, cleaving

Scanditronix PC-2048, 1983

- **Lutetium Oxyorthosilicate - LSO (1990s, Melcher)**
  - pros: high light output, fast, high density, high atomic number, rugged, nonhygroscopic
  - cons: intrinsic radioactivity

ECAT ACCEL, 2000

Characteristics of Selected Scintillators

	LSO	BGO	GSO	NaI
Density (g/cc)	⇒ 7.4	7.13	6.7	3.67
Effective atomic number	66	⇒ 75	59	51
Mean Free Path (cm)	1.16	⇒ 1.05	1.43	2.88
Hygroscopic?	⇒ no	no	no	yes
Rugged?	⇒ yes	yes	no	no
Decay Time (nsec)	⇒ 40	300	56,600	230
Relative Light Output	75	15	25	⇒ 100
Energy Resolution	10%	10.1%	9.5%	7.8%

Scintillation properties of primary crystals in PET

Material	Denstiy (g/cm^3)	Decay time (ns)	[a]Light Yield	Initial Photon Rate (ph/MeV-ns)	Energy resolution %@662 keV
NaI:Tl	3.67	230	100	164	6.5
$Bi_4Ge_3O_{12}$(BGO)	7.13	300	22	27	9.3
Gd_2SiO_5:Ce(GSO)	6.71	60	27	167	7.8
Y_2SiO_5:Ce(YSO)	4.54	70	70	377	9.0
Lu_2SiO_5:Ce(LSO)	7.40	40	80	750	7.9
[c]$Lu_{2(1-x)}Y_{2x}SiO_5$:Ce(LYSO)	7.11	40	100	845	7.5~9.5
[d]$Lu_{2(1-x)}Gd_{2x}SiO_5$:Ce(LGSO)	7.40	40	61	575	12.4
$Lu_2Si_2O_7$:Ce(LPS)	6.23	38	70	692	9.5~12.5
BaF_2	4.89	[b]0.8	27	[b]2300	7~8
$LaBr_3$:$Ce^{0.5\%}$	5.29	35	162	1743	3.0

[a]Relative to NaI(Tl)=100
[b]It is the fast scintillating component of BaF_2.
[c]x=0.1
[d]x=0.1

Quadrant sharing design

- 8x8 crystal matrix; two layer LSO
  LSO-fast/LSO-slow
- 128 single crystals in 2 layers
  $2.1 \times 2.1 \times 7.5\ mm^3$

HRRT Detector Design

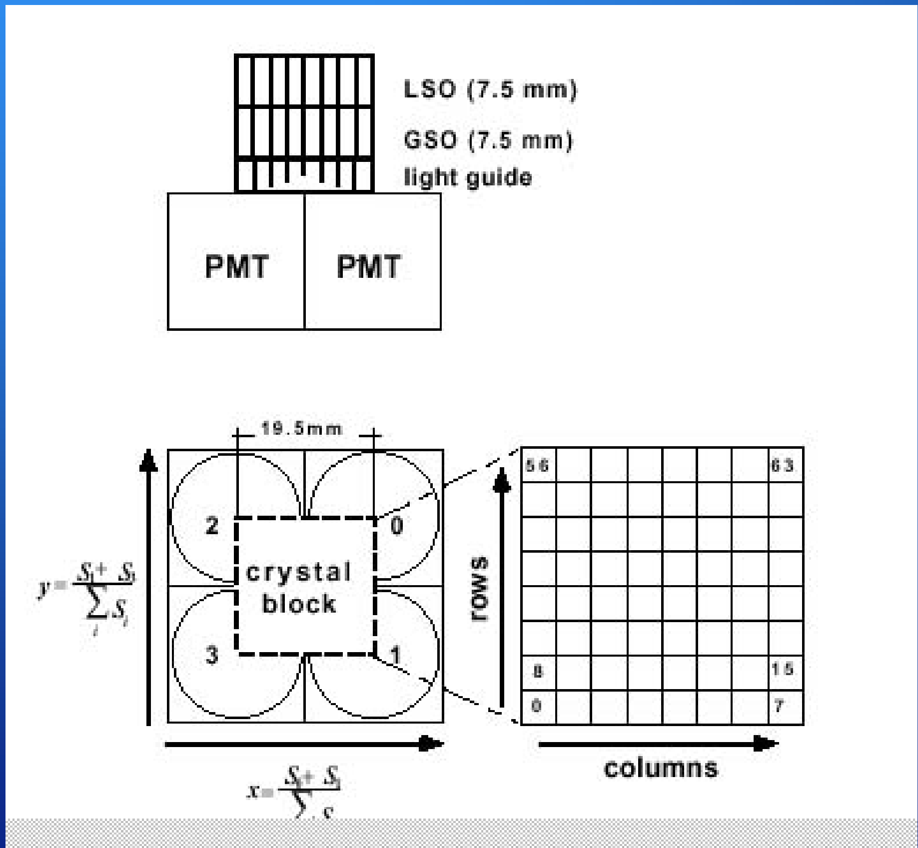

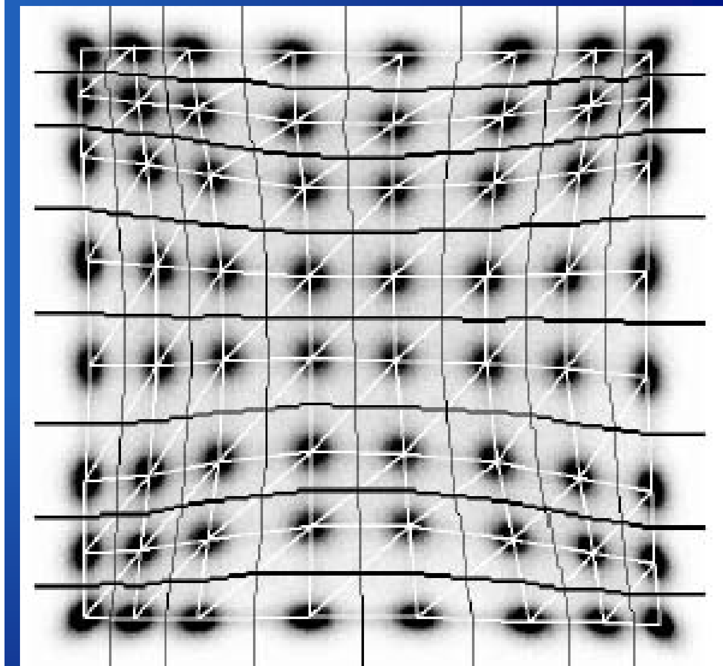

Depth-of-Interaction (DOI) Detector

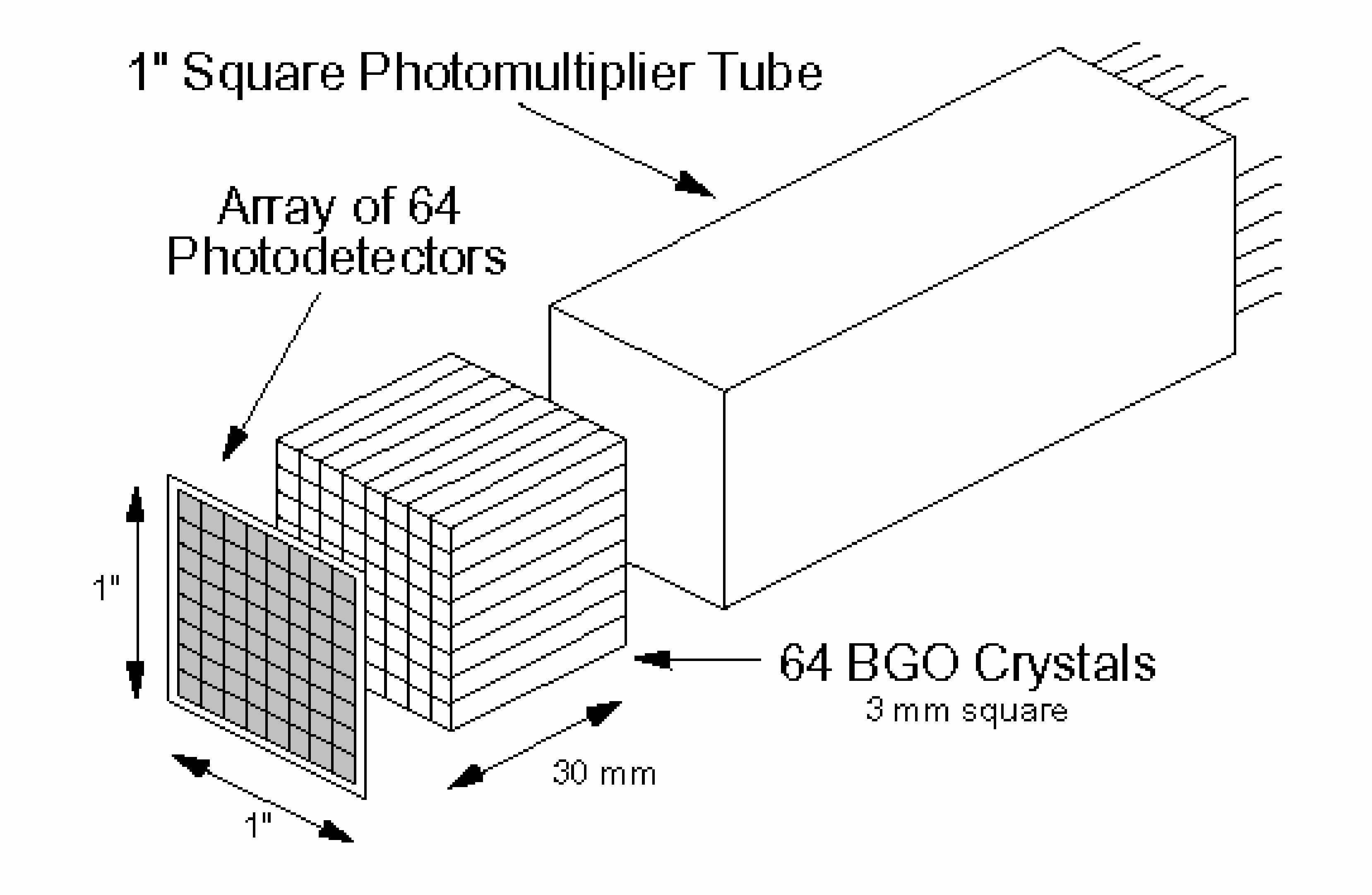

DOI Detector

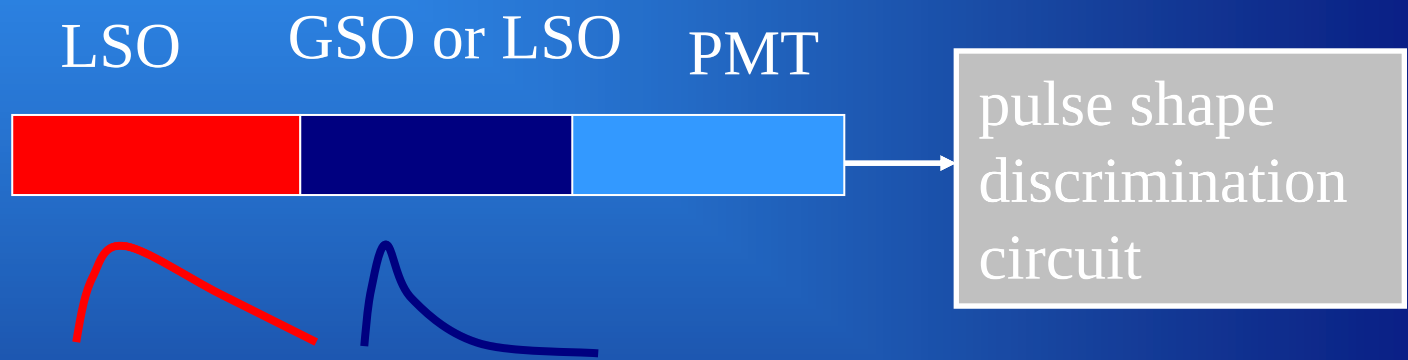

Phoswich detector

117 blocks per head

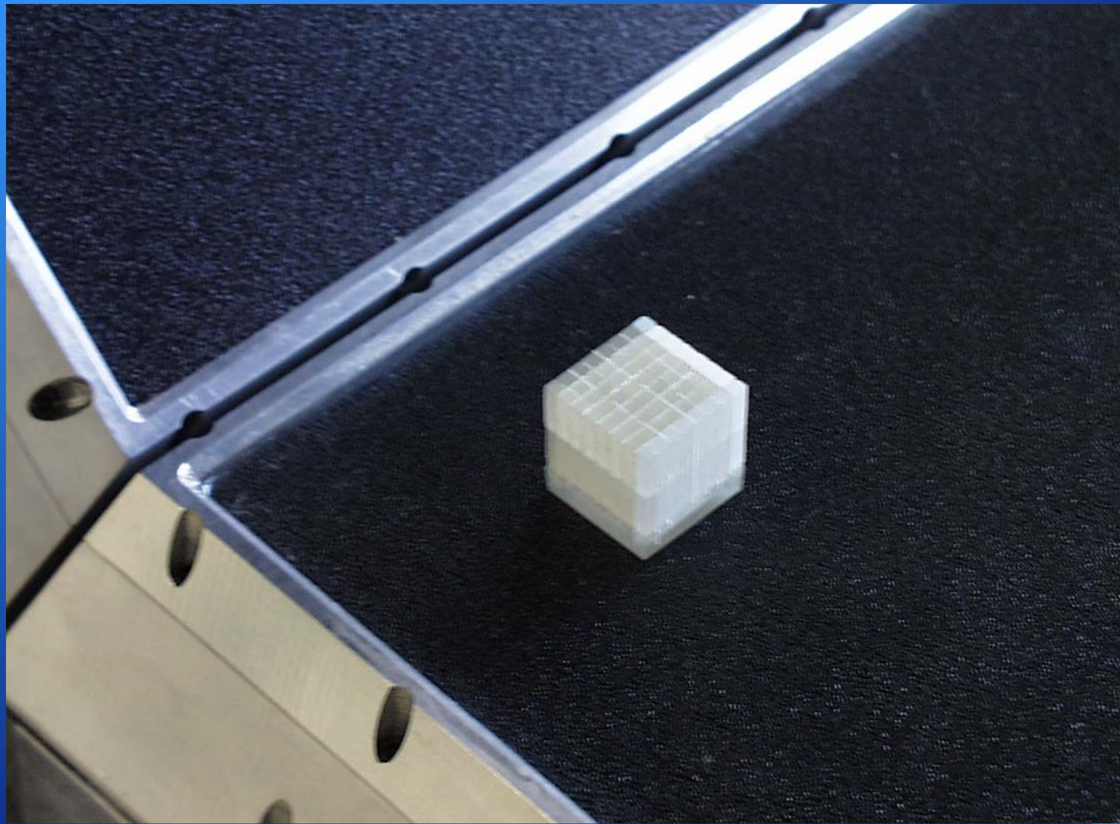

Octagon - 120,000 crystals

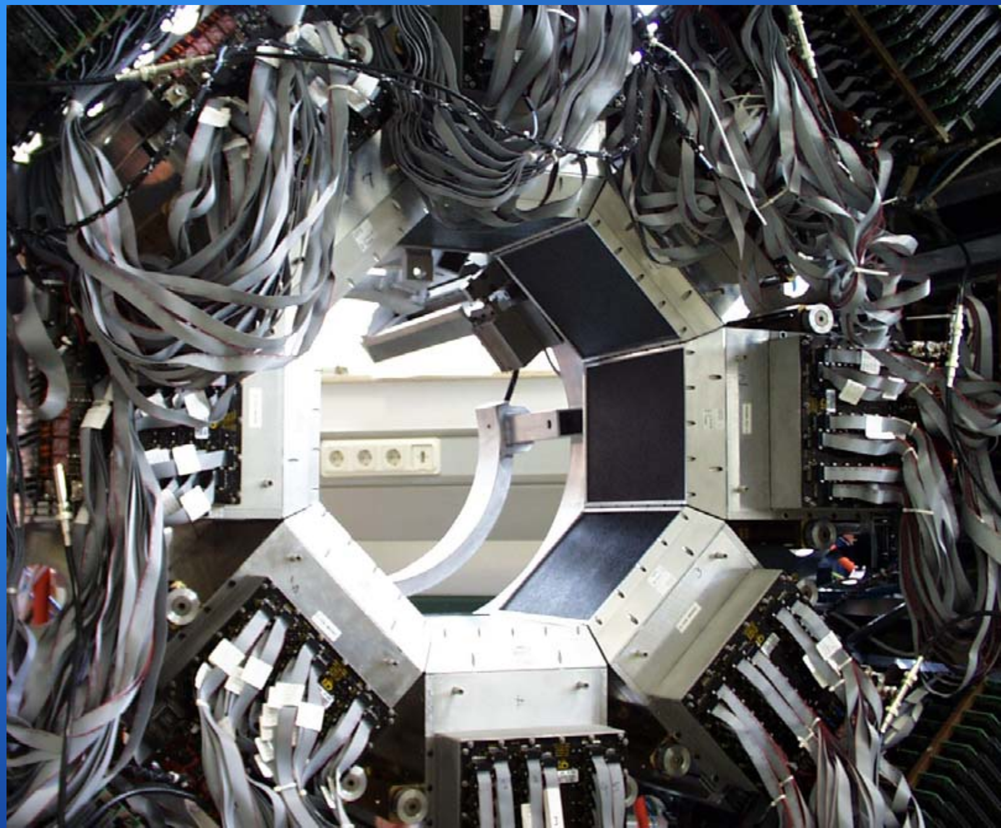

936 electronic channels
4.486*10^9 LORs

The neue Cologne Phantom

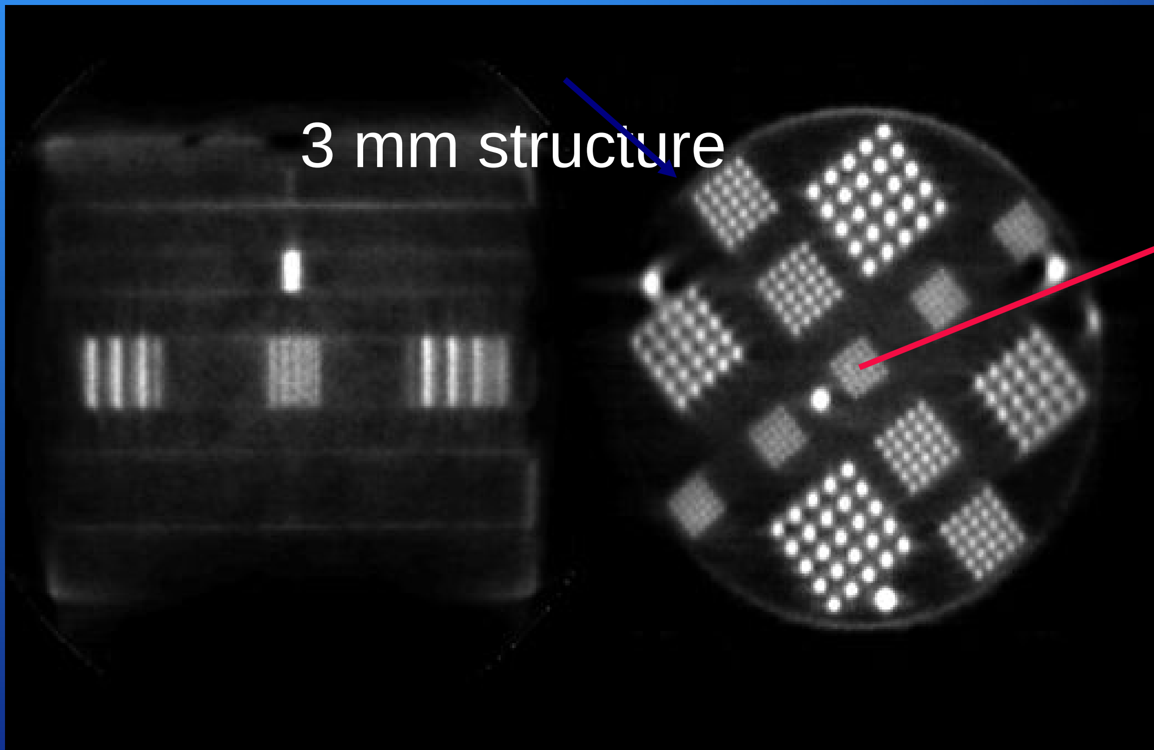

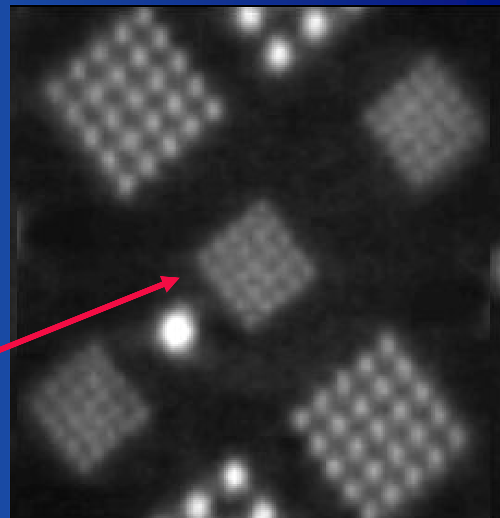

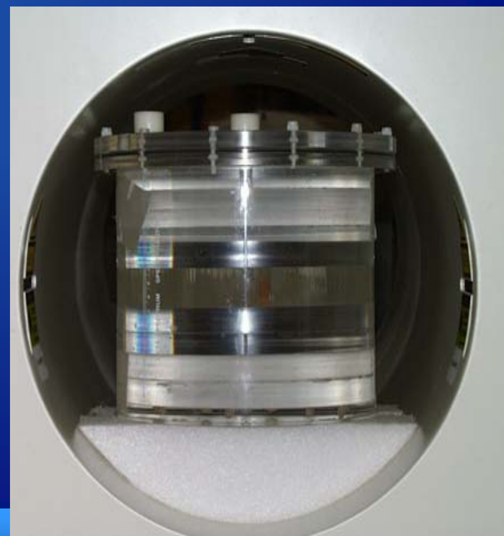

Parallax Errors

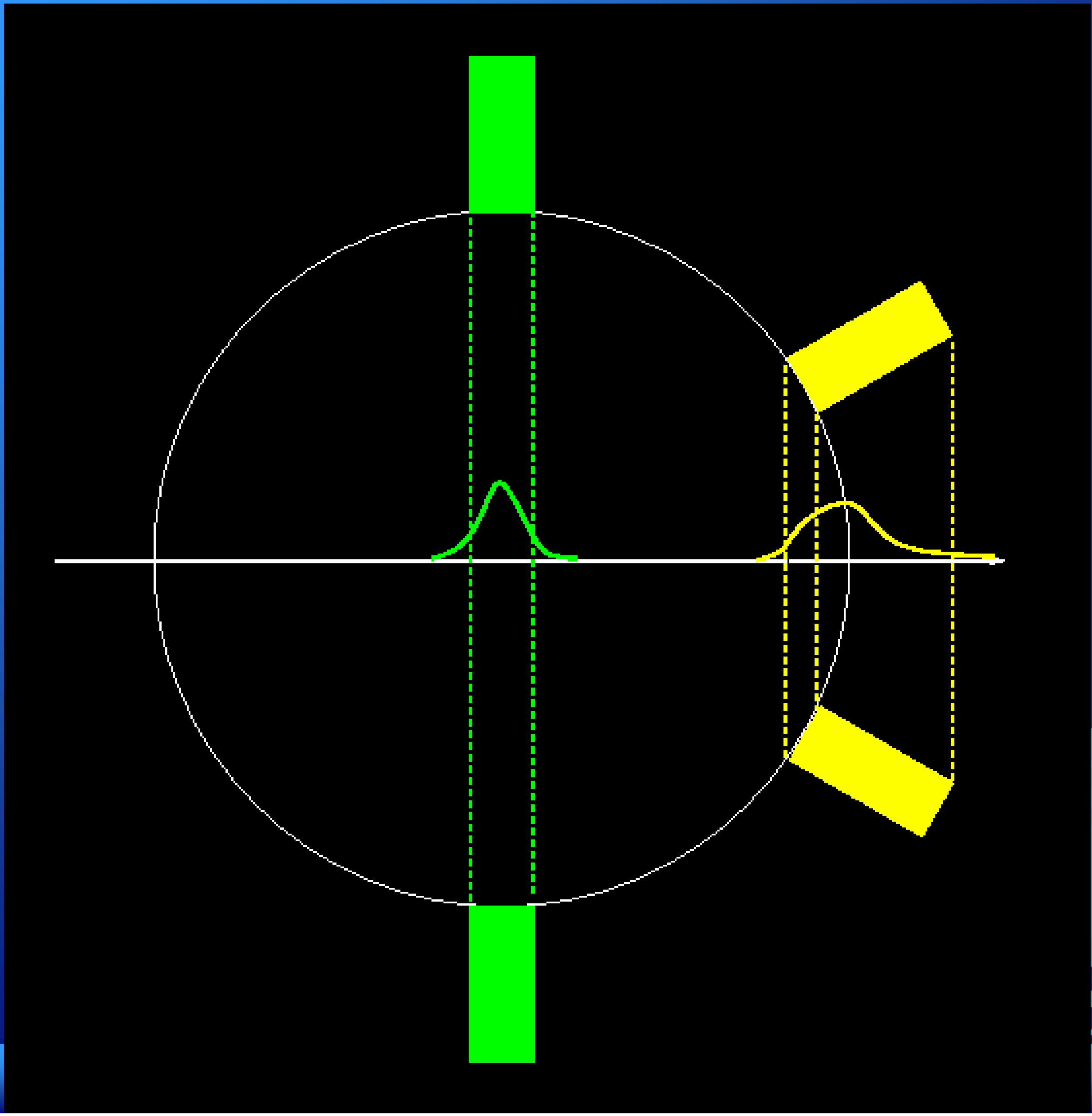

Signal Recovery for Parallax Errors

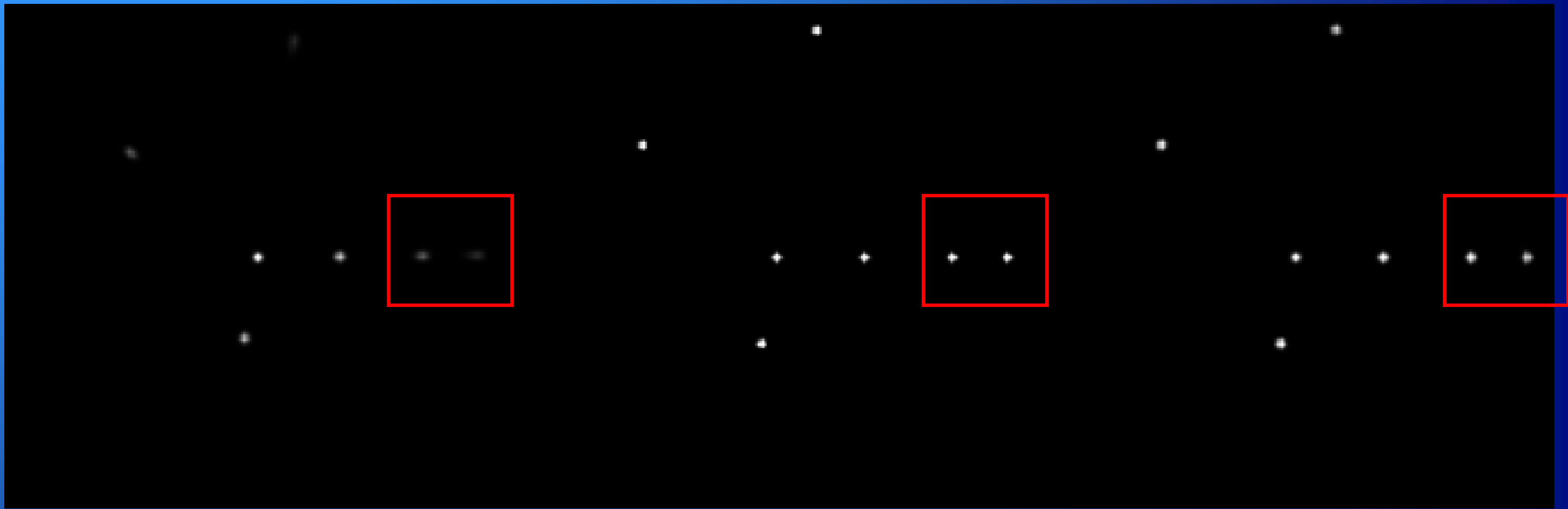

REBIN+FBP True SREM+FBP

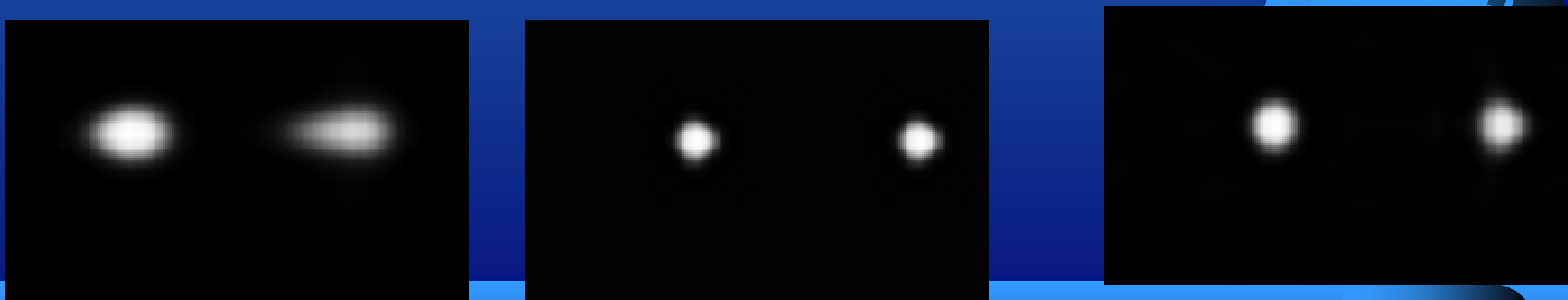

Compact PET
High-Performance Low-Cost (HPLC)

Compact - DOI *Conventional*

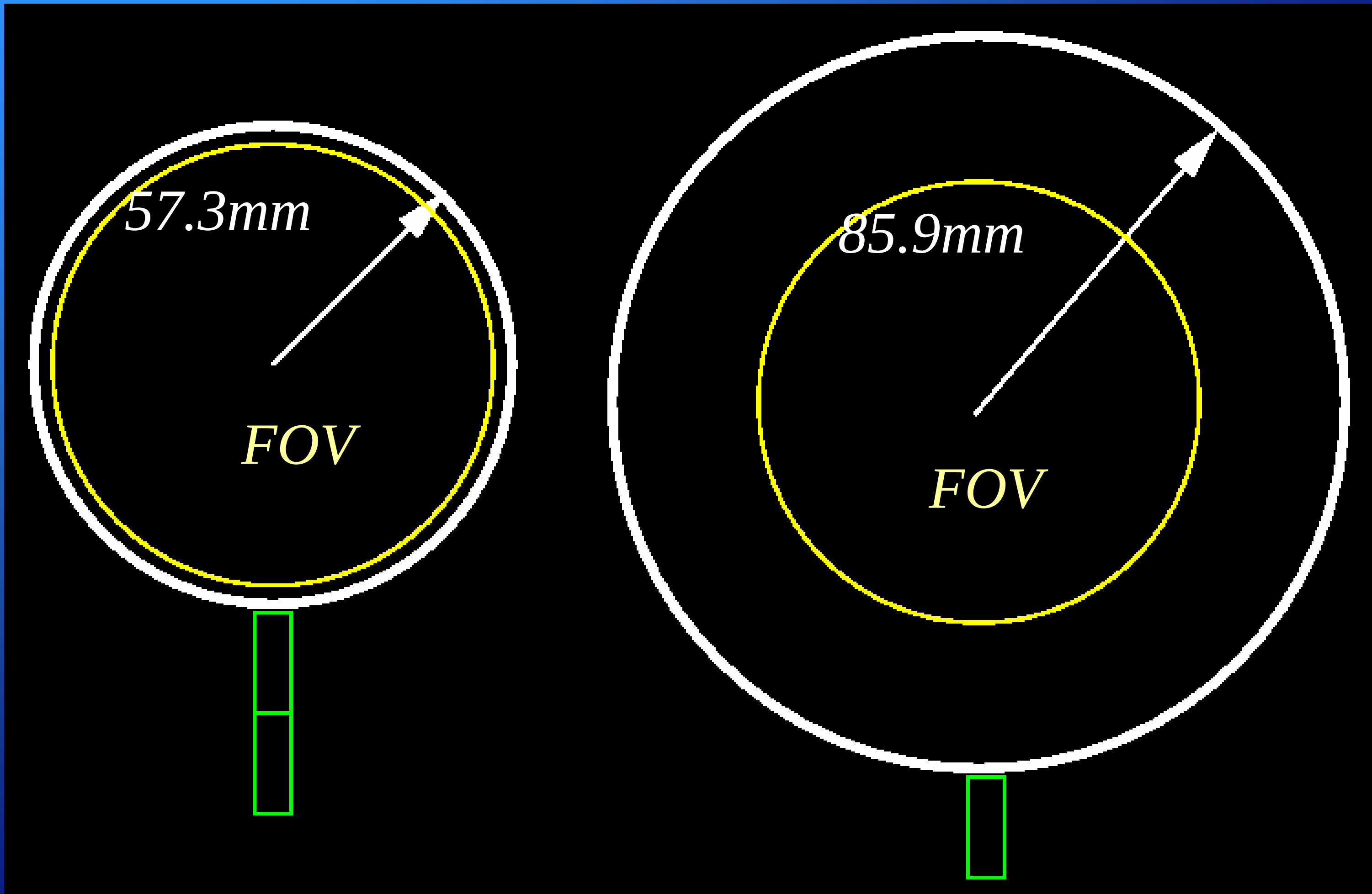

RFOV = 56.3mm

A Benchtop Prototype for High-Throughput Animal Imaging

- **HRRT modules**
  - **LSO crystals with DOI capability**
    - good spatial resolution
      - ~2.42mm crystal pitch
      - ~10mm DOI resolution
    - good detection sensitivity
    - high count rate
  - **large detection sensitive area**
    - ~25.2cm ×17.4cm
    - 72×104 crystals per layer
  - **off-shelf, well tested, cost-effective design**
  - **adjustable energy and coincidence windows**

Dual Planar Detector High-Throughput Animal PET Imager

Dual Layer D.O.I. Detectors (LSO)

Variable Detector Face-to-Face Spacing

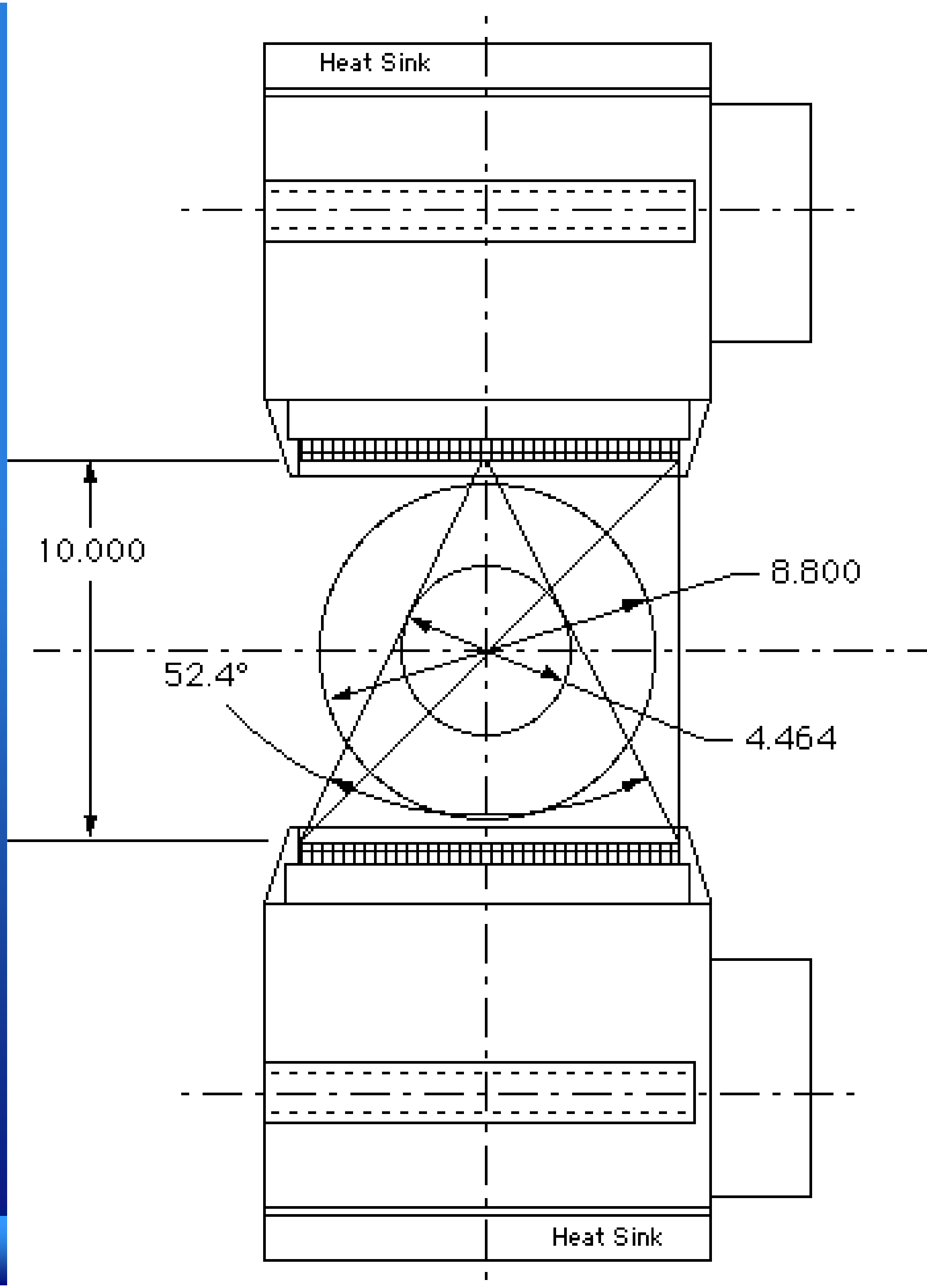

Example Reconstruction

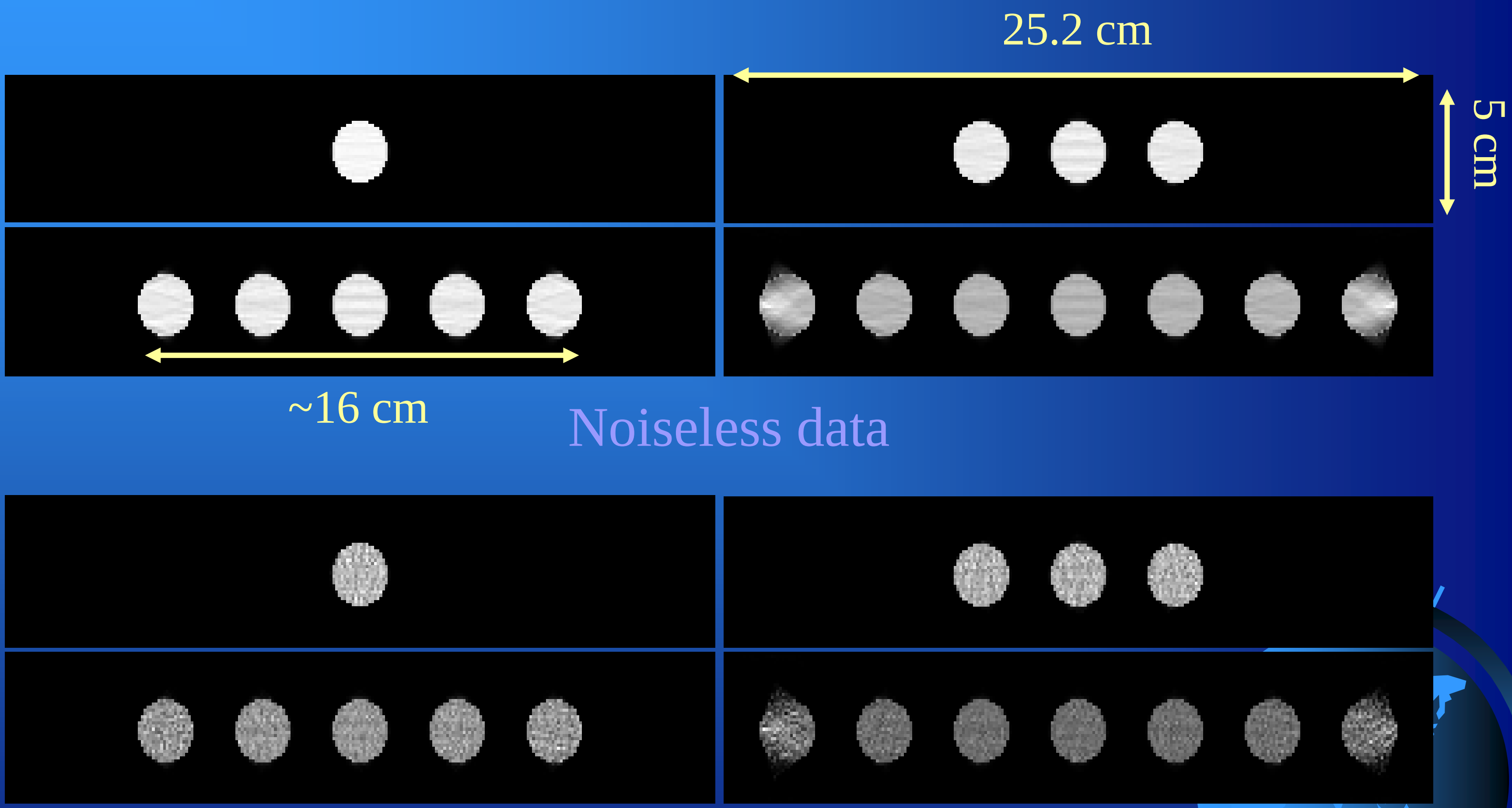

Noiseless data

Noisy data

Fully 3D Reconstruction without Angular Rotation

Chicago Tribune

Final Edition

$1.25 Sunday, May 8, 1988

Mysteries of the brain being revealed

By Ronald Kotulak
Science Writer

The brain is the body's last and greatest mystery, but it is beginning to yield its fabulous secrets.

Scientists are discovering the biological bases for mental disorders and are working on ways to actually see thoughts, raise IQs, improve memory and alter the 3-pound organ in ways not yet dreamed of.

Already new findings about the causes of mental illness have had a dramatic impact on the mentally ill, not only leading to new treatments but also easing the stigma by shifting the blame from the victim to brain chemistry—and thus encouraging more people to seek help.

But even bigger payoffs are looming as scientists develop ways to attack some of the brain's most common disorders—injury, mental retardation, learning and memory problems, stroke, Alzheimer's disease, Parkinson's disease, schizophrenia and aggressiv

The new era in b
being accelerated by
molecular biology t
scientists to take t
piece by piece and
gether to learn how
their new tools scient

● Peer inside the l
velous imaging devic
time, it is possible t

New view of the living human brain

Imaging technique: A side view of the brain of a 10-year-old girl suffering from focal encephalitis shows in a single image both the detailed structure and function of the brain. The computer technique, pioneered at the University of Chicago, combines in one image two separate tests. One test uses magnetic fields to make images of internal structures. A second test measures the brain's metabolic activity.

Test results: The combined image shows an infection at the top of the patient's brain that is paralyzing a foot. The yellow patch with a green core in an area that should be all red indicates infection.

PET scan color-coded by computer

Most active
More active
Less active
Least active

Chicago Tribune Graphic; Source: Dr. Charles Pelizzari, University of Chicago

● Probe the mind's secret for controlling the body. Tantalizing evidence that the brain and body are more profoundly interconnected than expected may outline the link between stress and disease and, conversely, uncover ways that the mind can be used to heal the body.

● Explore the mystery of learning and memory. Using powerful new technology, researchers can trace brain chemicals and neural pathways responsible for thoughts.

● Develop new treatments for such mental disorders as depression—which, because of recent advances in drugs and therapy techniques, can now be treated successfully in 9 out of 10 patients. One in 5 Americans suffers from a diagnosable mental disorder.

The neuroscience gold rush is largely due to the growing conviction that asking the brain to understand itself is no longer an unsolvable conundrum. Still, it is the

ed skies

Multi-Modality Image Fusion
Image Co-Registration
Hybrid Integrative Image Systems

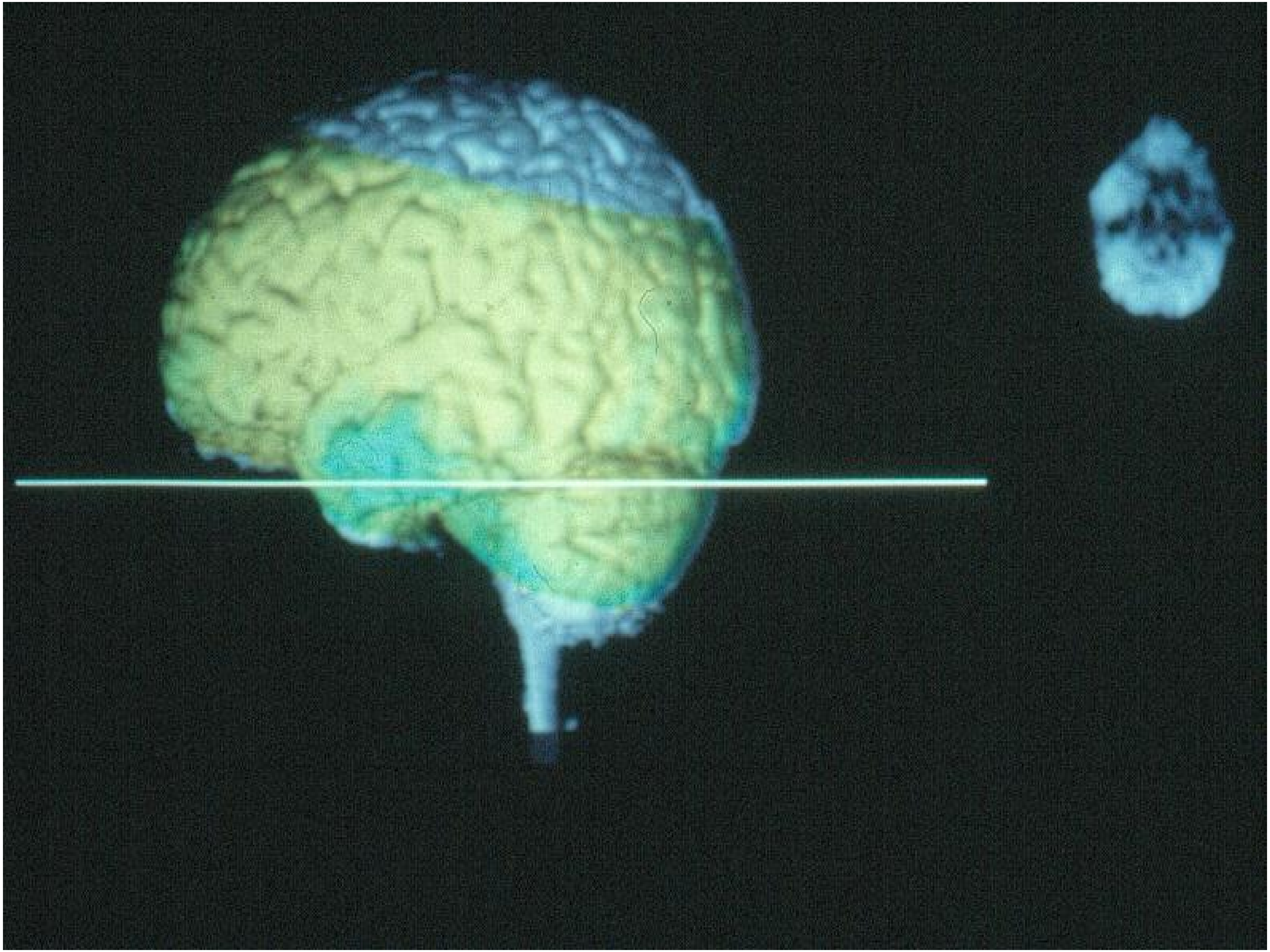

Hybrid Integrative Imaging System

PET / CT Scanner

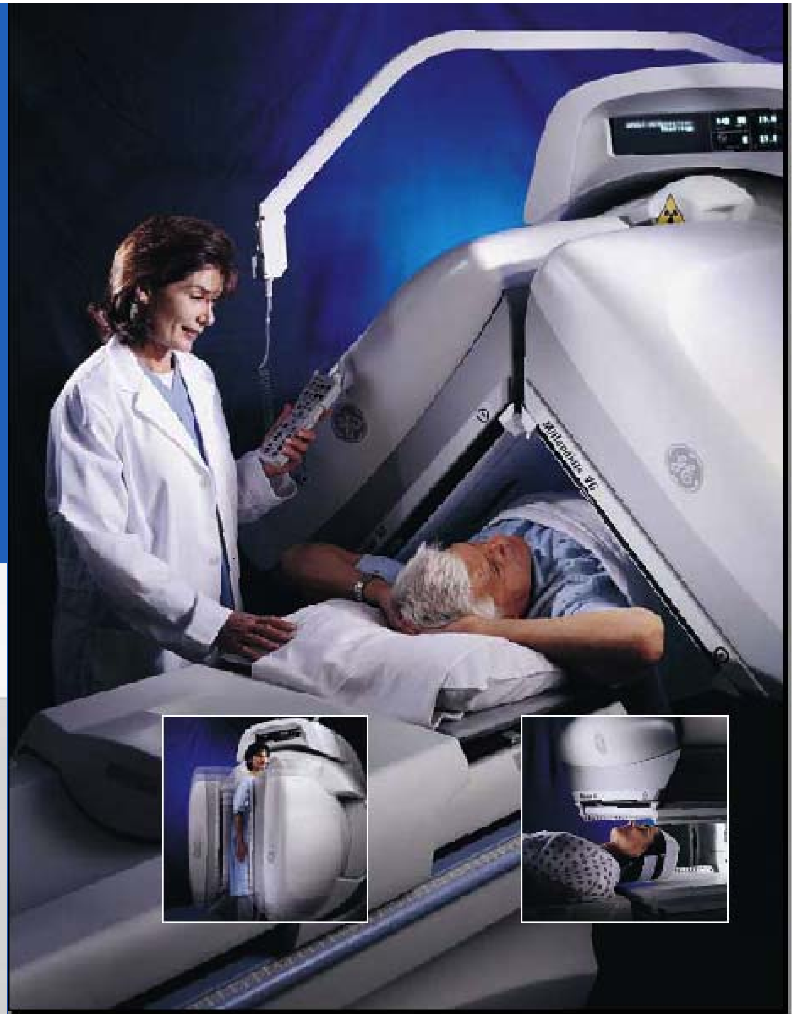

PET / SPECT / CT Scanner

Defining the Future of Diagnostic Imaging

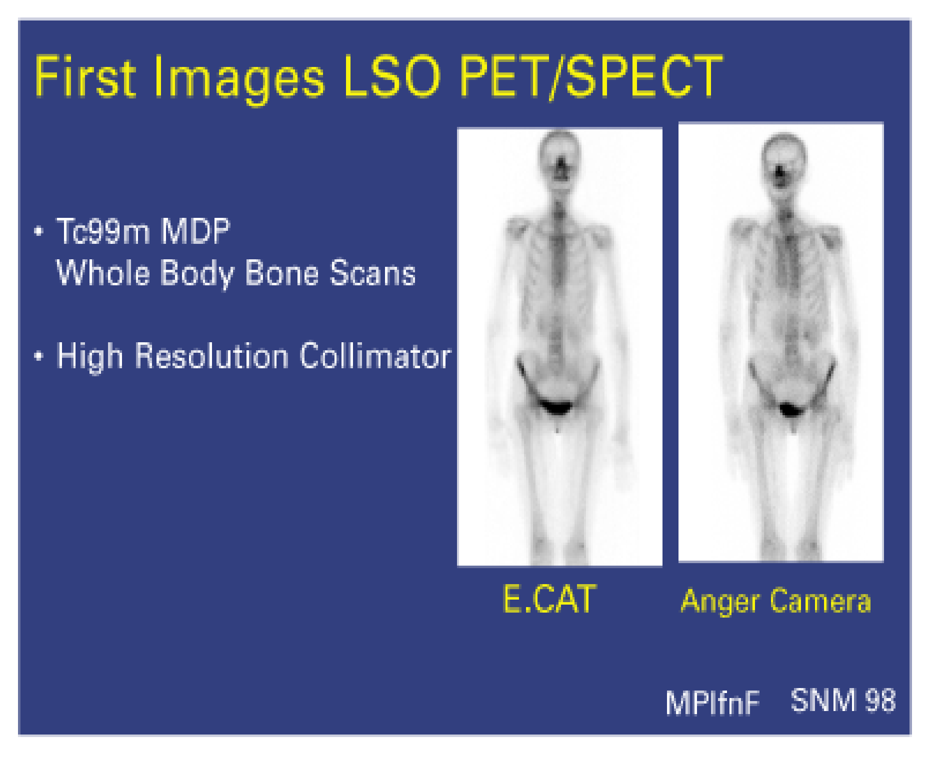

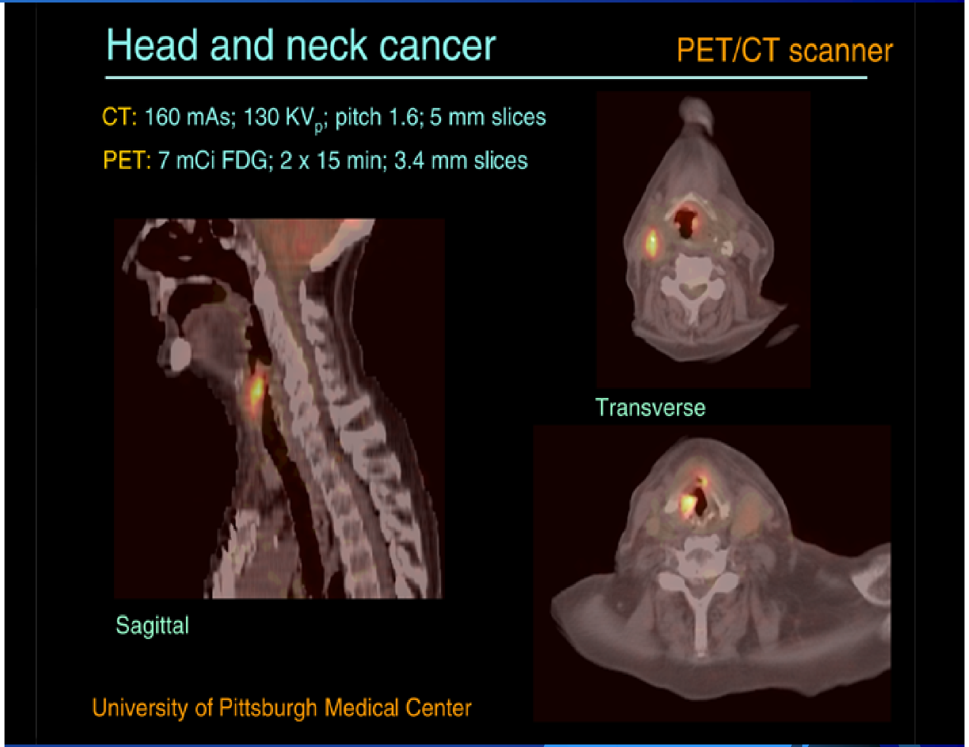

LSO PET/SPECT
1998 Society of Nuclear
Medicine Image of the Year

PET/CT
1999 Society of Nuclear
Medicine Image of the Year

Multi-Modality Integrative System

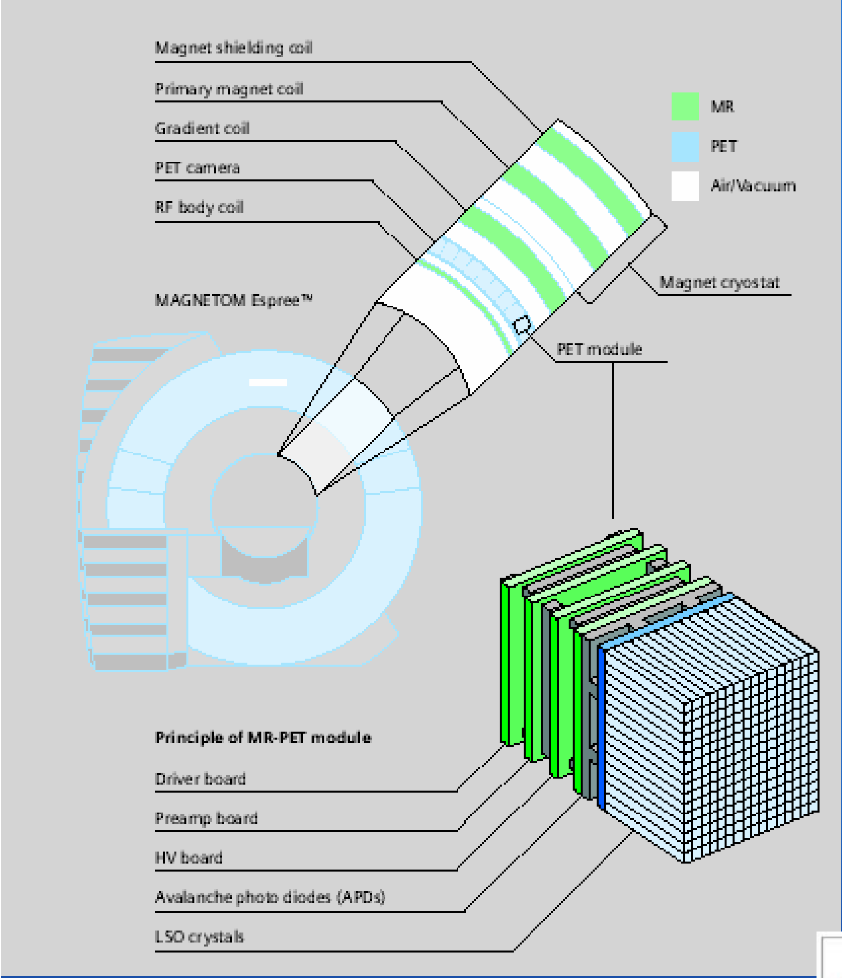

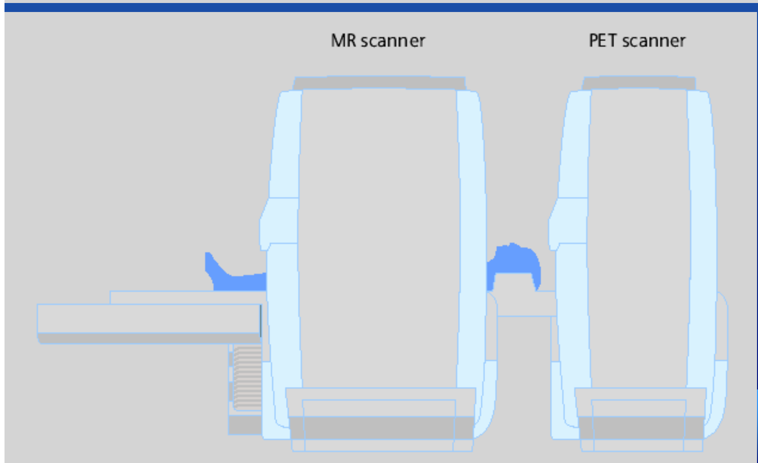

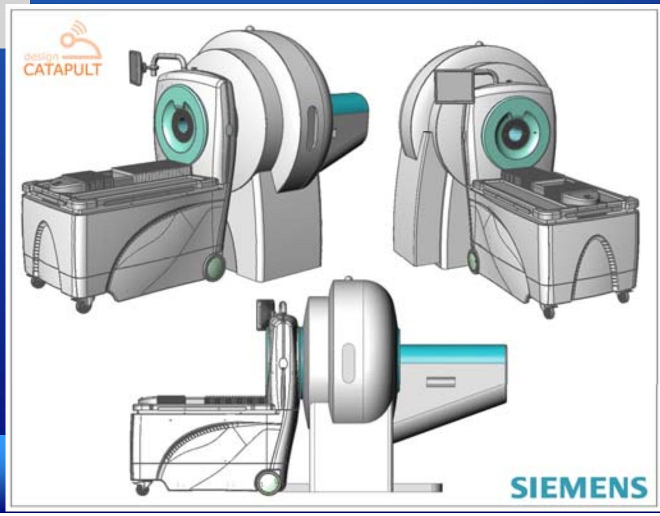

Siemens “Molecular Imaging”

REVEAL XVI
New Horizons in Clinical Applications

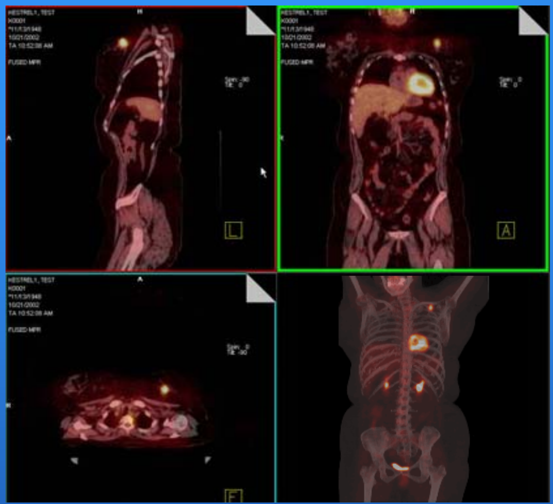

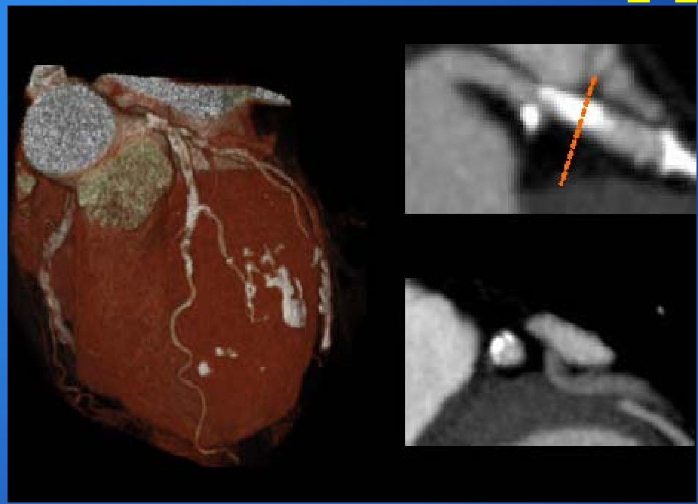

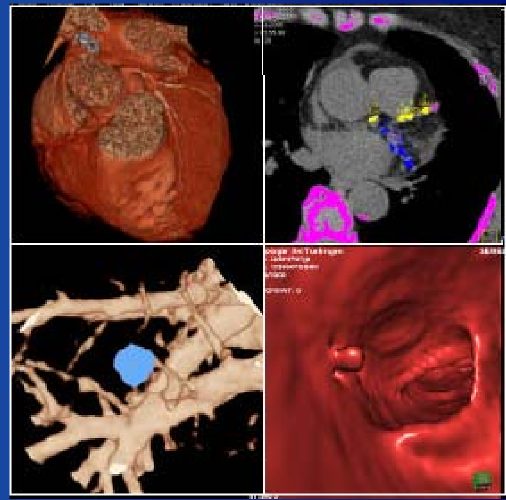

- **Oncology**
  - **Fused function & anatomy**
  - **10-minute PET/CT**
  - **Validated RTP integration**
  - **Image guided biopsy**
- Cardiology
  - High speed (0.4 sec/rotation)
  - CTA Vessel View
  - 4D Function (EF)
  - PET Viability & Perfusion
- Preventative
  - Fly-Thru Colonoscopy
  - Ca Scoring
  - CT Vision Fluoro
  - Lung nodule
  - CARE-dose pediatric

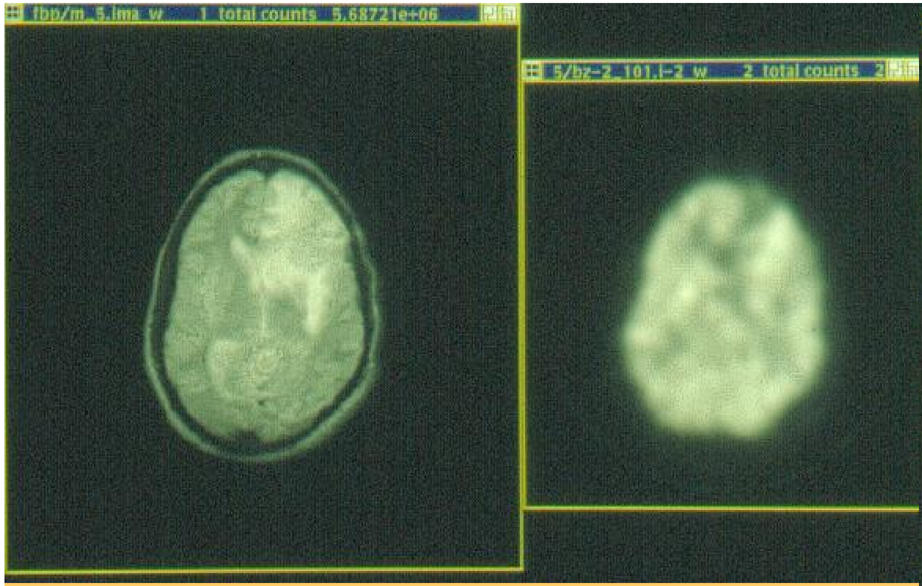

Multi-Modality Bayesian Image Reconstruction

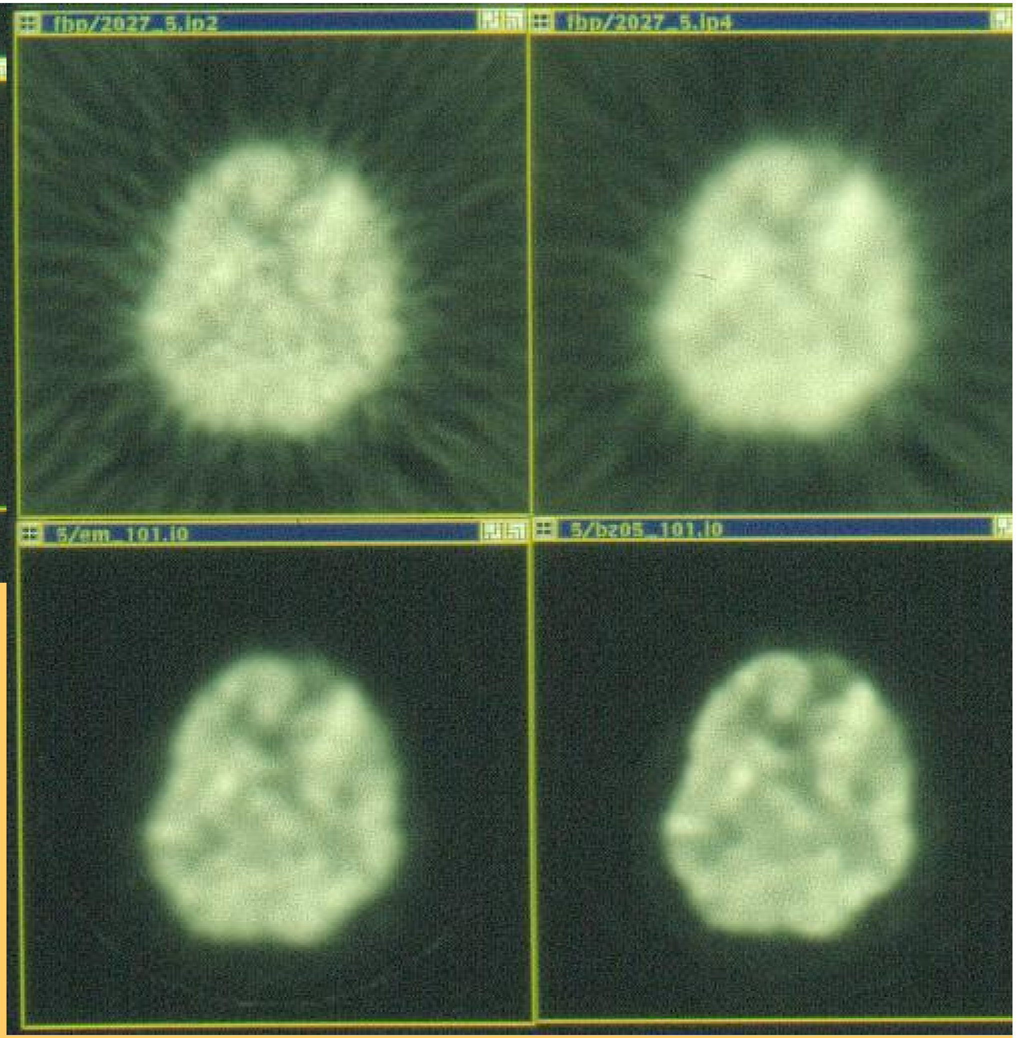

1. **Co-registration of PET/SPECT with CT/MRI**
2. **Incorporation of high-resolution information from the co-registered CT/MR images into a Bayesian image reconstruction framework to enhance image quality of PET/SPECT**
3. **Using the co-registered CT/MR images as an anatomic map in correction for attenuation and scatters in PET or SPECT**

Upper Two:
Filtered BackProj.
Lower Two:
Multi-Modality
Image Reconstru.
Chen, Kao, et al

Time-of-Flight Tomograph

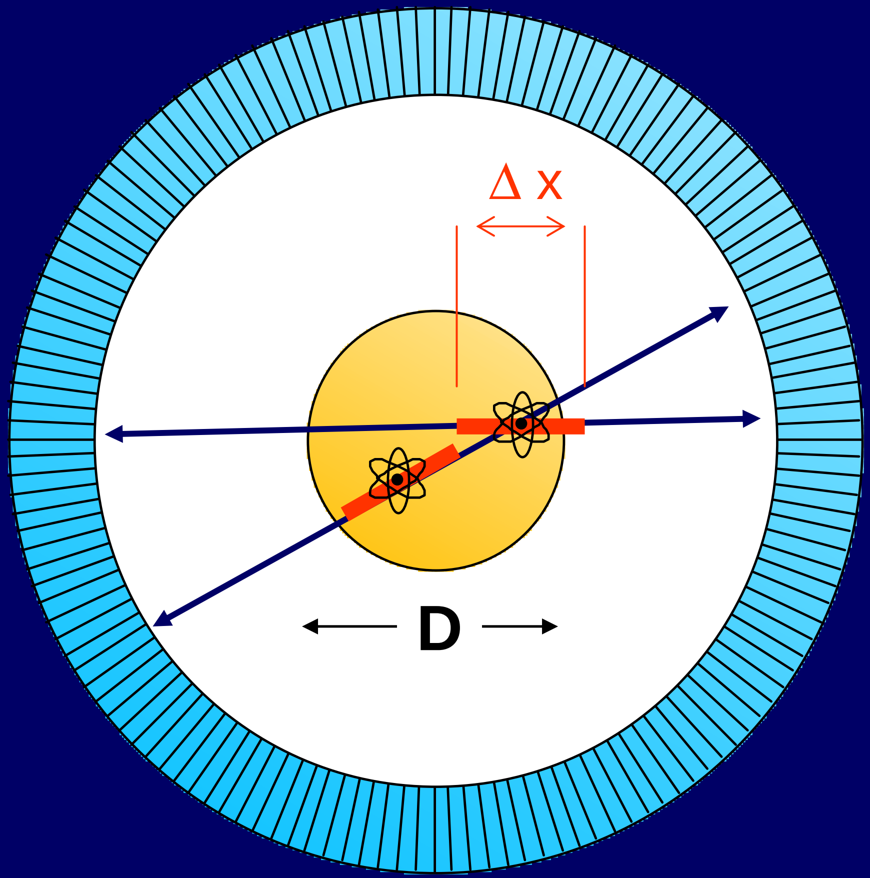

- Can localize source along line of flight - *depends on timing resolution of detectors*
- Time of flight information can improve signal-to-noise in images - *weighted back-projection along line-of-response (LOR)*

Δ x = uncertainty in position along LOR
= c · Δt/2

Karp, et al, UPenn

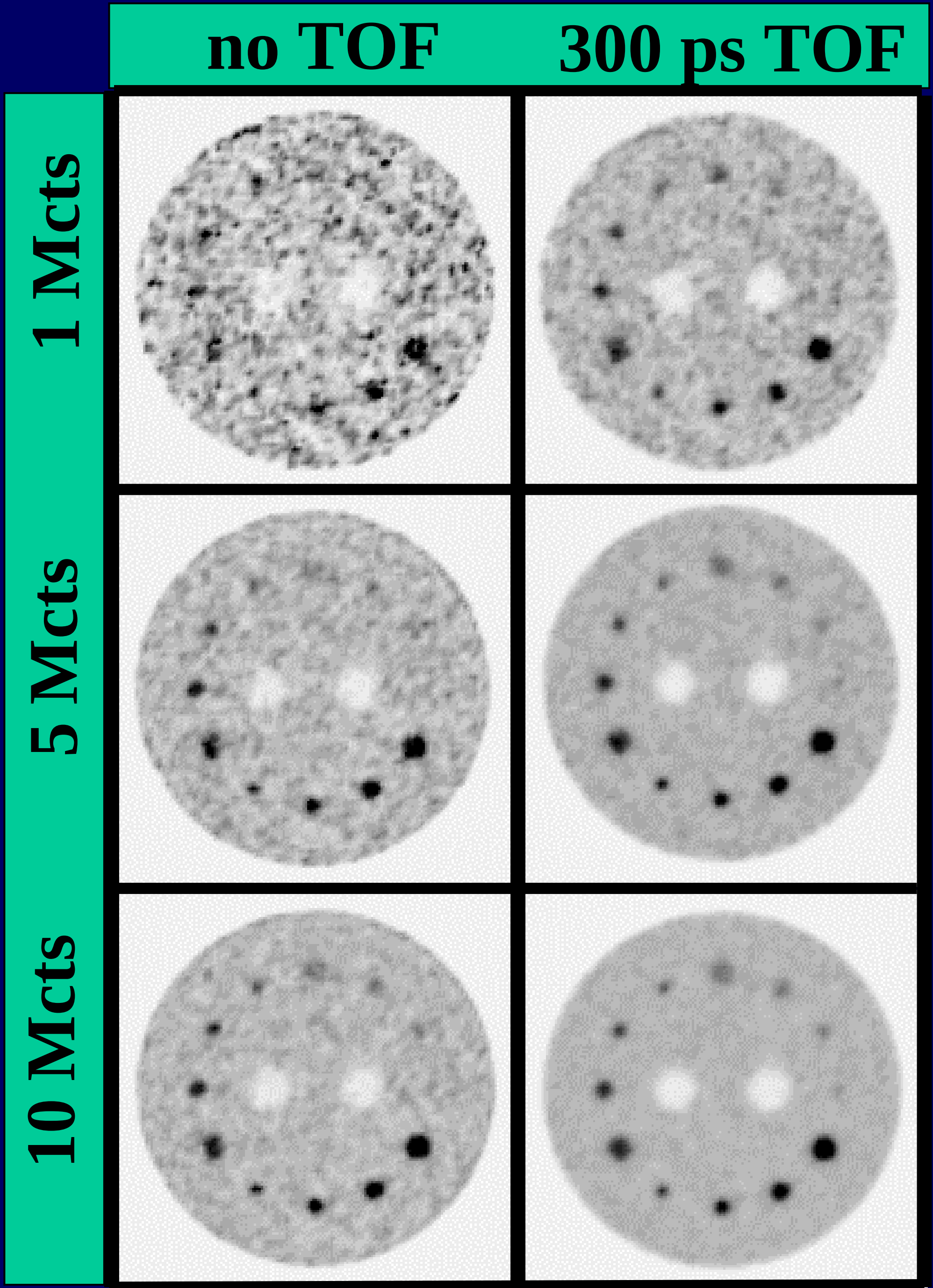

Benefit of TOF

Better image quality
Faster scan time

▫ 5Mcts TOF ∘ 5Mcts
▪ 1Mcts TOF • 1Mcts

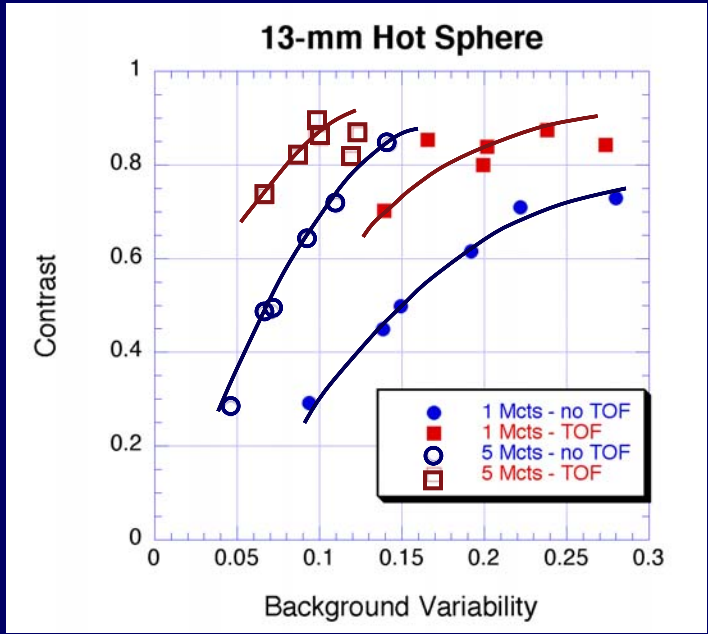

Karp, et al, UPenn

TOFPET DREAM

(A UC IS&FMI/HEP Collaboration)

30 pico-sec TOF

4.5 mm LOR Resolution (Human Scanner)

10 pico-sec TOF

1.5 mm LOR Resolution (Animal Scanner)

Histogramming

No “Reconstruction”

SiPM/PET Collaboration at ANL/UC/NIU

- Single photon response
- Pulsar-1156 SiPM in the test stand:

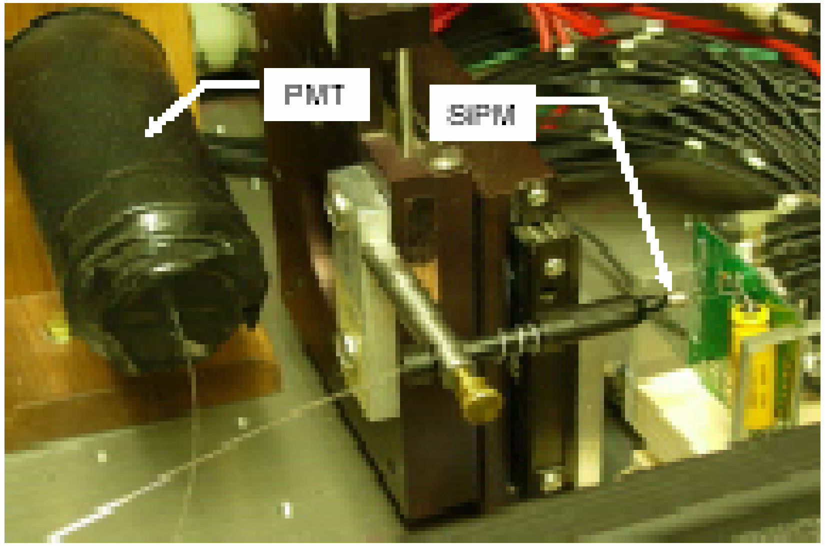

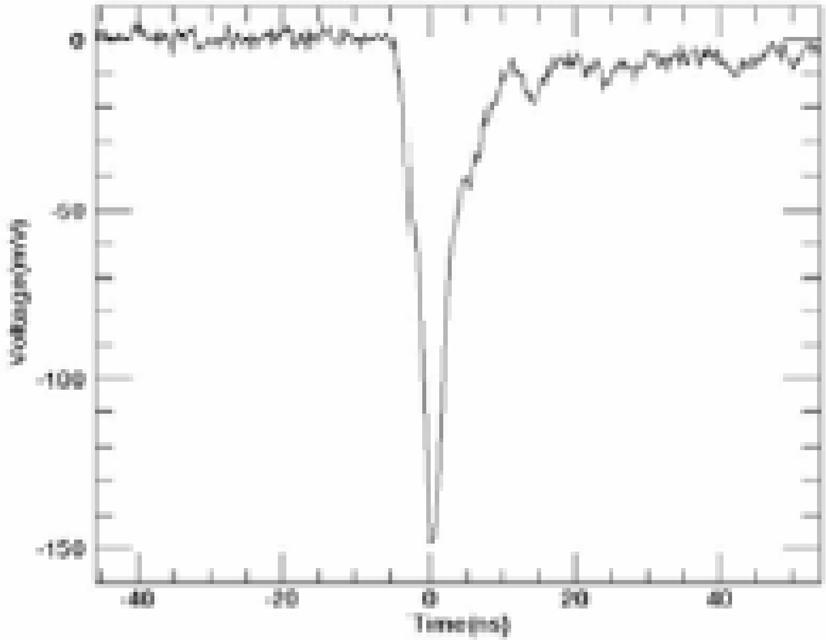

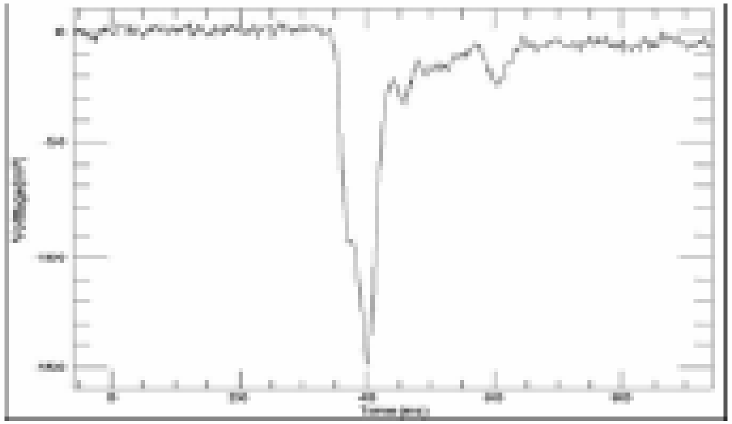

- Screen shots taken by Wagner and Xie:
  - No preamplifier

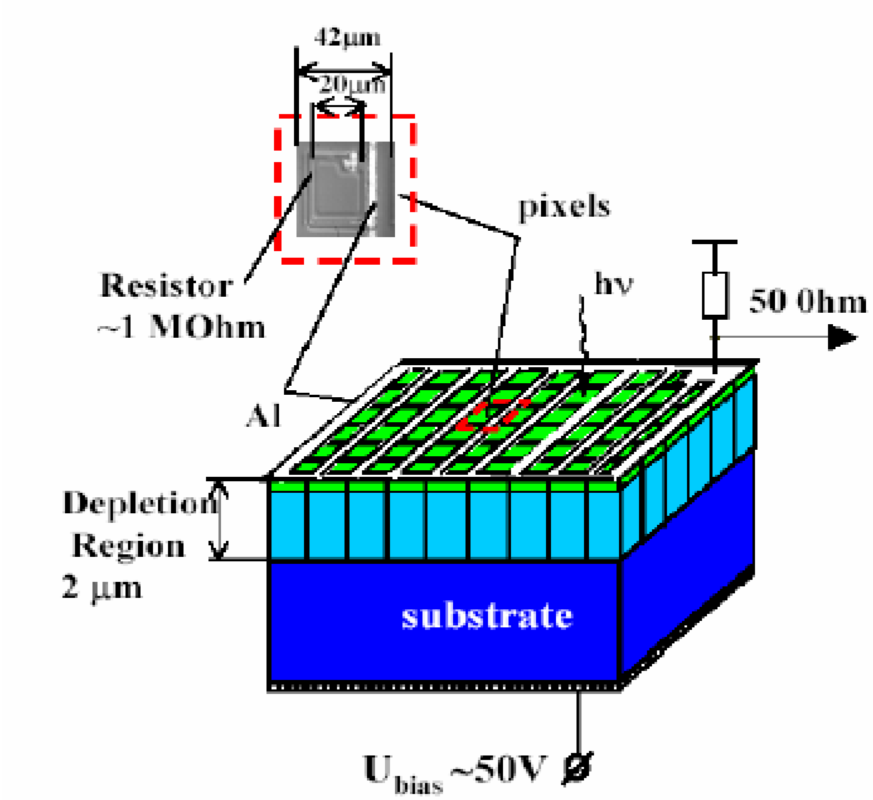
42µm
20µm
pixels
Resistor
~1 MOhm
hν
50 Ohm
Al
Depletion
Region
2 µm
substrate
U bias ~50V

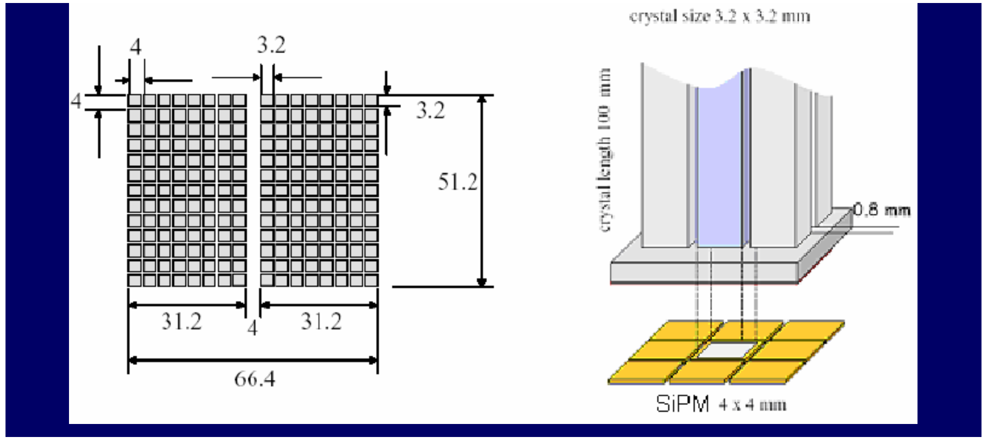
crystal size 3.2 x 3.2 mm
4
3.2
4
3.2
51.2
31.2
4
31.2
66.4
crystal length 100 mm
0.8 mm
SiPM 4 x 4 mm

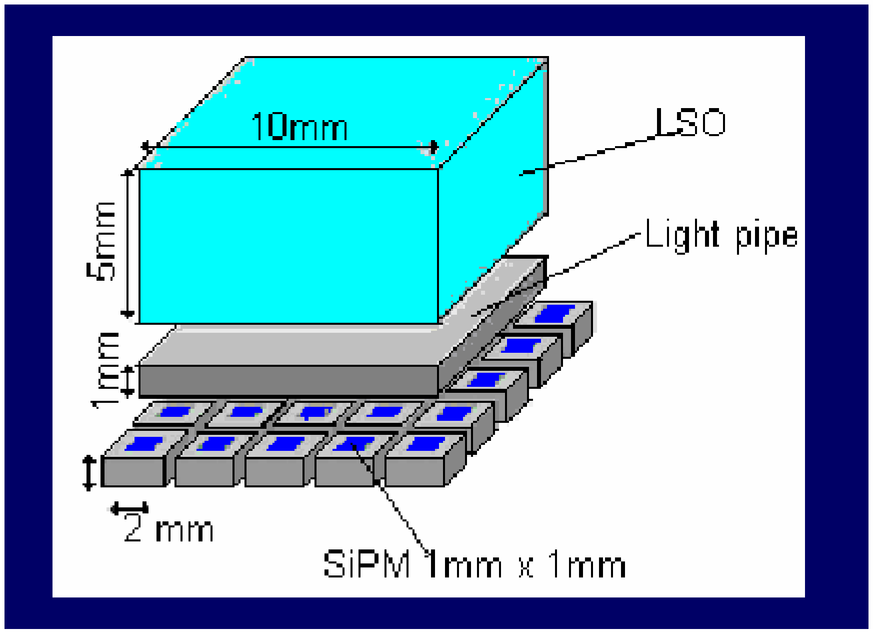
10mm
LSO
5mm
Light pipe
1mm
2 mm
SiPM 1mm x 1mm

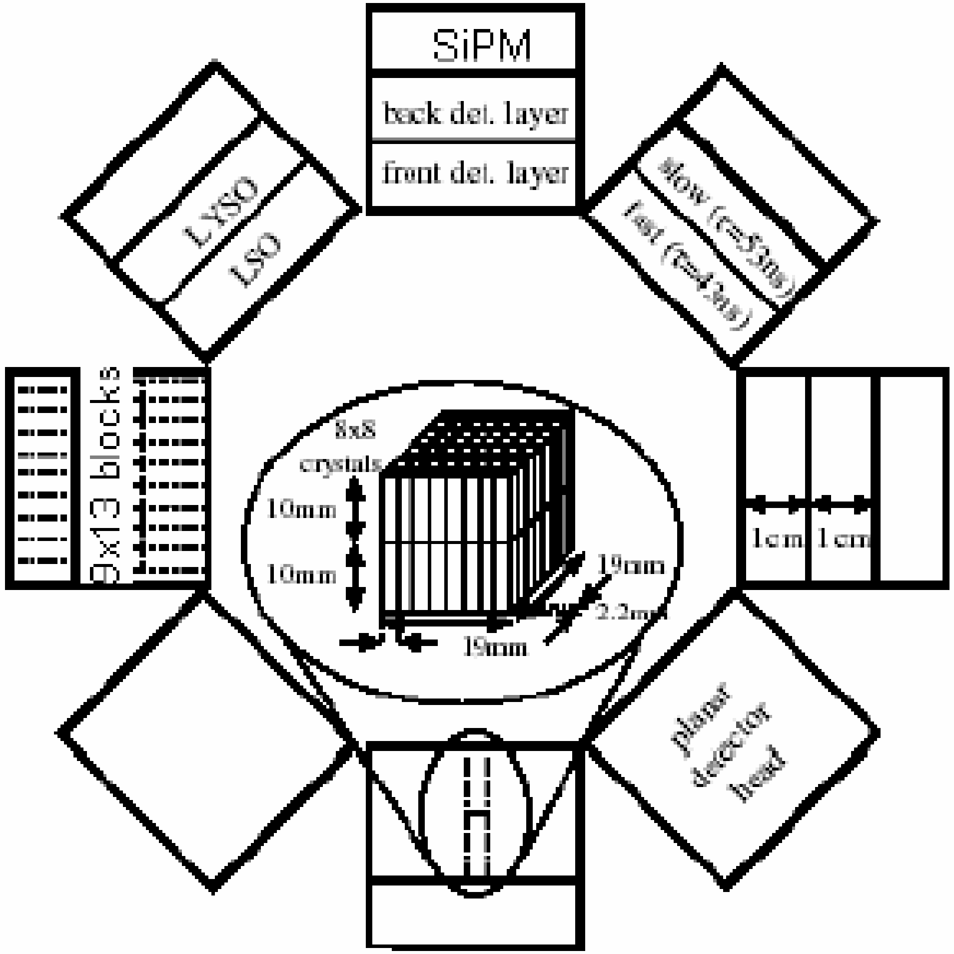
SiPM
back det. layer
front det. layer
LYSO
LSO
slow (τ=53ns)
fast (τ=43ns)
9x13 blocks
8x8
crystals
10mm
10mm
19mm
2.2mm
19mm
1cm
1cm
planar
detector
head

Geant4

– A Common Simulation Platform

High Energy Physics

Space and Radiation

Medical

Technology Transfer

High Energy Physics Space and Radiation Medical Technology Transfer

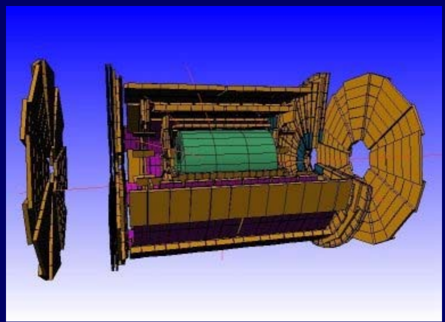

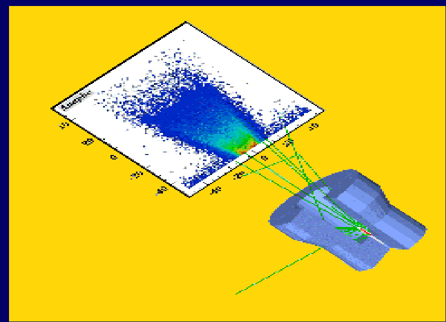

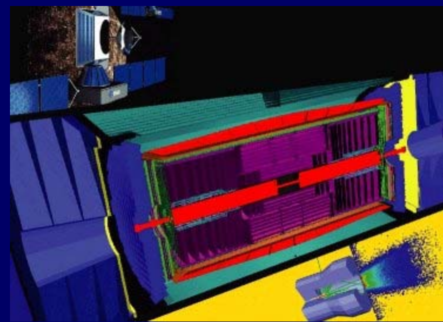

GATE
Geant4 Application for Tomographic Emission

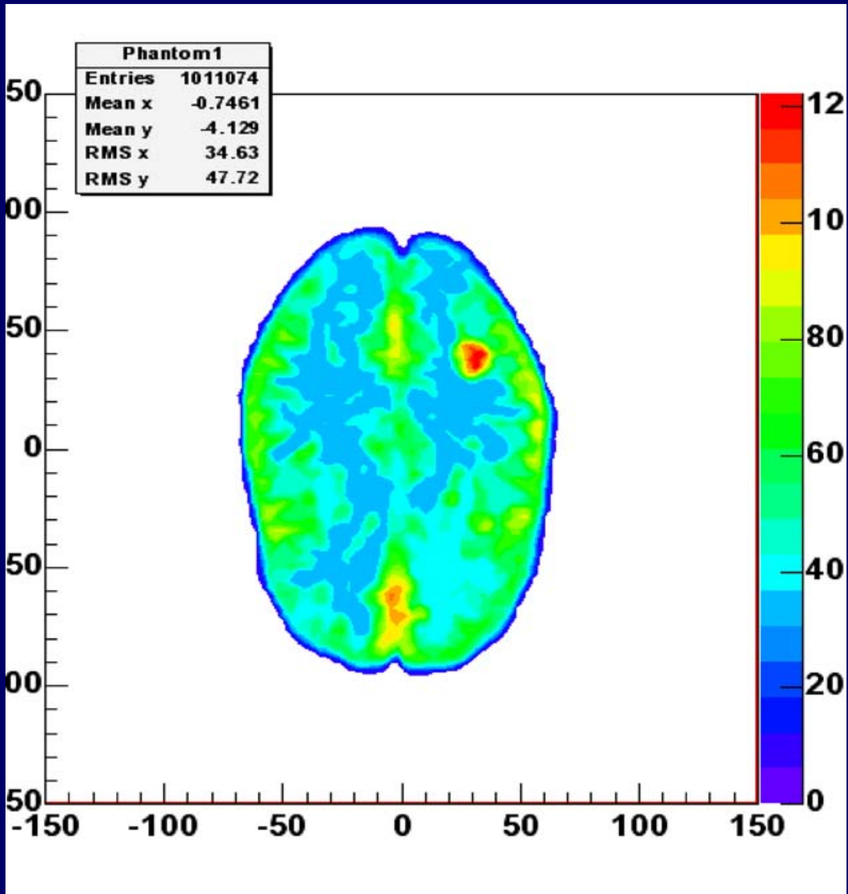

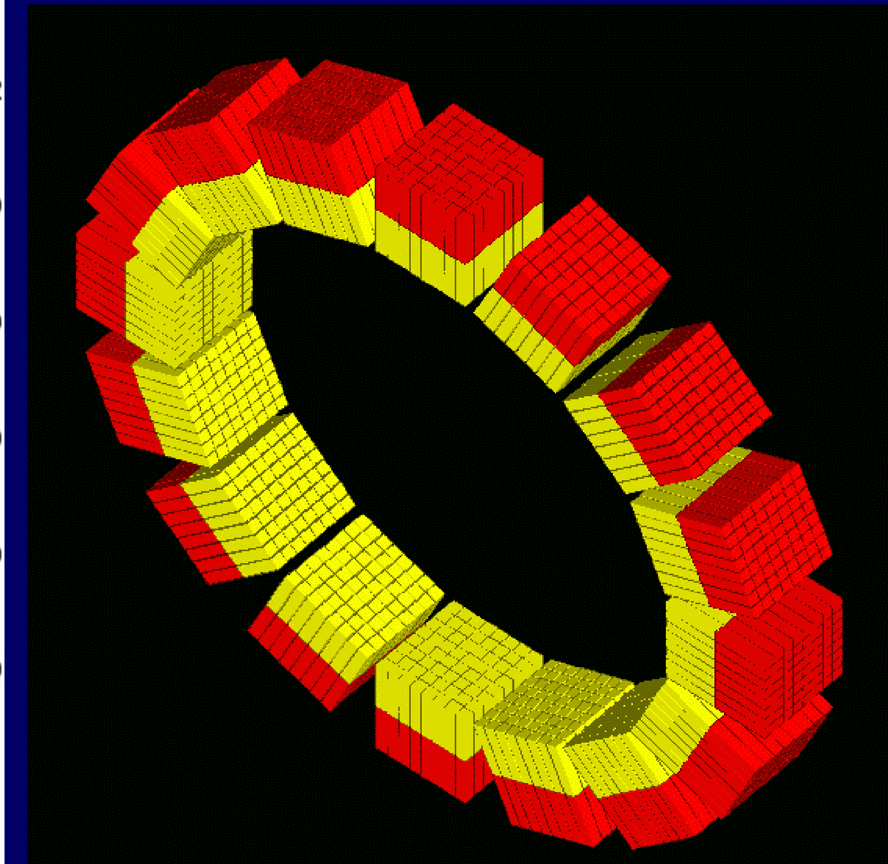

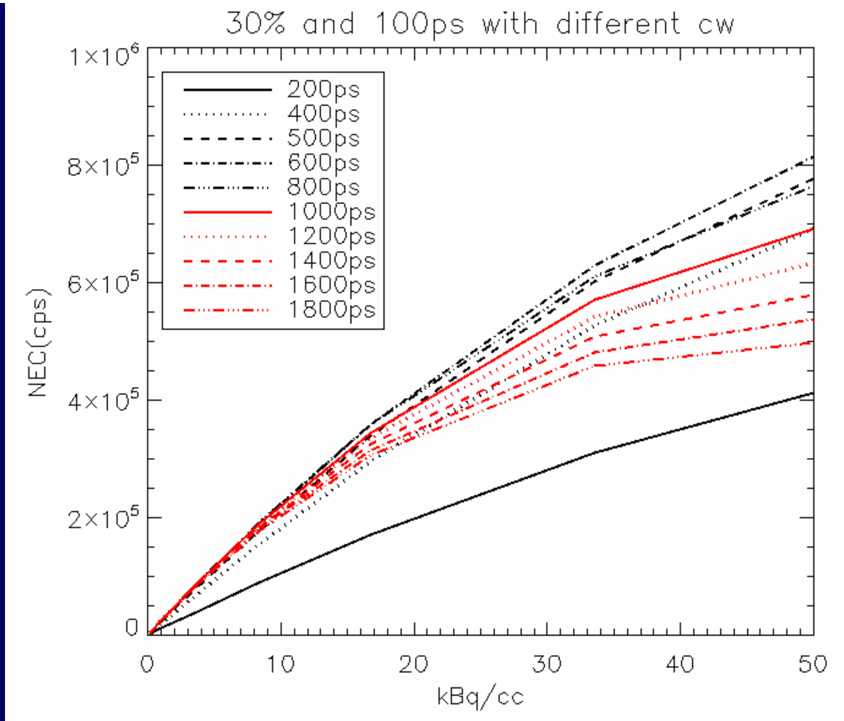
30% and 100ps with different cw
200ps
400ps
500ps
600ps
800ps
1000ps
1200ps
1400ps
1600ps
1800ps
NEC(cps)
kBq/cc

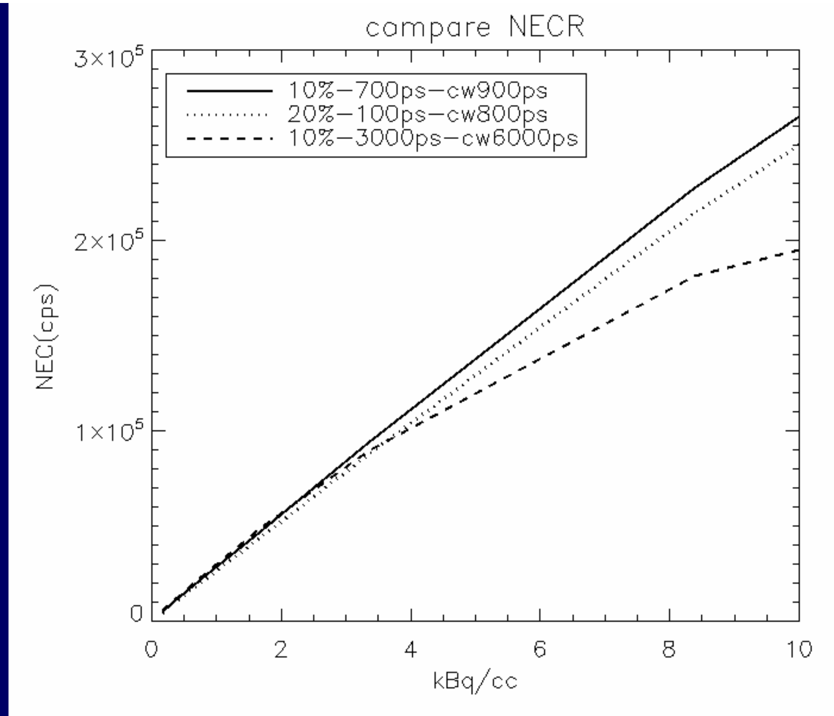
compare NECR
10%−700ps−cw900ps
20%−100ps−cw800ps
10%−3000ps−cw6000ps
NEC(cps)
kBq/cc

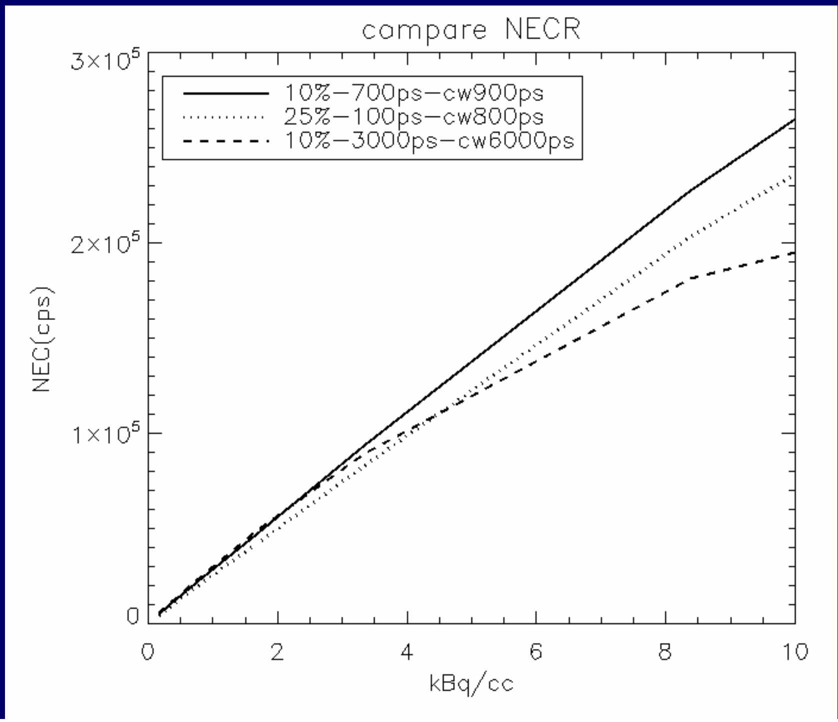
compare NECR
10%−700ps−cw900ps
25%−100ps−cw800ps
10%−3000ps−cw6000ps
NEC(cps)
kBq/cc

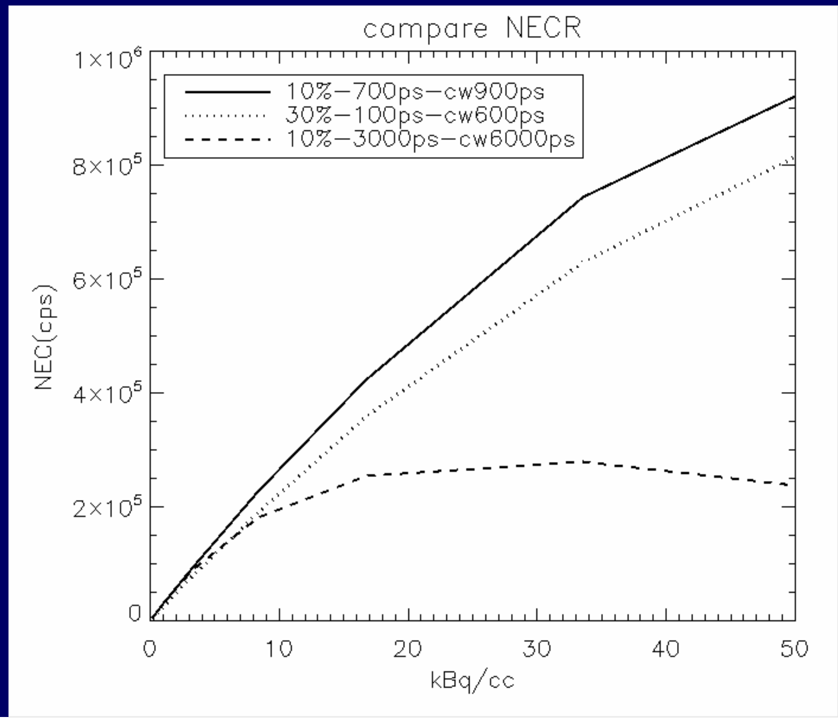
compare NECR
10%−700ps−cw900ps
30%−100ps−cw600ps
10%−3000ps−cw6000ps
NEC(cps)
kBq/cc

Acknowledgement

- UC/IS & FMI Group

  Chien-Min Kao, Ph.D. | Xiaochuan Pan, Ph.D.
  Patrick La Riviere, Ph.D. | Brian Roman, Ph.D.
  Bill O'Brien-Penney, Ph.D. | Daniel Appelbaum, M.D.
  Yonglin Pu, M.D., Ph.D. | Jeffrey Souris, Ph.D.
  Qingguo Xie, Ph.D. | Yun Dong

- UC HEP Group

  Henry Frisch, Ph.D. | Fukun Tang
  Harold Sanders | Tim Credo

- Argonne HEP Group

  Hendrik Weerts, Ph.D. | Alexandre Vaniachine, Ph.D.
  Robert Wagner, Ph.D. | Gary Drake
  Karen Byrum, Ph.D.

- NIU/Fermi Group

  Gerald C. Blazey, Ph.D. | Vic Rykalin, Ph.D.

- National Health Research Institute (in Taiwan)

  Christian Wietholt, Ph.D.